ΠΑΝΕΠΙΣΤΗΜΙΟ ΠΕΙΡΑΙΩΣ

UNIVERSITY OF PIRAEUS

Department Of Digital Systems

Postgraduate Programme

"Digital Communications & Networks"

Master Thesis

"THz Wireless Link Design"

Student

Ευάγγελος Παπασωτηρίου

Evangelos Papasotiriou

Supervision

Associate Professor Ms. Angeliki Alexiou

Piraeus 2018

Abstract

The proliferation of wireless devices in recent years in combination with the need of high throughputs per user and zero latency (less than 1 ms) pushes current technologies and available spectrum to the limit. Even though wireless world is moving to the 5G (fifth generation) era, which contains many promising technological advances e.g massive MIMO (Multiple Input Multiple Output) systems, full duplexing e.t.c, still there is a lack of efficiency and flexibility in handling huge amount of QoS/QoE (Quality of Service / Experience) oriented data. To overcome these problems and provide unprecented capacity using ultra wide bandwidths THz band (0.1-10 THz) looks very promising. But high frequencies of THz band create a novel source of noise (colored), which in combination with severe losses give it new peculiar propagation characteristics. Furthermore transmissions depend on the environmental conditions since water vapor concentration and atmospheric temperature effect the propagation. Current work focuses on the initial research of the achievable information theoretical results in the spectrum ranges of 275-400 GHz and 0.1-1 THz. Metrics of capacity, spectral efficiency and symbol error rate for various link distances are employed using frequency bands of the 0.1-1 THz. They are located around the local minima of molecular loss, using a threshold of 3dB defining transmission windows for a certain distance. Next they are divided in equally sized sub bands, where the assumptions of locally flat noise is made to employ the aforementioned metrics. Results suggest that losses imposed by the channel to the transmitted signal are severe, reducing significantly received SNR (Signal to Noise Ratio). Capacity is calculated within the spectrum of 275-400 GHz assuming antenna gains and different environmental conditions showing that beamforming yields better results improving received SNR independently of the changes in weather conditions. Conclusion of this work is that techniques of MIMO, pencil beamforming and high gain transceivers must be used in order to achieve unprecented bandwidth and throughput possibilities given by THz.

Abbreviations

QoS/QoE	Quality of service/Experience
5G	Fifth Generation
MIMO	Multiple Input Multiple Output
mm-Wave	milli meter Wave
Tbps / Gbps	Terra/Giga bits per second
THz/GHz	Terahertz/Gigahertz
AWGN	Additive White Gaussian Noise
LoS / NLoS	Line of Sight/ Non Line of Sight
EM	Electro Magnetic
PSD	Power Spectral Density
SER	Symbol Error Rate
SISO	Single Input Single Output
FSPL	Free Space Path Loss
v.m.r	Volume mixing ratio
SNR	Signal to Noise Ratio

Table 1. Abbreviations of frequently used terms.

Contents

1 Introduction

Over the last decade the number of wireless devices along with the demand for high quality services, has dramatically increased the need for spectral bandwidth alongside with the requirement for high data rate transmissions. In the meantime while wireless communications world is gradually moving towards the 5G era and many technological solutions have been proposed such as massive MIMO, full duplexing and mm-Wave communications. Still major significant limitations need to be overcome regarding the ability to efficiently handle massive amount of data, while providing sufficient QoS/QoE, super high data rates and zero latency. Under this scope wireless Tbps (Tera bits per second) connections and their supporting backhaul network infrastructure are expected to become a major technology trend of the near future. Networks beyond 5G are expected to provide unprecented performance not only by Tbps data rates but also by supporting a wide variety of novel use cases and applications that combine high data rates with agility, reliability, zero response time and artificial intelligence [1]. Examples of highly anticipated use cases are: virtual presence, 3D printing, cyber physical systems for intelligent transport and industry. So although 5G includes several game changing design principles like virtualization, softwarazation and commoditization of resources, in order to enhance scalability, flexibility and efficient resources use. It can be easily understood that fundamental performance limitations, related to available transmission bandwidth, transmission and processing delays, cost and energy consumption still define the boundaries of 5G capabilities. To overcome these obstacles in networks beyond 5G little explored resources and technologies need to be validated and exploited by directing research to de-risking technological concepts, components, architectures and system concepts. Under this scope THz frequencies can be used to enable wireless networking beyond 5G. THz band lies between 0.1-10 THz [1], [19] and the majority of its spectrum is still mostly unlicensed [21]. These high frequencies can now be exploited since transceivers capable operating at THz band are gradually being constructed [22]. Due to the possibility of large available bandwidths within this band large data rates even of 1Tbps could be achieved. So wireless THz communications and their supporting backhaul network infrastructure are expected to become an attractive complementing technology to the less flexible and much costlier optical fiber connections as well as for the lower data rate systems such as microwave links and WiFi [20]. This suggests that THz band will be used for wireless access and backhaul networking, hence influencing the development of near future networks. The implementation of THz networks will have to fully apply any novel technological breakthroughs [2], examples of these are the joined design of baseband digital signal processing for the complete optical wireless link, the development of broadband and highly efficient RF frontends operating at frequencies higher than 275 GHz [6], new standardized electrical/optical interfaces. Furthermore to address the extremely large bandwidths and propagation peculiarities of THz band, improved channel modeling, MAC (Medium Access Control) schemes and antenna array configurations are required [2].

Such technologies will bring fiber optic speeds to the wireless connections. Next follow the main application scenarios and their key requirements [2]. THz wireless backhaul: As it is known at most cases users at rural areas experience low connectivity. This due to the fact that deploying fiber optical networks is costly, time consuming and needs to capitalize the scheduled road reconstructions. So using THz links as a wireless backhaul extension of the optical fiber can guarantee high speed internet access. Moreover the growth of mobile and fixed users will require hundreds of Gbps (Giga bits per second) in the communication between cell towers (backhaul) or between towers and remote radio heads (fronthaul). Critical parameter is range, which should be in order of a few kilometers [2]. THz wireless local access: THz communications will enable seamless connectivity between high speed wired networks and wireless devices. This will accommodate the use of bandwidth demanding applications across static and mobile users, mainly for indoor and local access scenarios. Critical parameter here is apart from Tbps data rates the connection reliability with bit error rates as low as 10^{-5} , in an environment with few users [2]. THz wireless access for cyber physical systems: Fully adopting digital networking in industry, commerce and public services (e.g. traffic control, autonomous driving, remote health monitoring) places strict requirements for Tbps class access subject to fast response constraints. These cyber physical scenarios describe what is commonly known as tactile internet and impose the need for zero latency (less than 1 ms) [2]. Before reaching the ability of implementing any of the aforementioned THz band applications its peculiar characteristics should be studied, since it still remains highly unexplored. Due to the nature of those frequencies propagation of signal is highly affected by colored noise [1],[5],[6],[15], which is novel for telecommunications systems until now, where only AWGN (Additive White Gaussian Noise) was present. Also THz frequencies suffer from great propagation losses. So to implement the aforementioned applications of this band performance bound definitions must be extracted. Towards this end a new THz oriented information theoretic framework taking into account propagation and channel modeling studies [1],[5],[6],[15], contributions of Los/NLos, reflected and scattered components as well as molecular noise must be developed. This novel deterministic network information theoretic framework should be done for ultra wideband channels with more than 50GHz of bandwidth considering systems operating in ultra low SNR regimes. Current work aims to make the first step in this way by studying THz channel particularities in the 0.1-1 and 0.1 - 10 THz intervals. Particularly the distant dependent noise present in THz transmissions is shown and some initial information theory results for 0.1 - 1 THz using different bandwidths are shown and discussed.

2 THz channel model

2.1 THz channel particularities and characteristics

There are a few existing channel models that can be found in literature describing THz band communications. Since THz band lies within the boundaries of 0.1 - 10 THz it is profound that frequencies belonging to it have very small wavelength. This results to novel propagation characteristics and particularities in comparison with frequency regions used by systems until now. The most distinguishing feature of this band is the absorption of energy from the travelling EM wave by the atmospheric molecules. This phenomenon becomes ever increasing as one moves at higher frequencies within this band and at greater distances, leading to extreme path losses. Furthermore the energy absorbed by the molecules following the radiative transfer theory principles [4] is then reemitted at random directions adding an extra noise source to the receiver beyond the classic AWGN. In order to comprehend the propagation mechanism of THz waves a model must be derived. Such attempts have been done by [1], [5], [6]. The existing molecular absorption noise models are based on the sky noise [14], [15], [16]. This is a simple model of the absorption energy transfer in the atmosphere and can be applied to all absorbing atmospheres such as Earths. It is based on Kirchhoffs law of thermal radiation [17]. In the following sections of this chapter the parameters of absorption loss, noise temperature, PSD and power will be presented and explained.

2.1.1 Absorption coefficient

Different types of molecules present in the atmosphere resonate at different frequencies. An EM wave, at a specific frequency f of the THz band, propagating through the medium causes a specific type of molecule to absorb part of its energy and move to a higher energy state. According to radiative transfer theory **[**7**]** [8**]**, the energy difference between the two states is equivalent to the energy drawn from the wave by the molecule and from a communication perspective this is a loss. To measure the intensity of this phenomenon, absorption coefficient is used. To account for all the losses within THz band, due to the different types of molecules present in the medium, a stochastic process to model absorption coefficient is used. It depends on frequency and gives THz band its peculiar frequency selective absorption profile. To obtain absorption coefficient of all molecules and its isotopologues at various frequencies the simplest way is to use a spectroscopic database, such as HITRAN (high resolution transmission molecular absorption database) [18]. It contains line by line parameters for the most common molecules and its isotopologues (two isotopologues of the same molecular species differ to one another only to their elements number of neutrons), data which are used to calculate absorption coefficient at any frequency. Following the stochastic process of absorption coefficient is presented [6].

$$k_a^i(f) = \mu_i N \sigma_i(f) \ (m^{-1}) \tag{1}$$

Where μ_i is the fraction of molecules of kind i. This is a dimensionless number expressing the percentage concentration of the *i-th* molecular species in the total volume of the atmospheric medium. Hence μ_i is known as v.m.r (volume mixing ratio). N is the number density of all different kinds of molecules present in the medium.

$$N = \frac{p}{k_B T} \ (molecules/m^3) \tag{2}$$

Where p is the air pressure in Pa, k_B Boltzmann's constant in J/K, T air temperature in K.

$$\sigma_i(f) = S^i(T)G^i(f)(cm^2/molecule) \tag{3}$$

Equation (3), gives the absorption cross section of the *i-th* molecular species (e.g. all isotopologues of O_2). Absorption cross section gives the effective area in which a molecule can act as an EM wave energy absorber. It is a product between the spectral line intensity and the spectral line shape. Spectral line intensity can be directly obtained by HITRAN at the reference temperature of T_0=296 K, to calculate it at T, the following equation is used.

$$S^i(T) = S_0^i(T_0)\frac{Q(T_0)}{Q(T)}\frac{e^{-\left(\frac{hcE_i^L}{k_B T}\right)}}{e^{-\left(\frac{hcE_i^L}{k_B T_0}\right)}}\left(\frac{1-e^{-\left(\frac{hcf_c^i}{k_B T}\right)}}{1-e^{-\left(\frac{hcf_c^i}{k_B T_0}\right)}}\right)\left(\frac{cm^{-1}}{cm^{-2}molecule}\right) \tag{4}$$

Where $S^i_o(T_o)$ is the spectral line intensity at 296K from HITRAN. $Q(T_o)$, $Q(T)$ are the partition sum functions of *i-th* isotopologue from HITRAN [18**]** f^i_c is the center frequency of the *i-th* absorption line, k_B Boltzmann constant, c light speed in vacuum, E^i_L the lower energy state of the transition. $G^i(f,p,T)$ is the spectral line shape obtained by equation (8)**.** Spectral line intensity indicates the strength of the absorption per absorption line and spectral line shape the width and shape of the spectral lines. The center frequency of an absorption line is:

$$f_c^i = f_0^i + \delta_i \frac{p}{p_0}(Hz) \tag{5}$$

where p is the air pressure in atm, p_o is the reference pressure (1 atm), f_o^i is the center frequency of the absorption line at p_0, δ_i the linear pressure shift in cm^{-1}/atm. These values are obtained by HITRAN **[**10**]**. As explained in **[**11**]** the discrete absorption lines experience pressure broadening modeled by the Lorentz half width

$$a_i^L = \left[(1-\mu_i)a_0^{air} + \mu_i a_0^i\right]\left(\frac{p}{p_0}\right)\left(\frac{T_0}{T}\right)^{\gamma}(Hz) \tag{6}$$

where T_0 is the reference temperature(296 K), γ is the broadening coefficient of temperature dependence, $\alpha^{air}{}_0$ and $\alpha^i{}_0$ are the air and self broadened half widths respectively in cm^{-1} / atm. Self broadening is caused by collisions between molecules of the same species, while foreign broadening due inter molecular collisions. All

aforementioned values are obtained by HITRAN database. The most well known line shape is Lorentz [1], [6]

$$F_L^i(f) = \left(\frac{a_L^i}{\pi}\right)\left(\frac{f}{f_c^i}\right)\left[\frac{1}{\left(f-f_c^i\right)^2+\left(a_L^i\right)^2}+\frac{1}{\left(f+f_c^i\right)^2+\left(a_L^i\right)^2}\right](Hz^{-1}) \quad (7)$$

but it overestimates the absorption at far wings as it never reaches zero. To overcome this Van Vleck Weisskopf line shape is used **[**12**]**, **[**13**].**

$$G^i(p,f,T) = \frac{f}{f_c^i}\frac{\tanh\left(\frac{hf}{2k_BT}\right)}{\tanh\left(\frac{hf_c^i}{2k_BT}\right)}\left[F_L^i\left(f-f_c^i\right)+F_L^i\left(f+f_c^i\right)\right](Hz^{-1}) \quad (8)$$

Using equations (1) to (8) total absorption coefficient at frequency *f* can be calculated. At this point should it be mentioned that HITRAN line by line parameters obtained by the database are not in SI units but in cgs (centimeter gram second), so in order for the aforementioned equations to have the appropriate SI units wherever cm^{-1} appears in calculations the equations must be multiplied by light speed, having units cm/s. Now that absorption coefficient is properly defined. The most common absorbing molecules of the atmosphere must be mentioned, which are: water, carbon dioxide, nitrous oxide, methane, molecular oxygen, molecular nitrogen (hitran molecular ids: 1,2,4,5,6,7,22) [10]. Furthermore it should be addressed that water vapor is the major absorber of energy in THz frequencies [6], meaning that different concentrations impact efficiency of these systems. From fig. 3 it is obvious that water vapor is mostly responsible for energy loss, water vapor absorption coefficient almost coincides with the total.

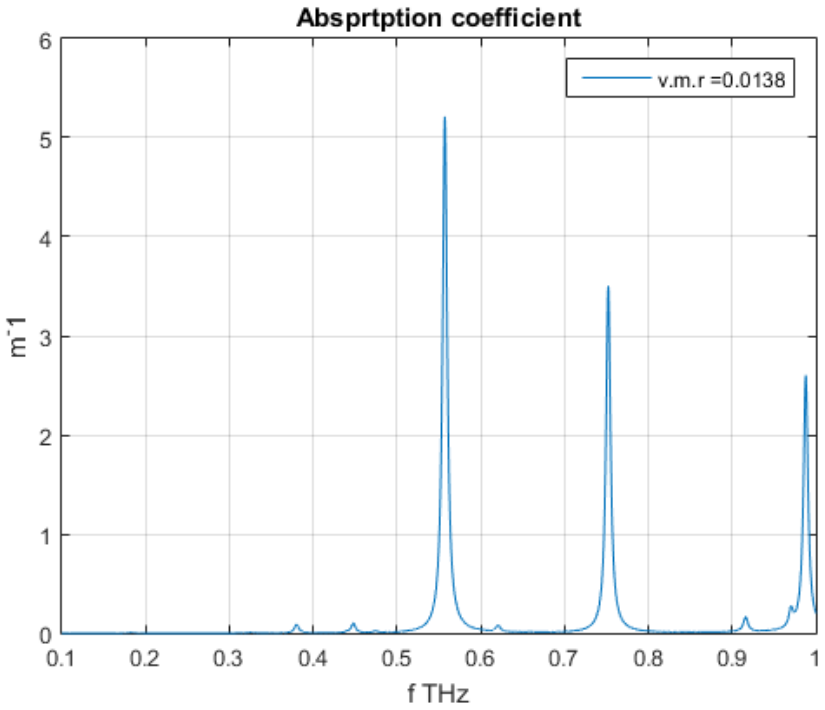

Figure 1. Absorption coefficient calculated with data from HITRAN database for molecules 1,2,4,5,6,7,22 (ids of database) for T_0 = 296 K, p = 1 atm, *v.m.r* = 0.0138 in the 0.1 - 1THz interval.

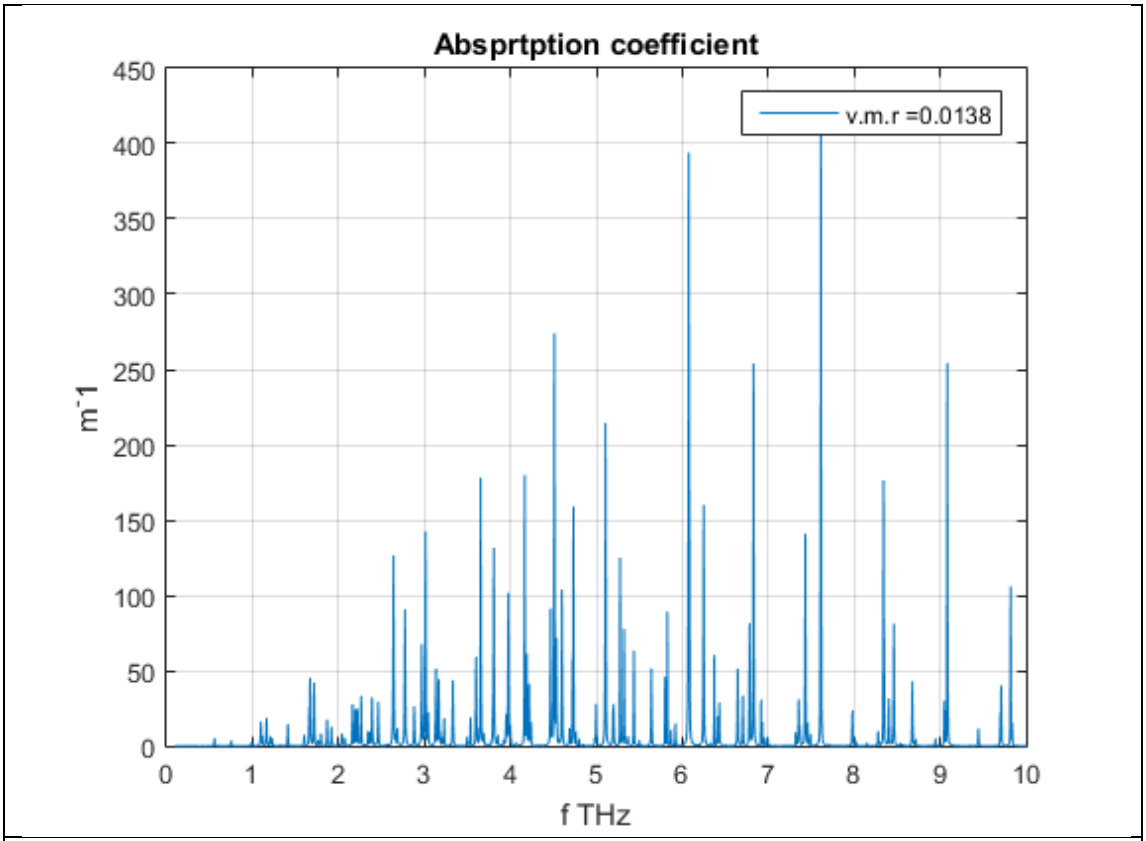

Figure 2. Absorption coefficient calculated with data from HITRAN database for molecules 1,2,4,5,6,7,22 (ids of database) for T_0 = 296 K, p = 1 atm, $v.m.r$ = 0.0138 in the 0.1 - 10 THz interval.

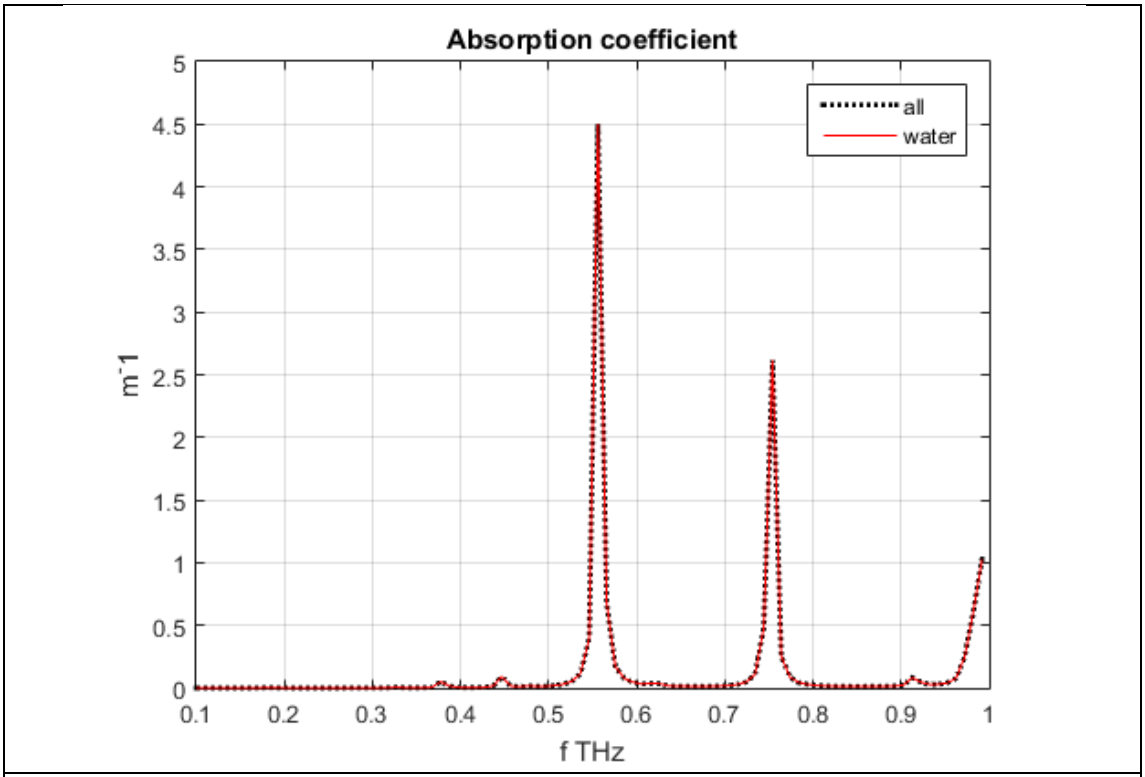

Figure 3. Absorption coefficient calculated with data from HITRAN database for molecules 1,2,4,5,6,7,22 (ids of database) for T_0 = 296 K, p = 1 atm, $v.m.r$ = 0.0138 in the 0.1 - 1 THz interval.

2.1.2 Transmittance

In the previous paragraph the intensity of absorption was presented. Now the amount of radiation at frequency *f* and distance *d* capable of propagating through the medium without being lost, using the Beer Lambert Law is the transmittance **[**1**],** [6], [11], [19].

$$\tau(f,d) = \frac{P_r(f,d)}{P_t(f)} = e^{-\sum_i k_a^i(f)d} \quad (9)$$

It is a function of both frequency and distance. Where f is the frequency of the travelling wave and *d* the distance between the transmitter and receiver antennas. Absorption coefficient at f is the summand for all individual molecules absorptions. $P_r\ (f)$, $P_t(f)$ in Watt are the received and transmitted signal powers respectively. Equation (9) is the foundation of THz research, because as will be presented through the following sections, molecular absorption loss, frequency-distant dependent noise, receiver noise temperature are directly derived through it. Transmittance is dimensionless and its maximum value never exits one. To better comprehend its physical meaning one could view it as a percentage by multiplying with 100 %. Next figures 4,5, give transmittance at various distances for the 0.1 - 1 and 0.1 - 10 THz bands.

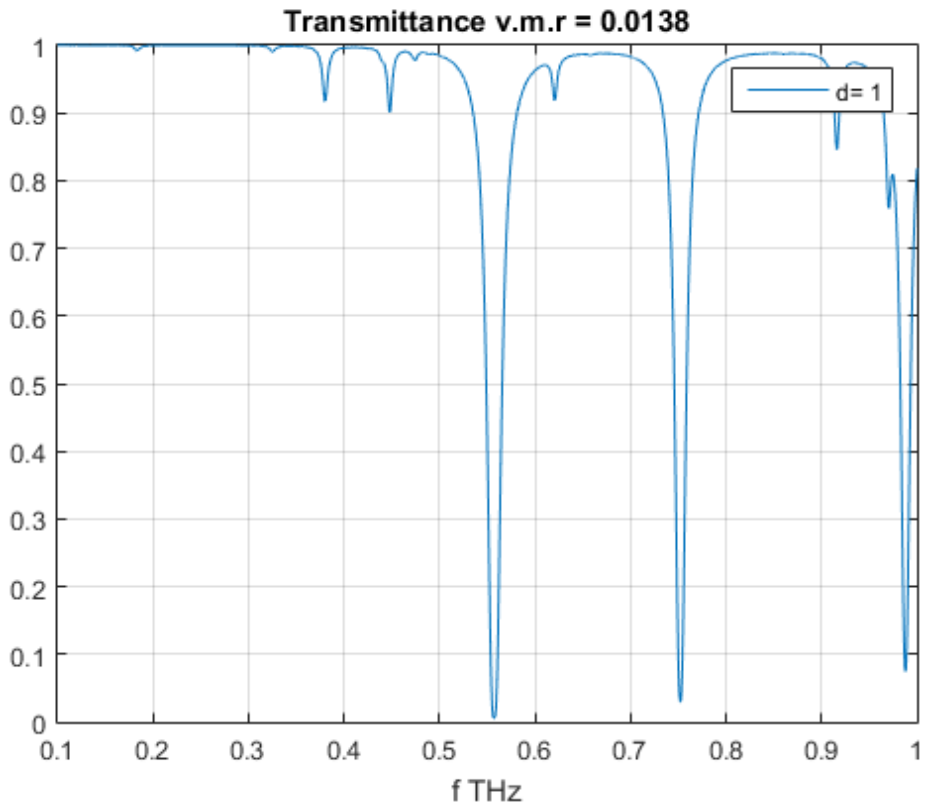

(a)

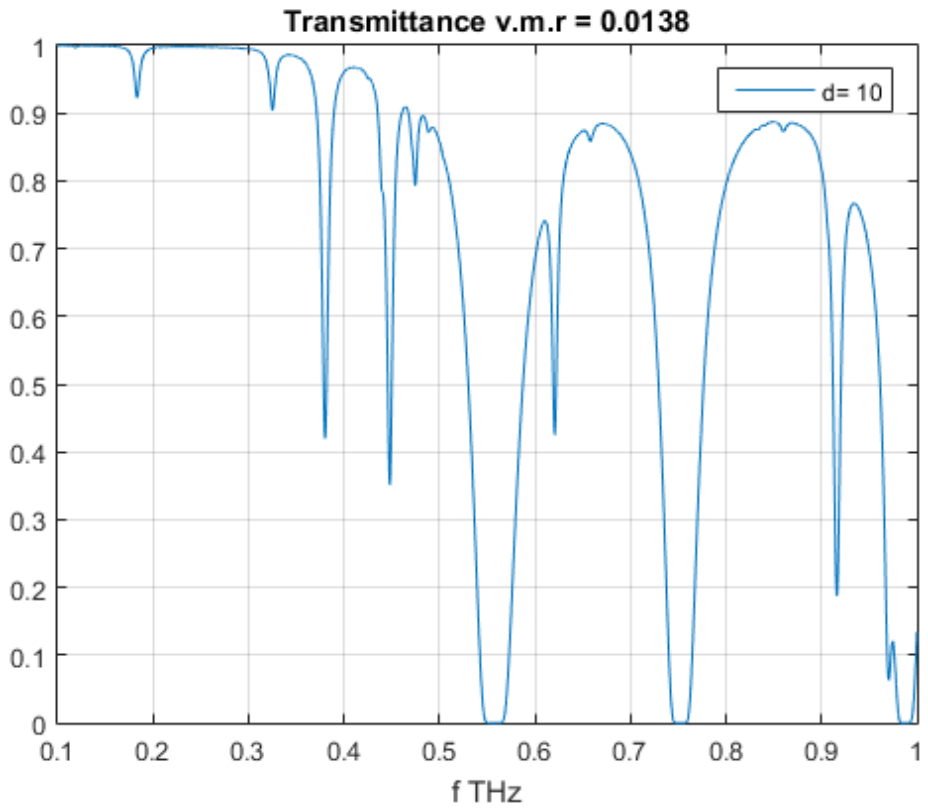
Transmittance v.m.r = 0.0138
d= 10
f THz

(b)

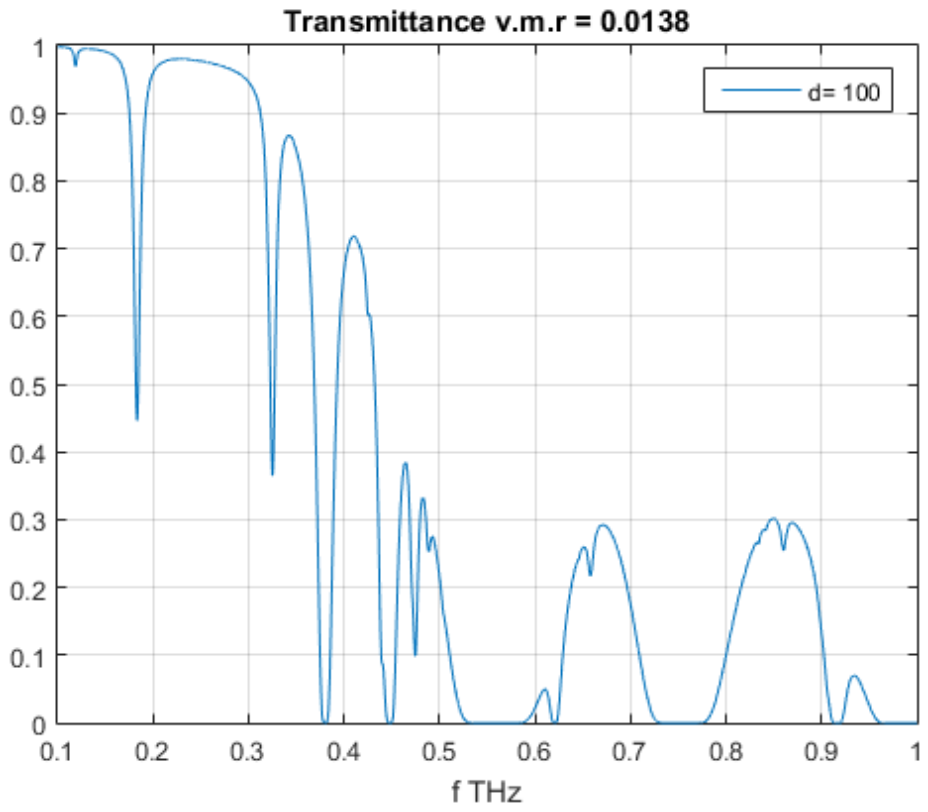
Transmittance v.m.r = 0.0138
d= 100
f THz

(c)

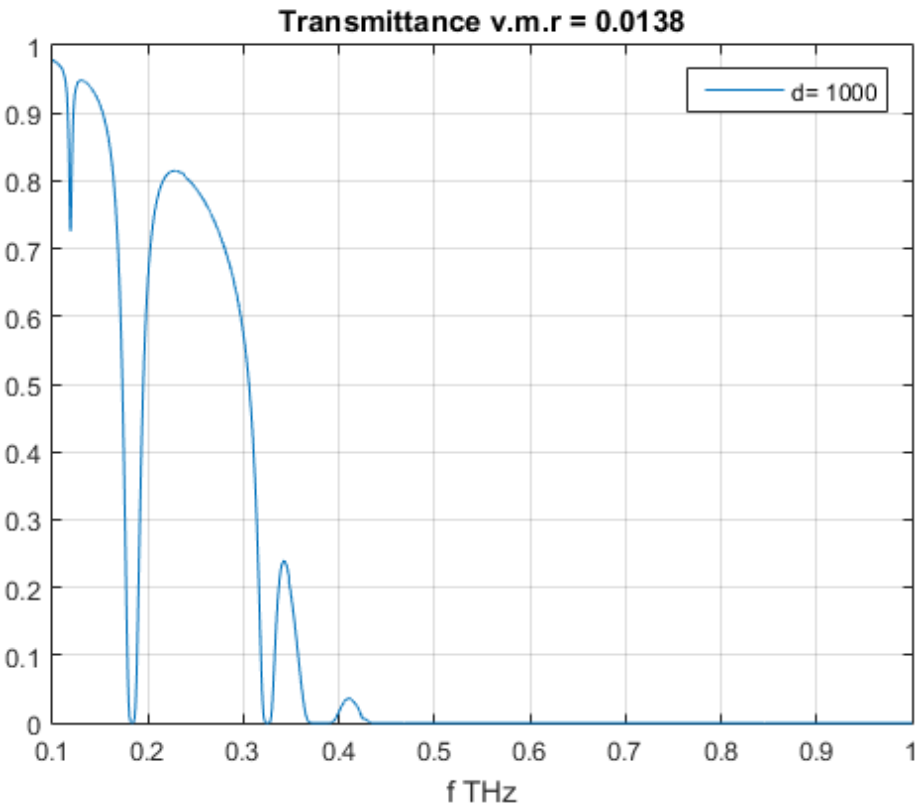

(d)

Figure 4. Transmittance in 0.1 - 1 THz band, with HITRAN database data for p=1 atm, T_0=296K, $v.m.r$ = 0.0138, at distances d = [1,10,100,1000] m.

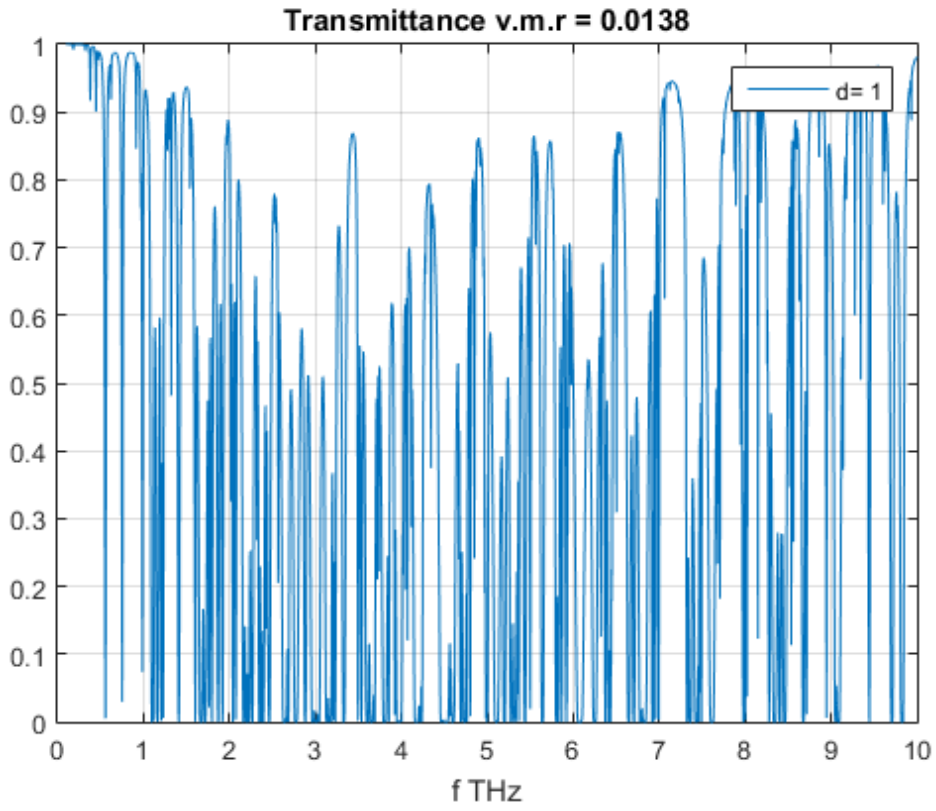
Transmittance v.m.r = 0.0138
d= 1
f THz

(a)

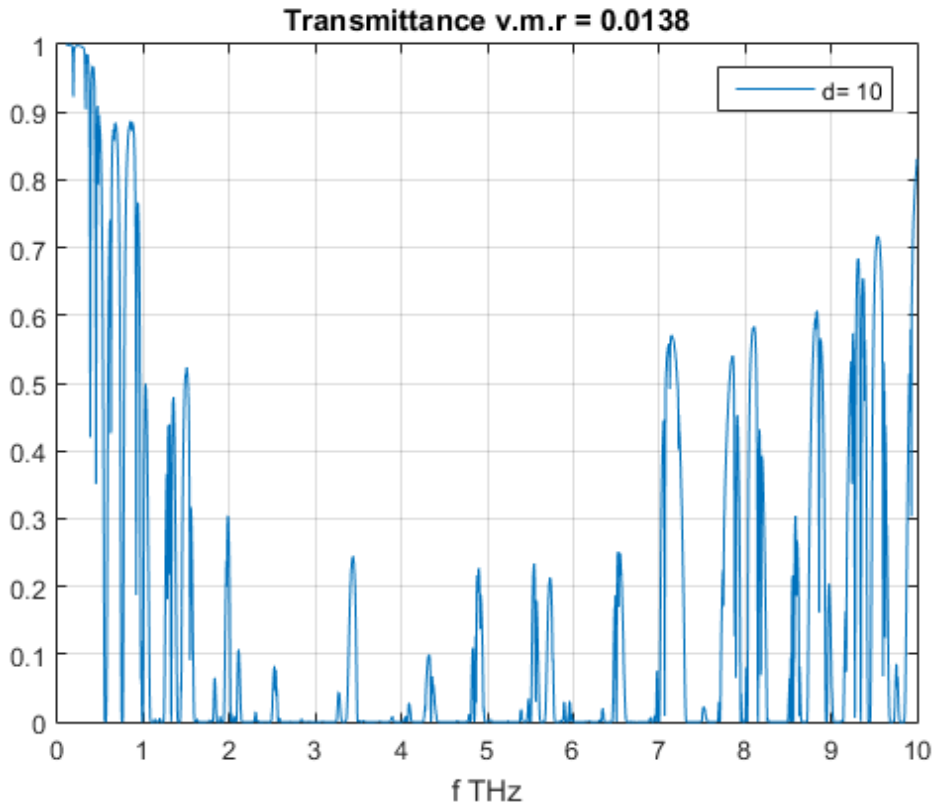
Transmittance v.m.r = 0.0138
d= 10
f THz

(b)

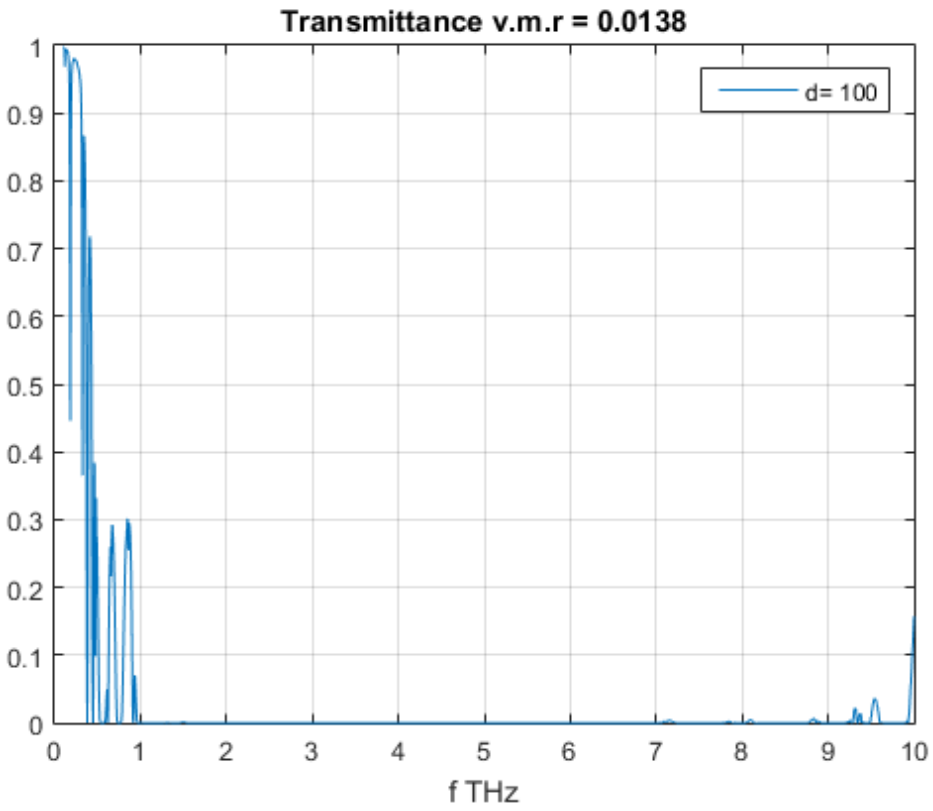

(c)

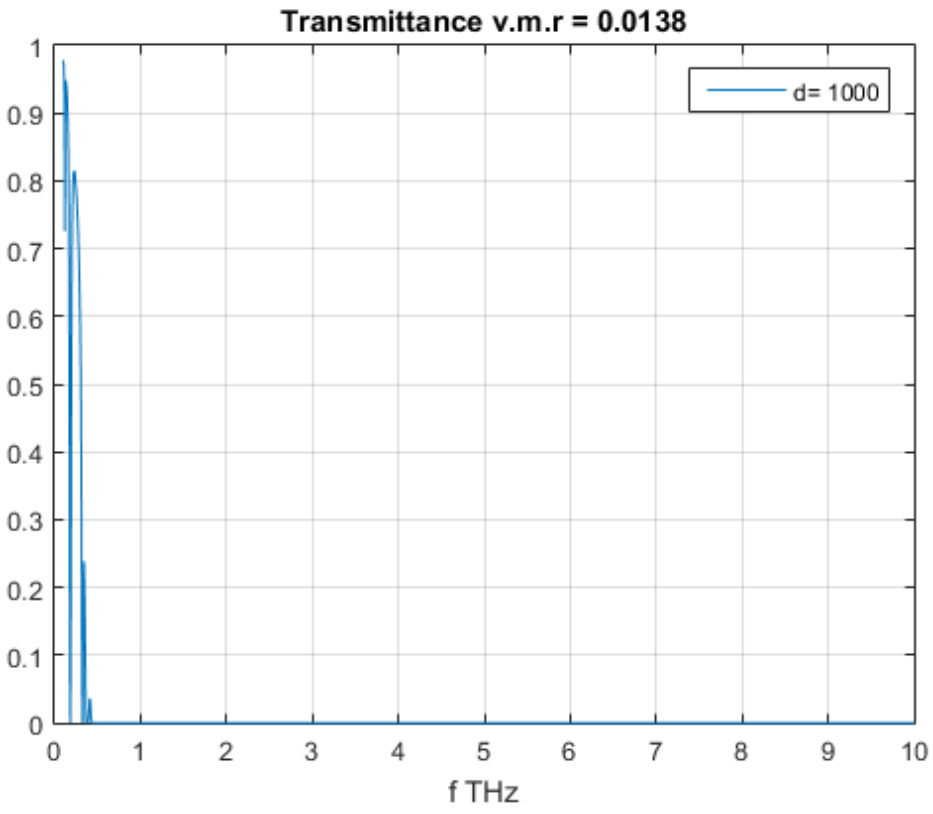

(d)

Figure 5. Transmittance in 0.1 - 10 THz band, using HITRAN database data for p=1 atm, T_0=296K, *v.m.r* = 0.0138, at distances d = [1,10,100,1000] m.

Figures 4,5 illustrate how transmittance is reduced along the spectrum, as a function of frequency and distance. From fig. 4(a) for the link distance of 1m, transmittance is above 0.9 almost in the entire spectrum. Except for the sub intervals of 0.5-0.6, 0.7-0.8 and close to 1 THz, where it gets close to 0.1. From fig. 4(b), as link distance increases to 10m transmittance gets close to 0.1 at wider ranges of the previous mentioned sub intervals. Furthermore it is deteriorating (dropping below 0.9) at more frequency intervals near 0.4 THz, within 0.4 - 0.5 THz, near 0.6 THz and within 0.9 - 1 THz. Hereafter in the next figures 4 (c) and (d) the aforementioned intervals get wider and transmittance lower. Significant is the result for link distance 1000m, where transmittance is zero for almost half the 0.1 - 1 THz band. Figures 5 (a) and (b), show that transmittance is below 0.6 for frequencies above 1 THz. Indicating that absorption is more evident higher in the band combined with distance increase. This is better shown in figures 5 (c) and (d), where transmittance is zero almost above 1 THz and 0.5 THz respectively. Figures 4, 5 aid to comprehend the growth of signal loss. Distance increase between transmit and receive antennas means that more molecules are present in the medium and absorb energy. Additionally the increase of frequency means that more molecular isotopolgues are able to resonate.

2.1.3 Pathloss

Regarding only the LOS loss mechanisms the two main losses in THz band occur from the FSPL as in every telecommunication system and the molecular absorption loss.

$$A_{abs}(f,d) = \frac{1}{\tau(f,d)} = e^{\sum_i k_a^i(f)d} \tag{10}$$

or in dB $$A_{abs}(f,d) = d\sum_i k_a^i(f)\, 10log_{10}(e) \tag{11}$$

Equations (10), (11) give the molecular absorption loss at f,d.

The FSPL of an EM wave due to its expansion at the medium is given by:

$$A_{spread}(f,d) = 20log_{10}\left(\frac{4\pi fd}{c}\right)(dB) \tag{12}$$

Adding equations (11), (12) the total path loss at *f, d* is given as:

$$A(f,d) = A_{spread(f,d)} + A_{abs}(f,d)(dB) \tag{13}$$

Next follow, figures (6,7) of FSPL and molecular absorption loss. At the 0.1 - 1 and 0.1 -10THz intervals for different distances.

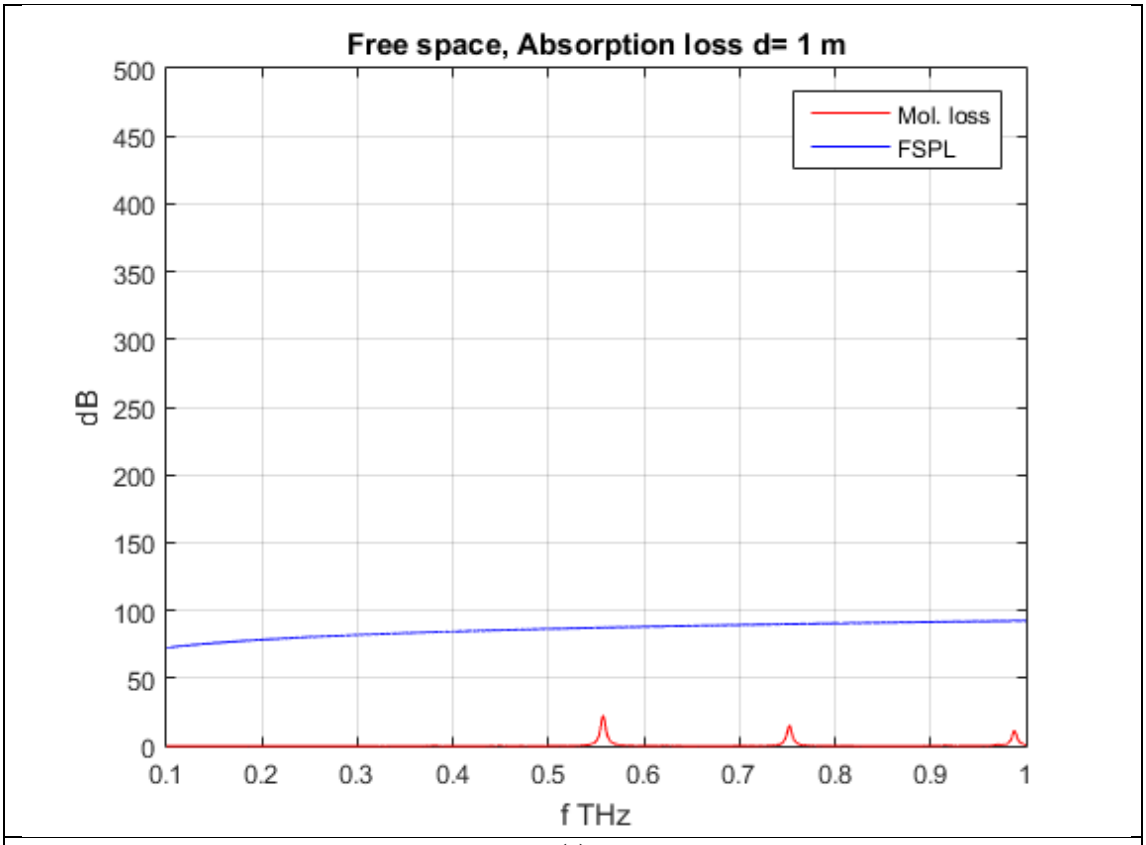
Free space, Absorption loss d= 1 m
Mol. loss
FSPL
dB
f THz
0
50
100
150
200
250
300
350
400
450
500
0.1
0.2
0.3
0.4
0.5
0.6
0.7
0.8
0.9
1

(a)

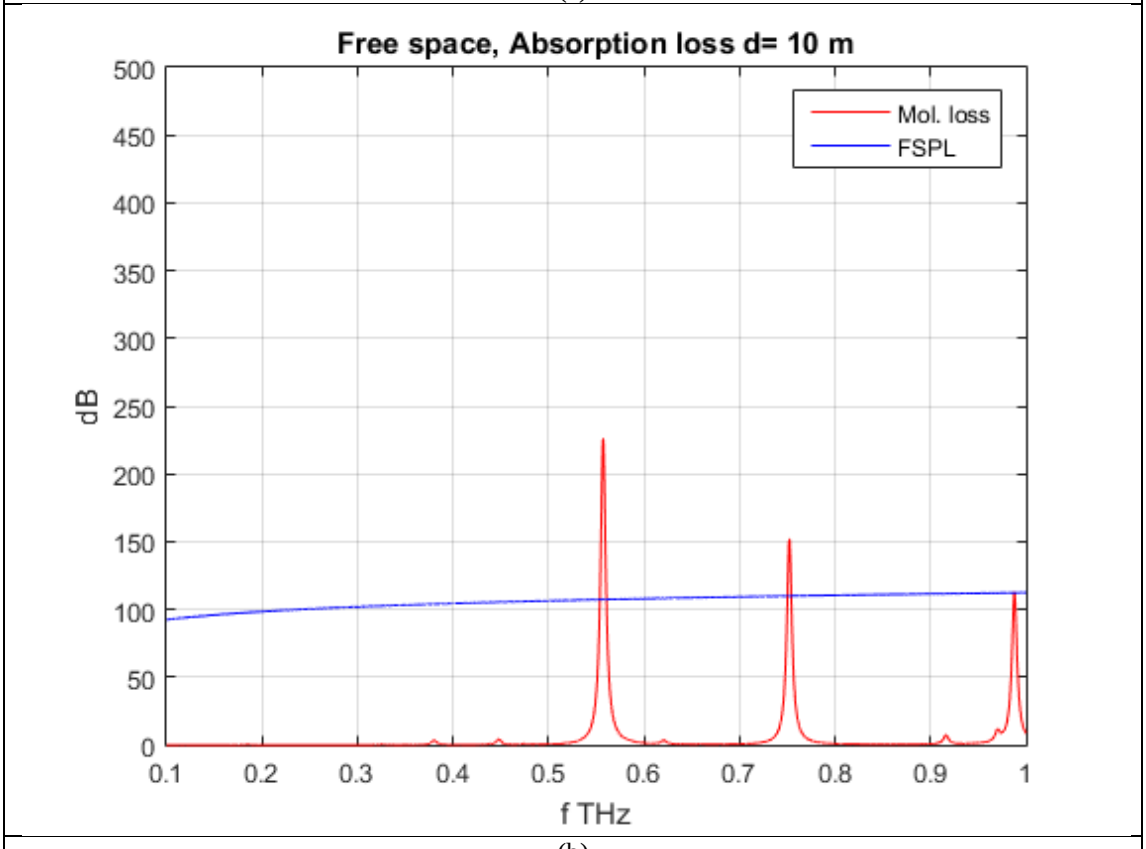
Free space, Absorption loss d= 10 m
Mol. loss
FSPL
dB
f THz
0
50
100
150
200
250
300
350
400
450
500
0.1
0.2
0.3
0.4
0.5
0.6
0.7
0.8
0.9
1

(b)

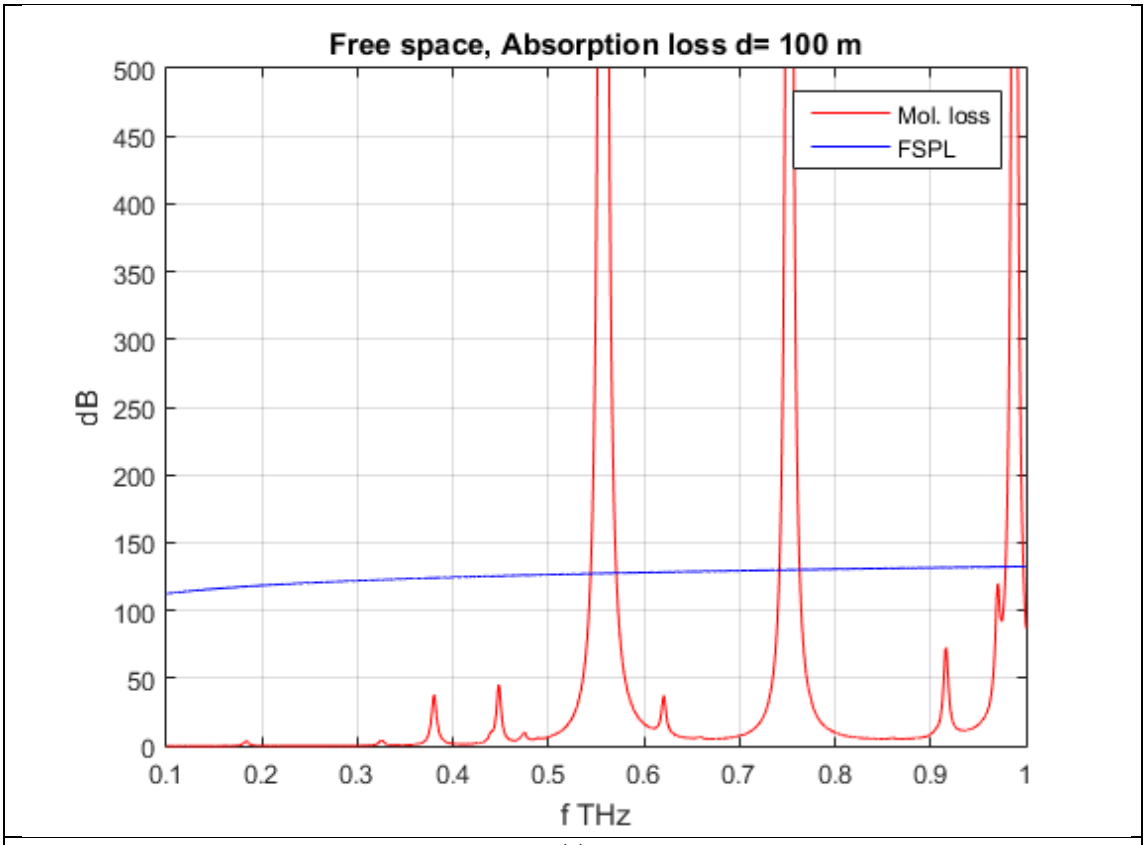

(c)

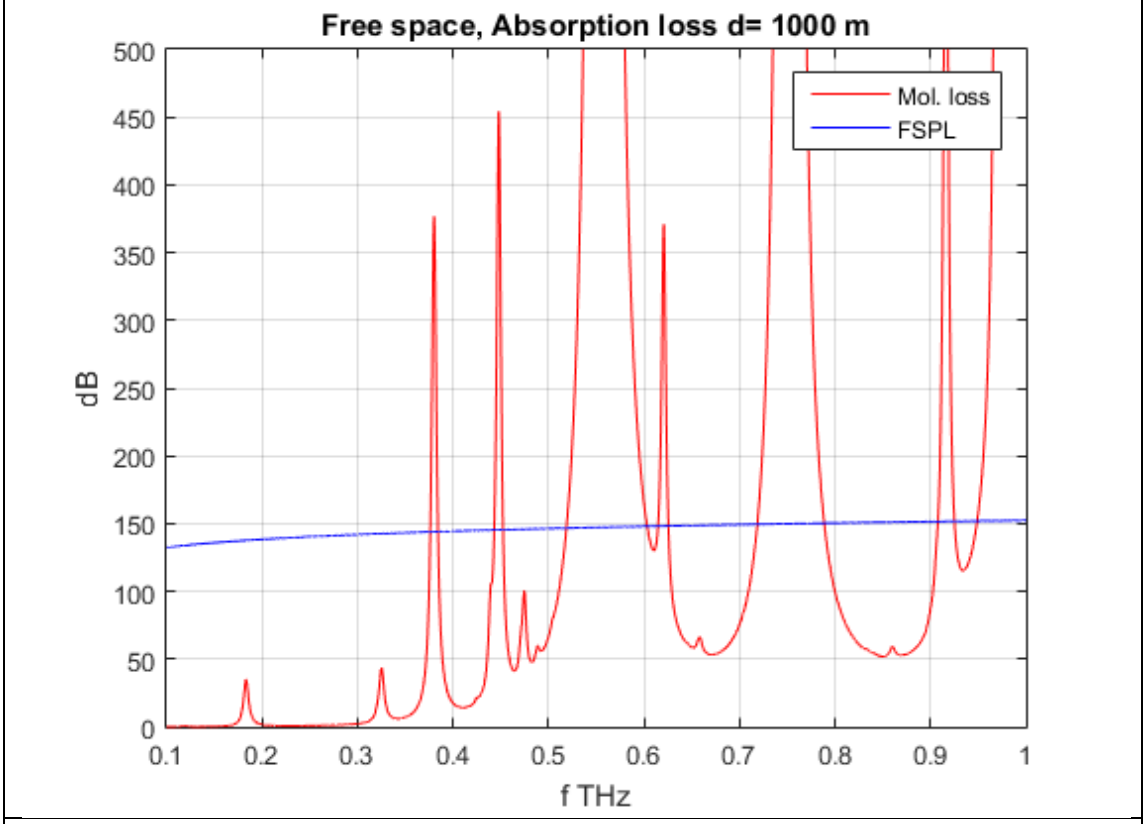

(d)

Figure 6. FSPL & Molecular absorption loss in 0.1 -1THz. Using HITRAN database for p = 1atm, T_0 =296K, *v.m.r* = 0.0138, d=[1,10,100,1000].

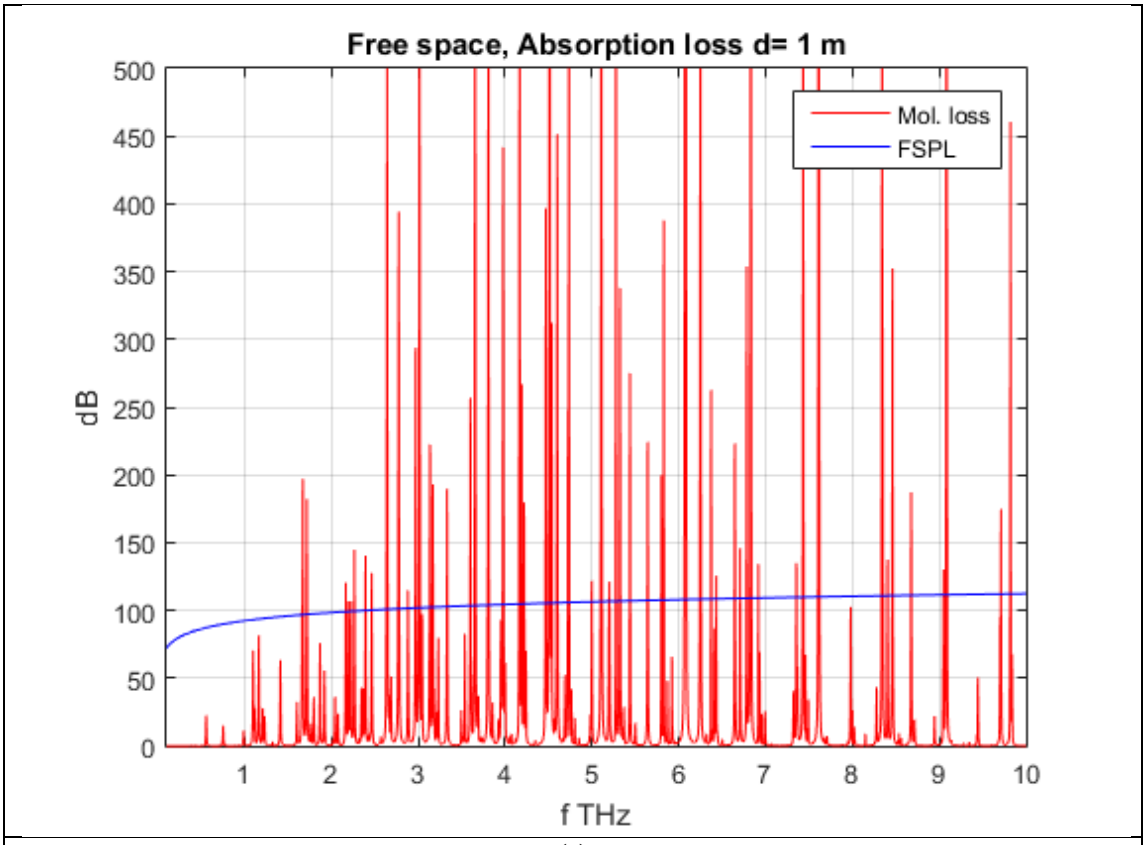
Free space, Absorption loss d= 1 m
Mol. loss
FSPL
dB
f THz
0
50
100
150
200
250
300
350
400
450
500
1
2
3
4
5
6
7
8
9
10

(a)

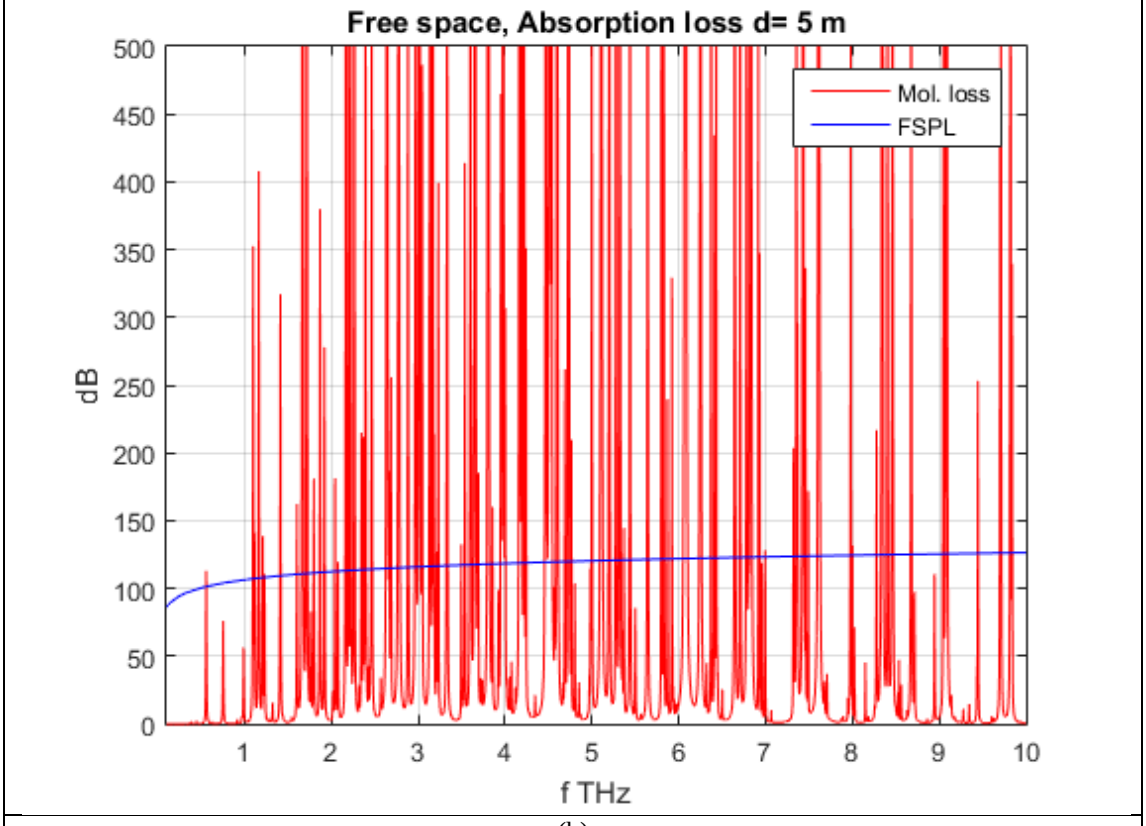
Free space, Absorption loss d= 5 m
Mol. loss
FSPL
dB
f THz
0
50
100
150
200
250
300
350
400
450
500
1
2
3
4
5
6
7
8
9
10

(b)

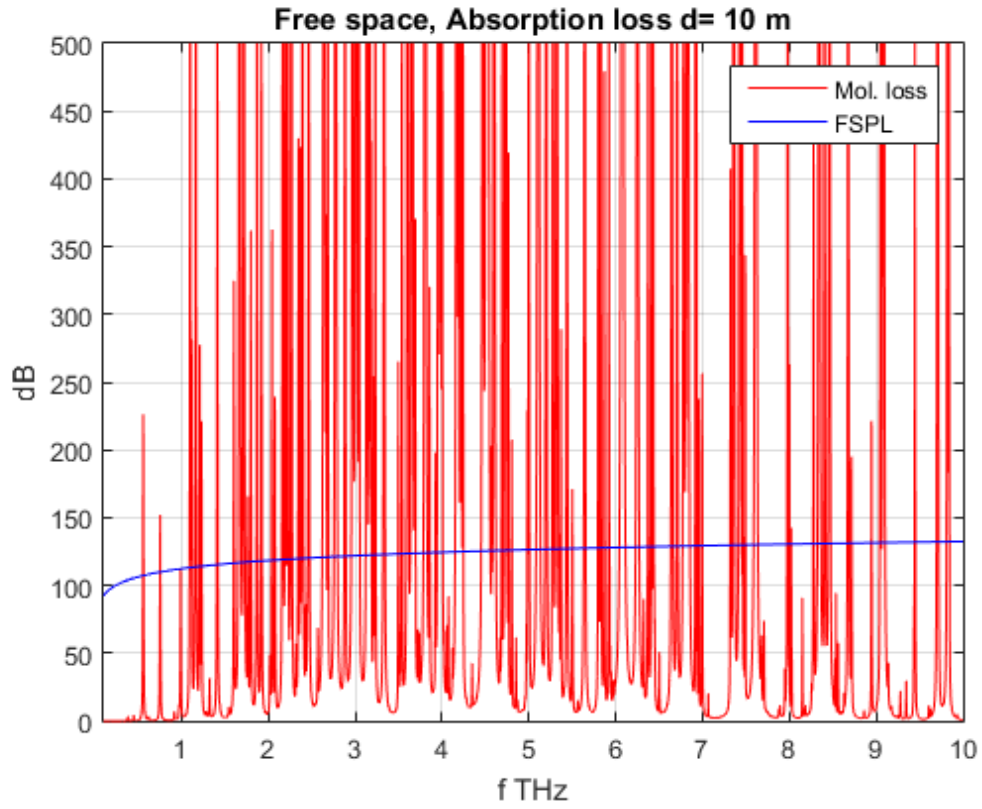

(c)

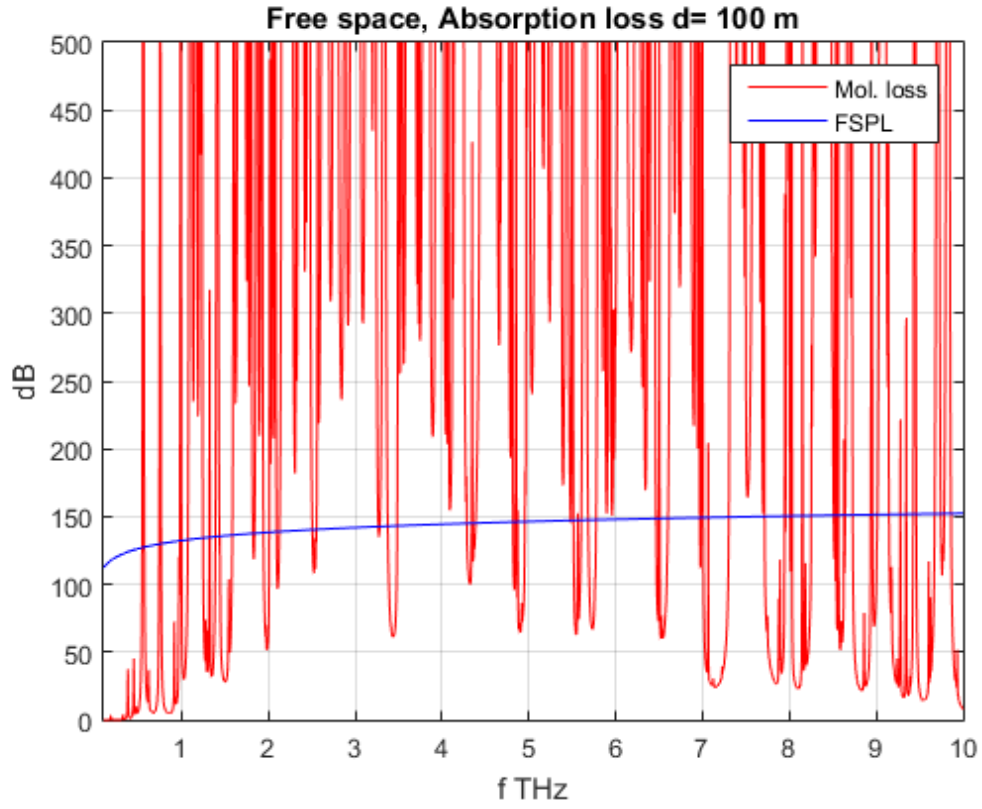

(d)

Figure 7. F.S.P.L & Molecular absorption loss in 0.1 -10THz. Using HITRAN database for p = 1atm, T_0 =296K, $v.m.r$ = 0.0138, d=[1,5,10,100].

Figures 6 (a) to (d) illustrate the FSPL and molecular absorption loss as a function of frequency and distance. Fig. 6 (a), verifies the fact that molecular loss is inversely proportional to transmittance (fig. 4 (a)). At link distance 1m, molecular loss is almost flat, when compared to FSPL. Some local maxima peaks of molecular loss appear within sub intervals of 0.5 - 0.6, 0.7 - 0.8 and 0.9 - 1 THz, but still FSPL dominates the losses. Next in fig. 4 (b) the previous intervals of molecular absorption peaks become wider occupying the entire aforementioned frequency regions and exceed FSPL, while peaks of absorption at different band regions, close to 0.4 THz and in the interval of 0.4-0.5 THz can be seen to emerge. In fig. 4 (c) as distance further increases to 100 m molecular loss at the intervals of 0.5-0.6, 0.7 - 0.8, 0.9 - 1 THz, reaches local maxima way exceeding the FSPL, while in meantime significant peaks in the rest of the spectrum appear. Finally from fig. 6 (d) beyond the frequency intervals, where the peaks exceeded FSPL in previous distances. New peaks at different frequency regions appear exceeding FSPL. Figures 7 (a) to (d) give similar results having high molecular absorption peaks along almost the entire 0.1 - 10 THz band. This agrees with the transmittance being close to zero above 1THz, as one moves further into the THz band. In general FSPL is already high, because of the THz frequencies. But what is very interesting, is that with the increase of distance molecular absorption loss at some frequencies takes very large values in the form of local maxima. This is due to its exponential increase, when FSPL increases by a square distance d^2 factor. The natural meaning of molecular absorption loss increase as link distance becomes wider, is that more absorbing molecules are present in the medium. Combining molecular and FSPL, total pathloss becomes much more severe.

2.1.4 Noise in THz frequencies

Up to this point it has been shown that molecules of the atmospheric medium cause attenuation to the propagating THz waves. As mentioned previously in this chapter different molecules resonate at different frequencies. Part of the energy absorbed by them following the preservation of energy theory is then re - radiated in the medium, at the same frequency as the absorption occurred. This effectively is a source of noise. The parameter that measures this phenomenon is called emissivity.

$$\varepsilon(f,d) = 1 - \tau(f,d) \tag{14}$$

This leads to a new source of noise temperature at the receiver antenna, when and only a transmission occurs. The molecular noise temperature.

$$T_{mol}(f,d) = T_A\varepsilon(f,d) = T_A(1 - \tau(f,d)) \text{ (K)} \tag{15}$$

Where T_A is the temperature of the ambient atmosphere (current work considers T_A=T_o=296K HITRAN reference temperature). An important observation is that molecular noise can have maximum temperature of T_A .The total noise temperature comprehended by the receiver is:

$$T_{noise}(f,d) = T_{sys} + T_{mol}(f,d) + T_{other}\ (K) \tag{16}$$

where T_{sys} is the receiver's electronics thermal noise temperature and T_{other} accounts for other noise sources.

$$T_{sys} = T_{ref}(NF - 1)(K) \quad (17)$$

Where T_{ref} is the reference temperature of the system (here T_{ref} =296 K), and NF the noise figure at the input of the receiver. Using the previous equations noise PSD and power are defined as.

$$Noise_{psd}(f, d) = k_B T_{noise}(f, d)(W/Hz) \quad (18)$$

$$Noise_{power}(f, d) = \int_B Noise_{psd}(f, d)df = k_B \int_B T_{noise}(f, d)df \quad (19)$$

where B stands for the used bandwidth around frequency f. In the case where no transmission takes place the receiver only detects AWGN noise.

2.2 Distance and frequency dependence of THz propagation

In the previous sections of this chapter fundamental equations regarding transmission in THz band were defined. This section tries to make clear the dependence between frequency and distance and the prohibitions they impose in the propagation of EM waves in this band. In particular the main concern is to evaluate the behavior of noise, since it is a fundamental criterion for any telecommunication system. From this point on a constant system noise temperature along the whole bandwidth of T_{sys}=300 K (NF=3dB) will be considered, along with the molecular noise temperature as it is expressed at different distances and frequencies. Other noise sources (T_{other}=0) will be neglected.

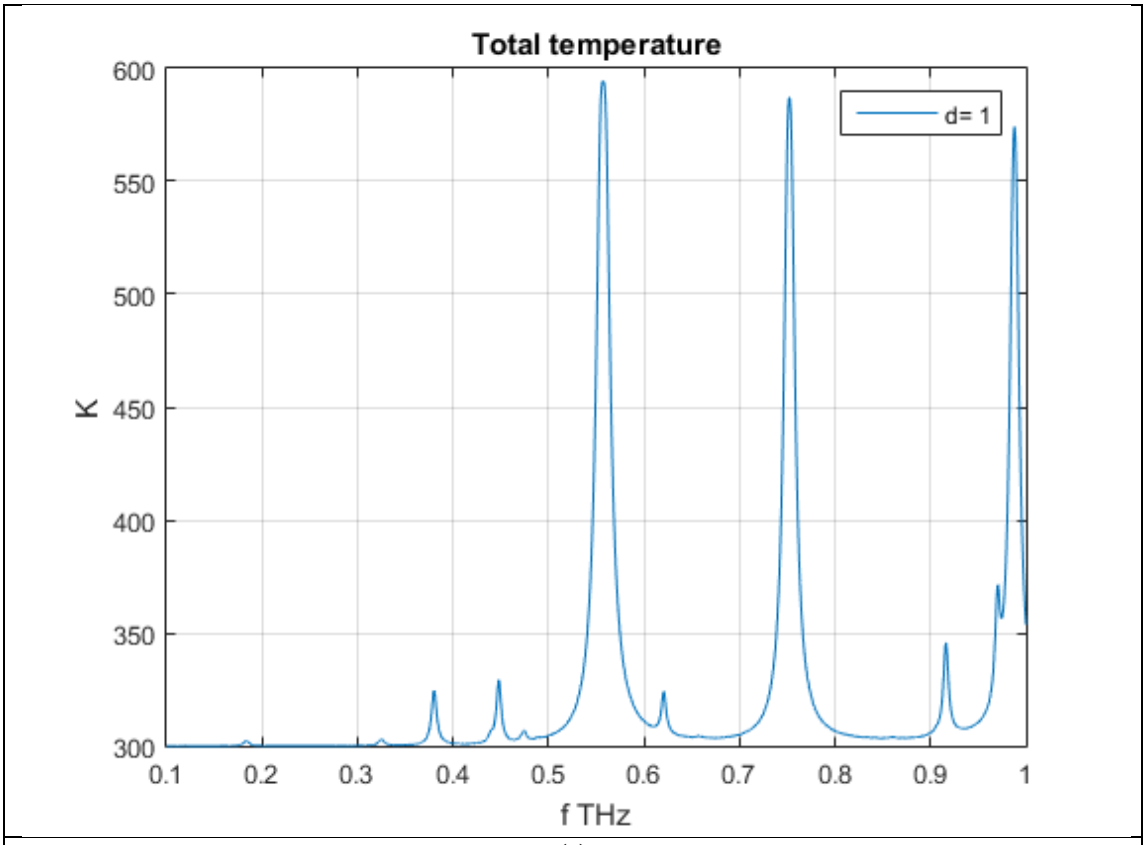
Total temperature
d= 1
K
f THz
600
550
500
450
400
350
300
0.1
0.2
0.3
0.4
0.5
0.6
0.7
0.8
0.9
1

(a)

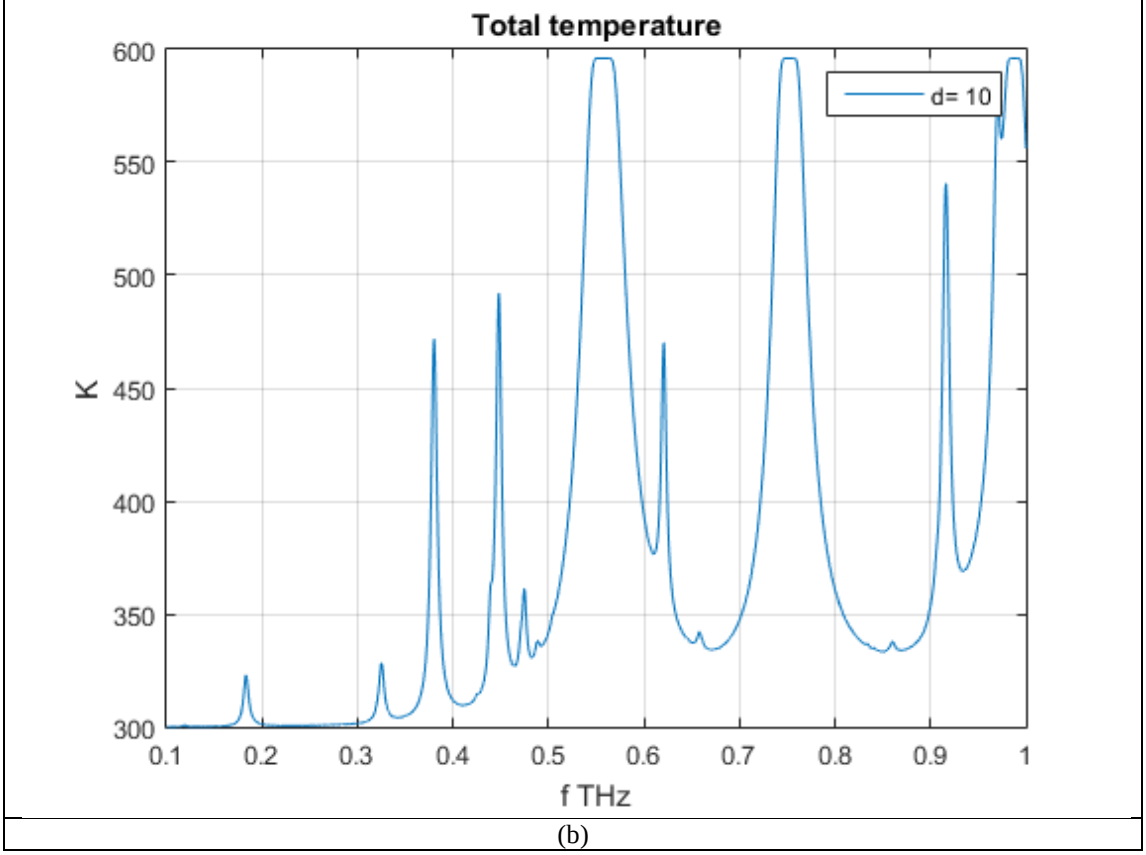
Total temperature
d= 10
K
f THz
600
550
500
450
400
350
300
0.1
0.2
0.3
0.4
0.5
0.6
0.7
0.8
0.9
1

(b)

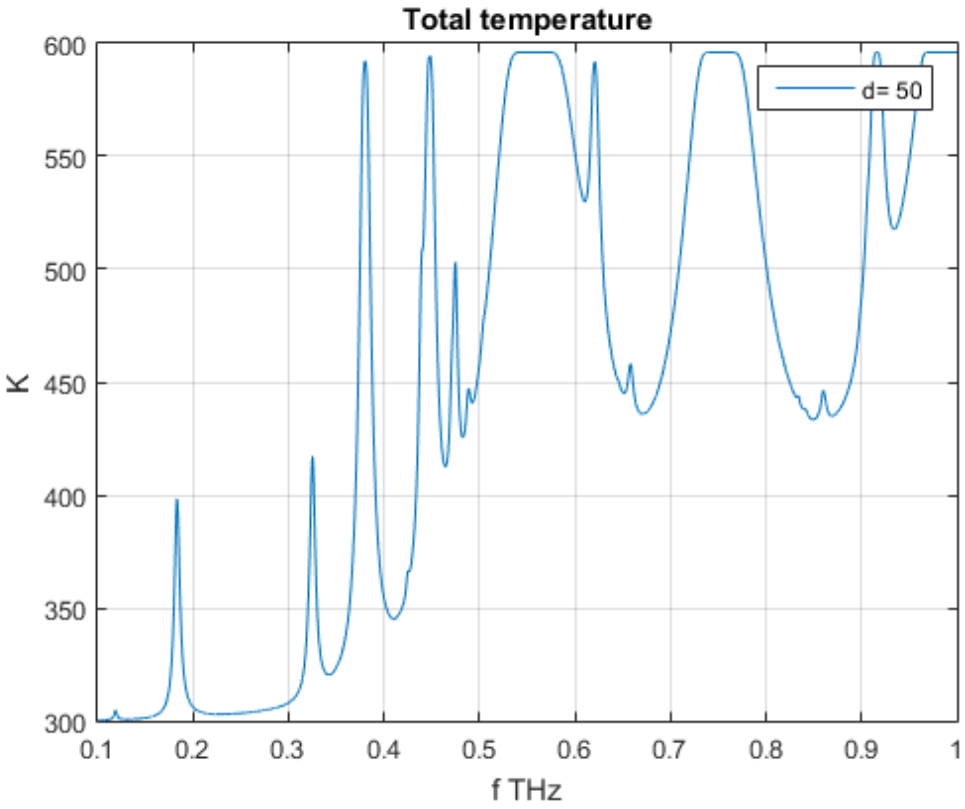

(c)

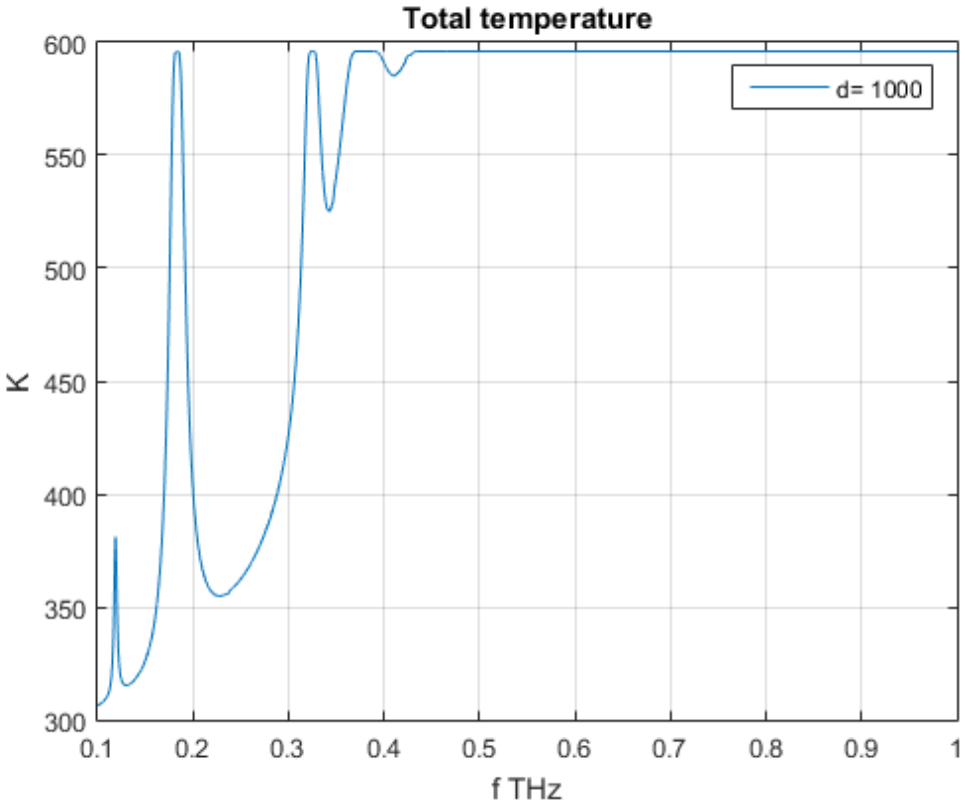

(d)

Figure 8. Total noise Temperature with 300K system noise in 0.1 -1THz. Using HITRAN database for p = 1atm, T_0 =296K, *v.m.r* = 0.0138, d=[1,10,50,1000].

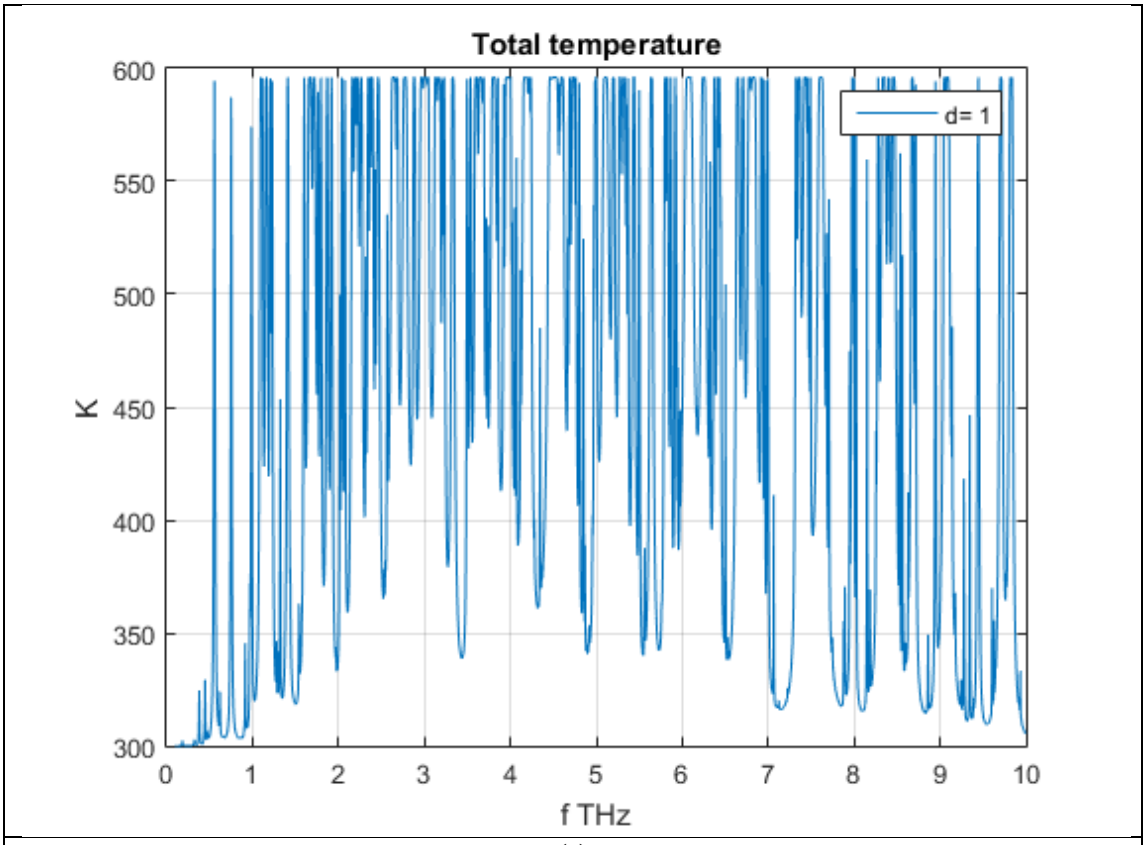
Total temperature
d= 1
K
f THz
600
550
500
450
400
350
300
0
1
2
3
4
5
6
7
8
9
10

(a)

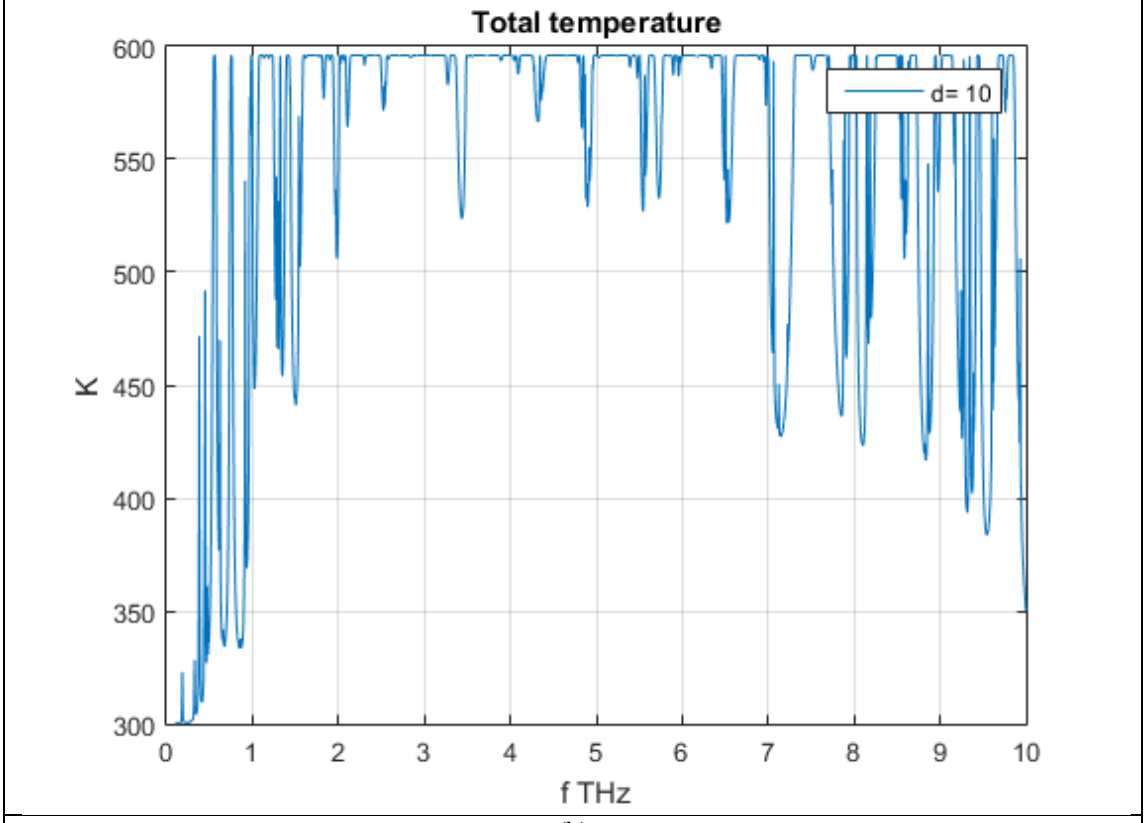
Total temperature
d= 10
K
f THz
600
550
500
450
400
350
300
0
1
2
3
4
5
6
7
8
9
10

(b)

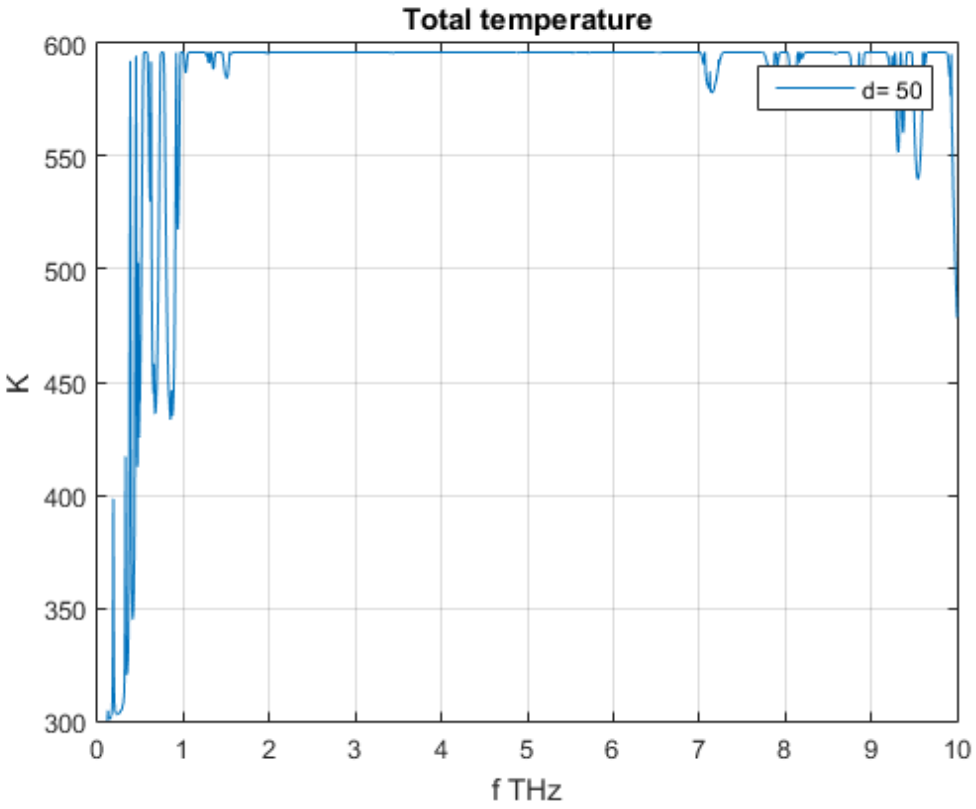

(c)

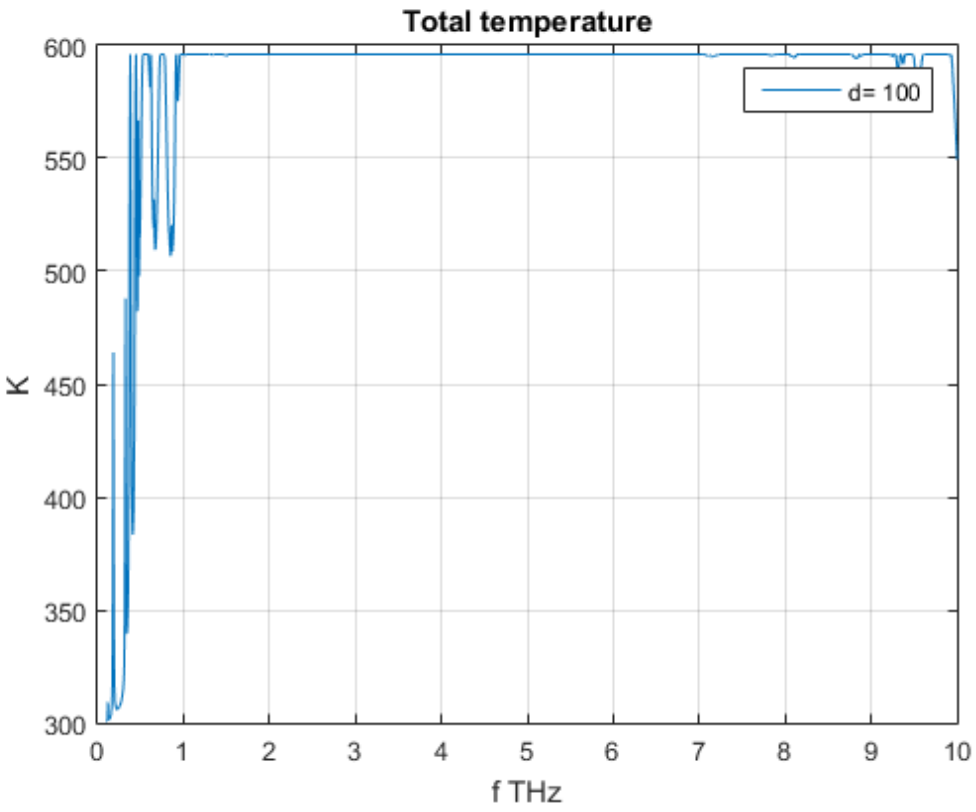

(d)

Figure 9. Total noise Temperature with 300K system thermal noise in 0.1 -10THz. Using HITRAN database for p = 1atm, T_0 =296K, *v.m.r* = 0.0138, d=[1,10,50,100].

Figures 8 and 9 illustrate the total noise temperature at the receiver as a function of frequency and distance (a constant thermal noise of 300 K is assumed, to get only molecular noise temperature subtract it from the total temperature). In fig. 8 (a) at frequency sub intervals belonging in the 0.5 - 0.6, 0.7 - 0.8, 0.9 - 1 THz peaks close to the upper bound of 600 K appear. In the rest of the spectrum temperature is below 350 K and in many occasions its value is almost flat. From fig. 8 (b) link distance increase to 10m, shows peaks reaching 600 K for wider ranges of the aforementioned intervals. In the meantime temperature peaks beyond 450 K appear close to 0.4, 0.6 and 0.9 THz and in the sub interval belonging to 0.4 - 0.5 THz. The frequency ranges where temperature can be considered flat are further reduced and temperature is higher. In fig. 8 (c) temperature reaches 600 K in wider regions of the aforementioned spectrum. Also new temperature peaks close to 400 K, near 0.2 THz appear. Again the spectrum where temperature is flat is further reduced and temperature is higher. In fig. 8 (d) for the link distance of 1km temperature reaches the upper bound in the entirety of the bandwidth and is only below 400 K in the lower spectrum till 0.3 THz. From fig. 9 (a) for frequencies above 1 THz peaks close to the upper bound of 600 K appear along the entire bandwidth. Yet also local minima below 400 K can be observed in the interval of 1 - 10 THz. Fig. 9 (b) indicates that increasing link distance to 10m temperature exceeds 500 K almost in the entire region of 2-7 THz, while spectrum regions with almost flat temperature are further reduced and their temperature is close to 450 K. This distance related temperature increase is more evident at fig. 9 (c), (d) having link distances 50, 100 m respectively. There temperature reaches the upper bound in the entire spectrum beyond 1 THz.

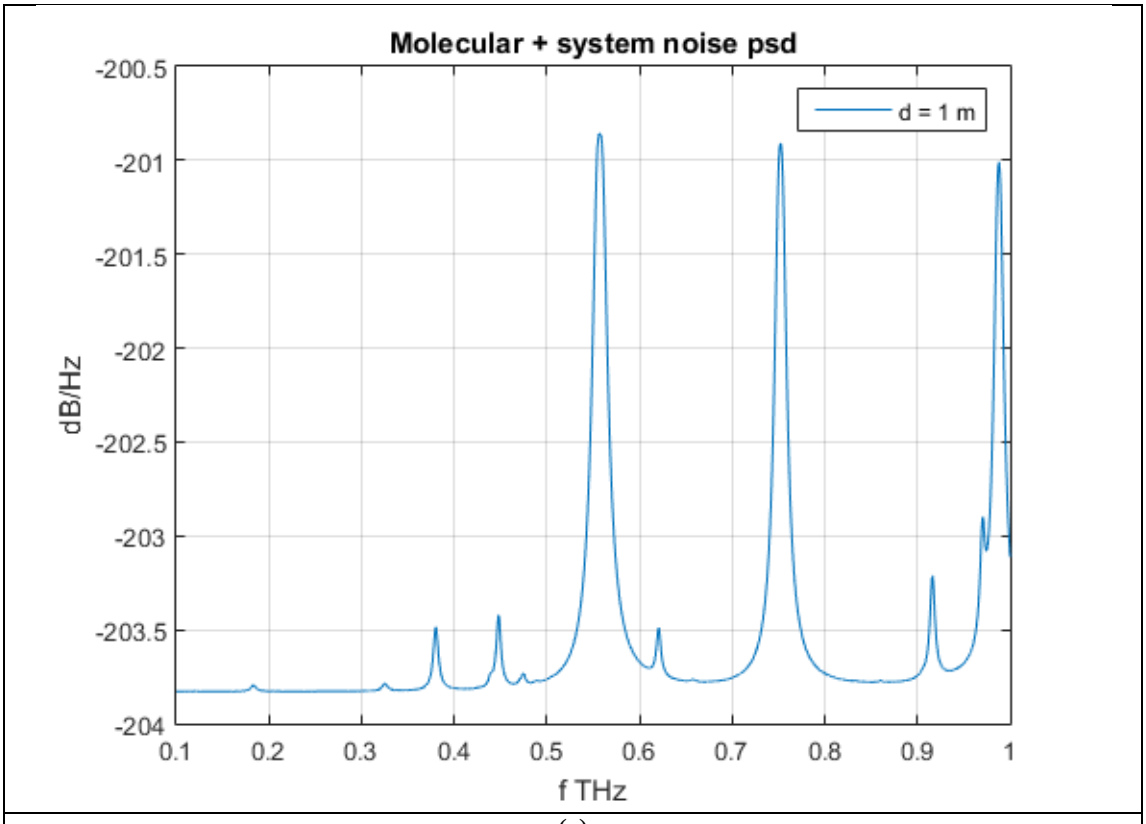

(a)

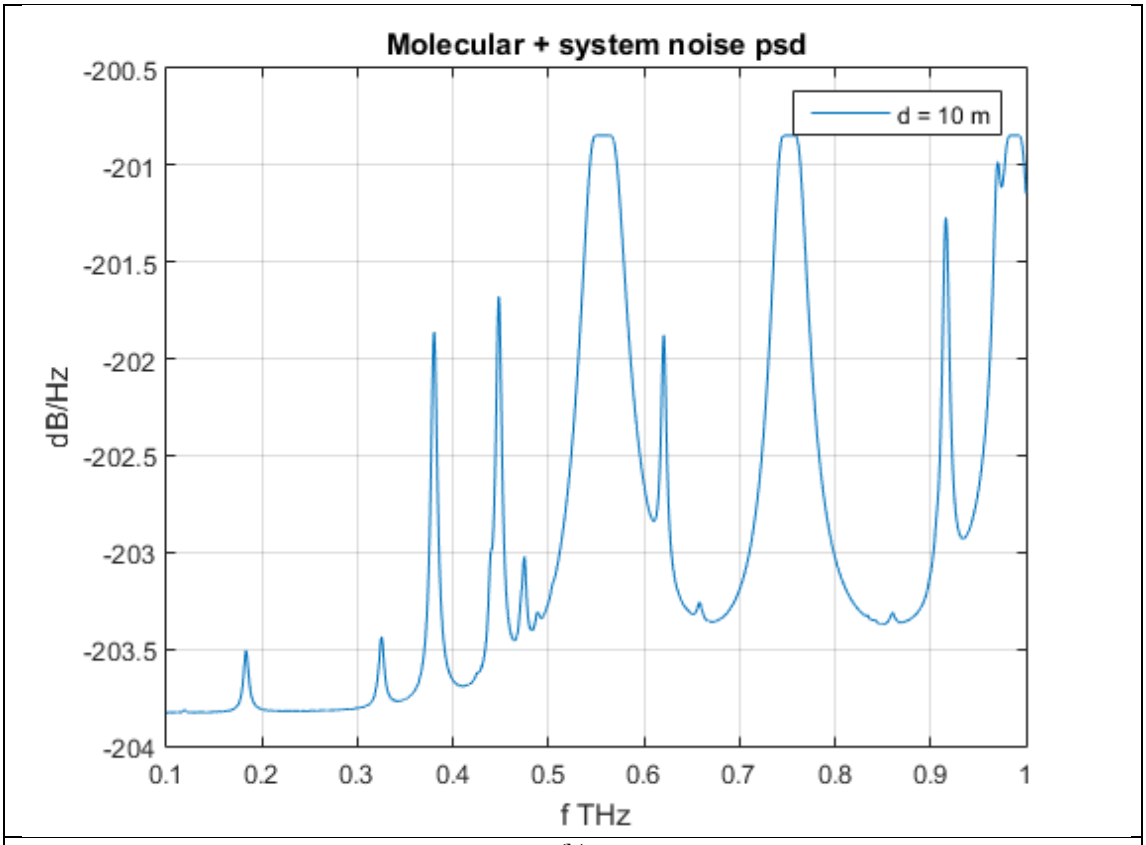
Molecular + system noise psd
d = 10 m
dB/Hz
f THz
-200.5
-201
-201.5
-202
-202.5
-203
-203.5
-204
0.1
0.2
0.3
0.4
0.5
0.6
0.7
0.8
0.9
1

(b)

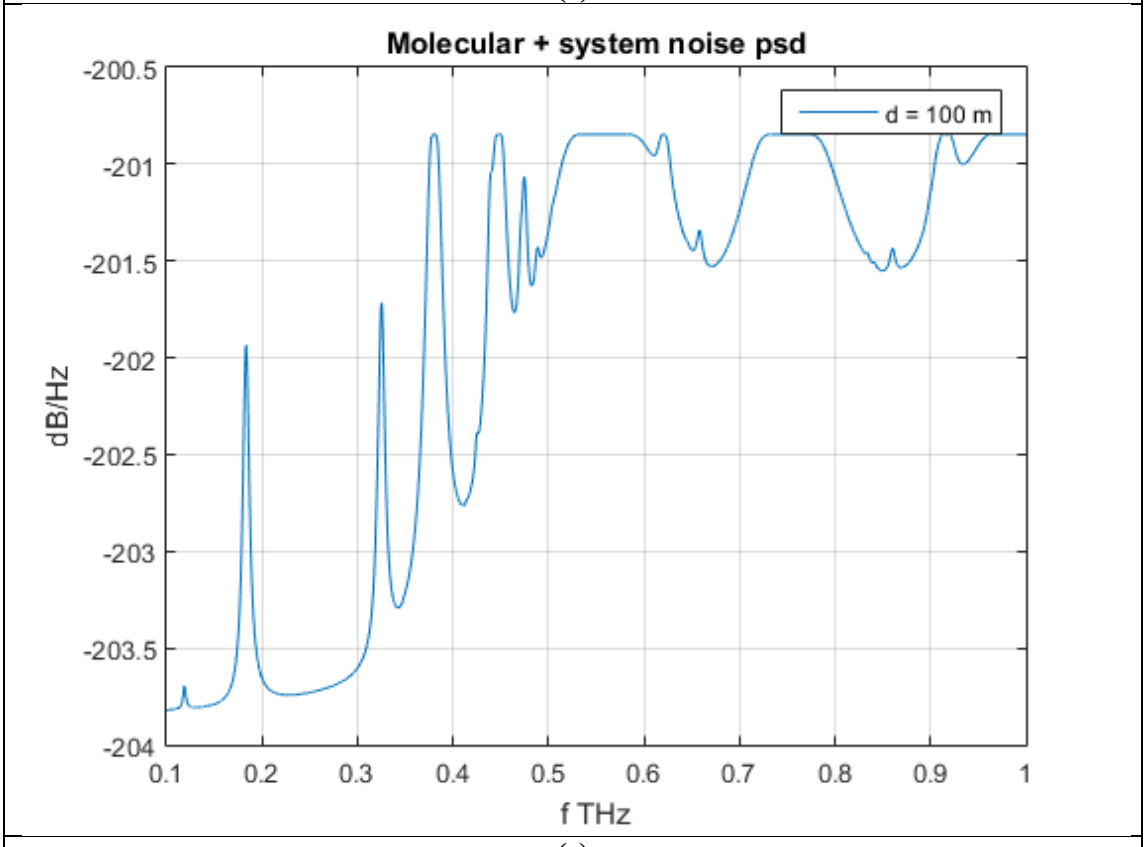
Molecular + system noise psd
d = 100 m
dB/Hz
f THz
-200.5
-201
-201.5
-202
-202.5
-203
-203.5
-204
0.1
0.2
0.3
0.4
0.5
0.6
0.7
0.8
0.9
1

(c)

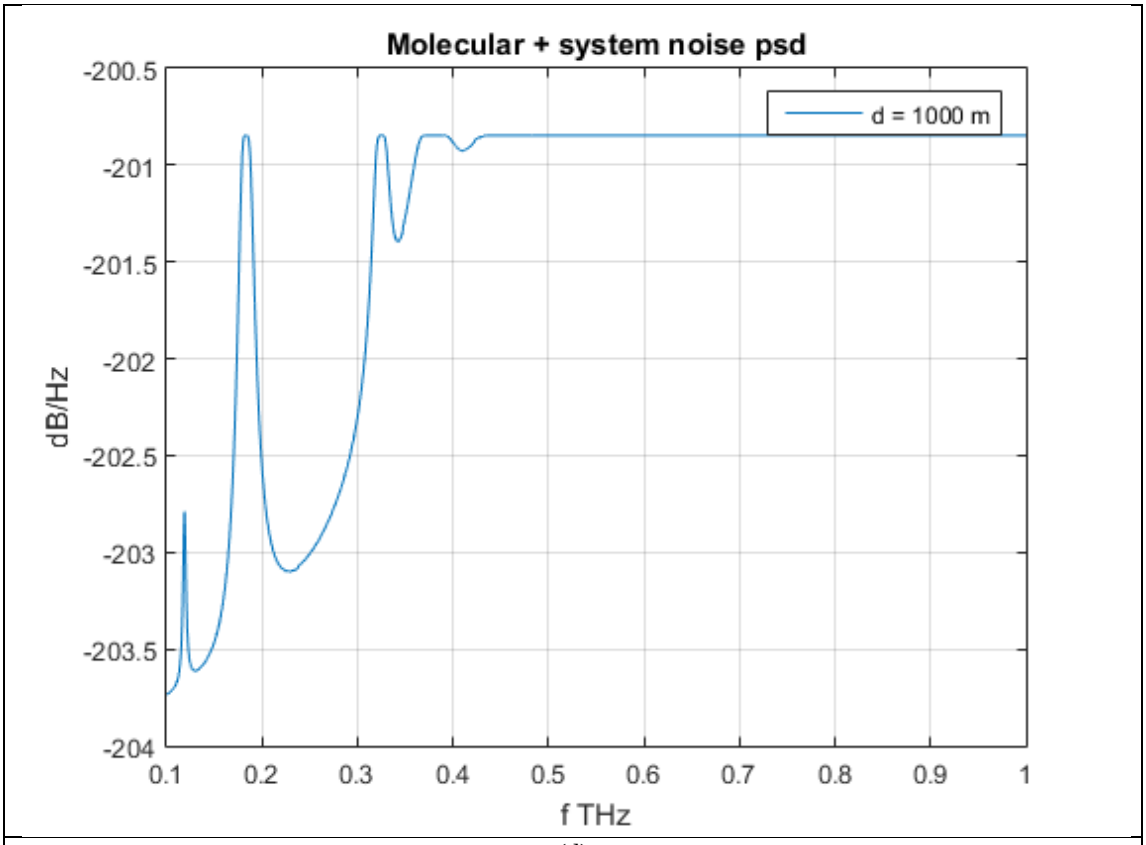

(d)

Figure 10. Noise PSD with 300K system thermal noise in 0.1 -1THz. Using HITRAN database for p = 1atm, T_0 =296K, $v.m.r$ = 0.0138, d=[1,10,100,1000].

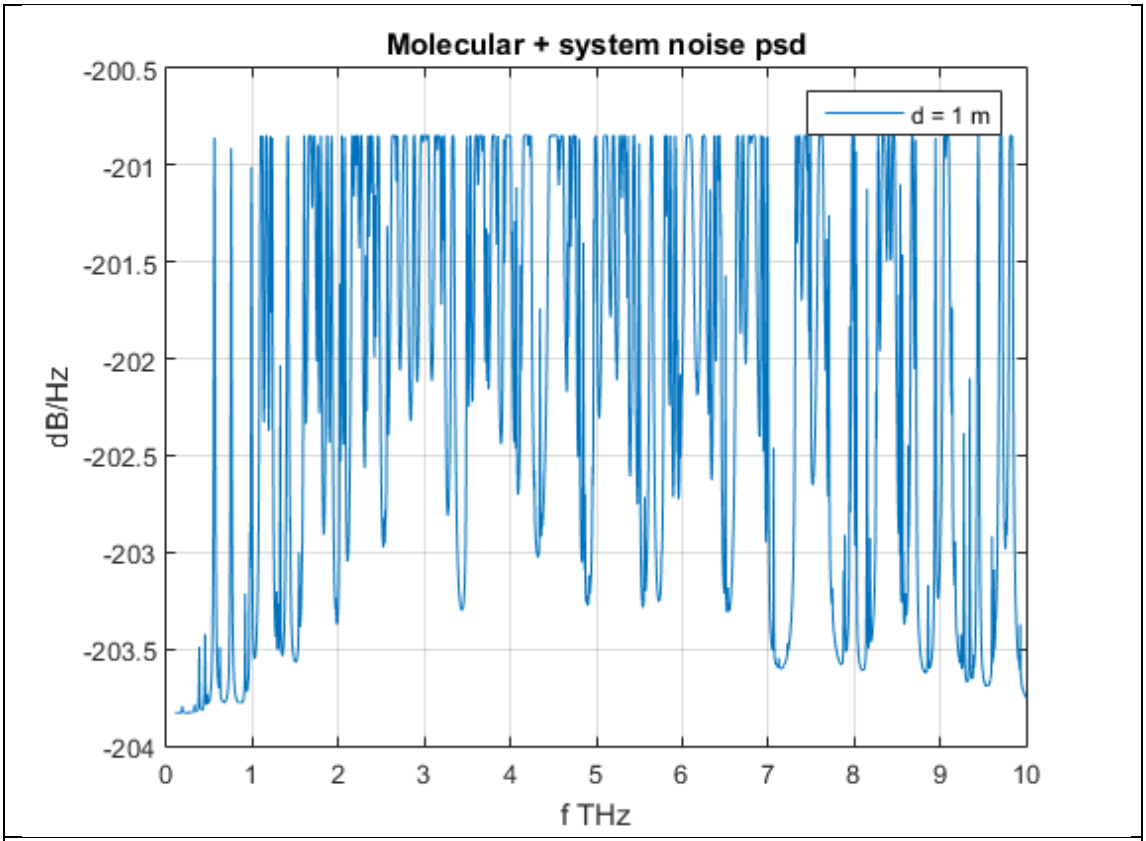

(a)

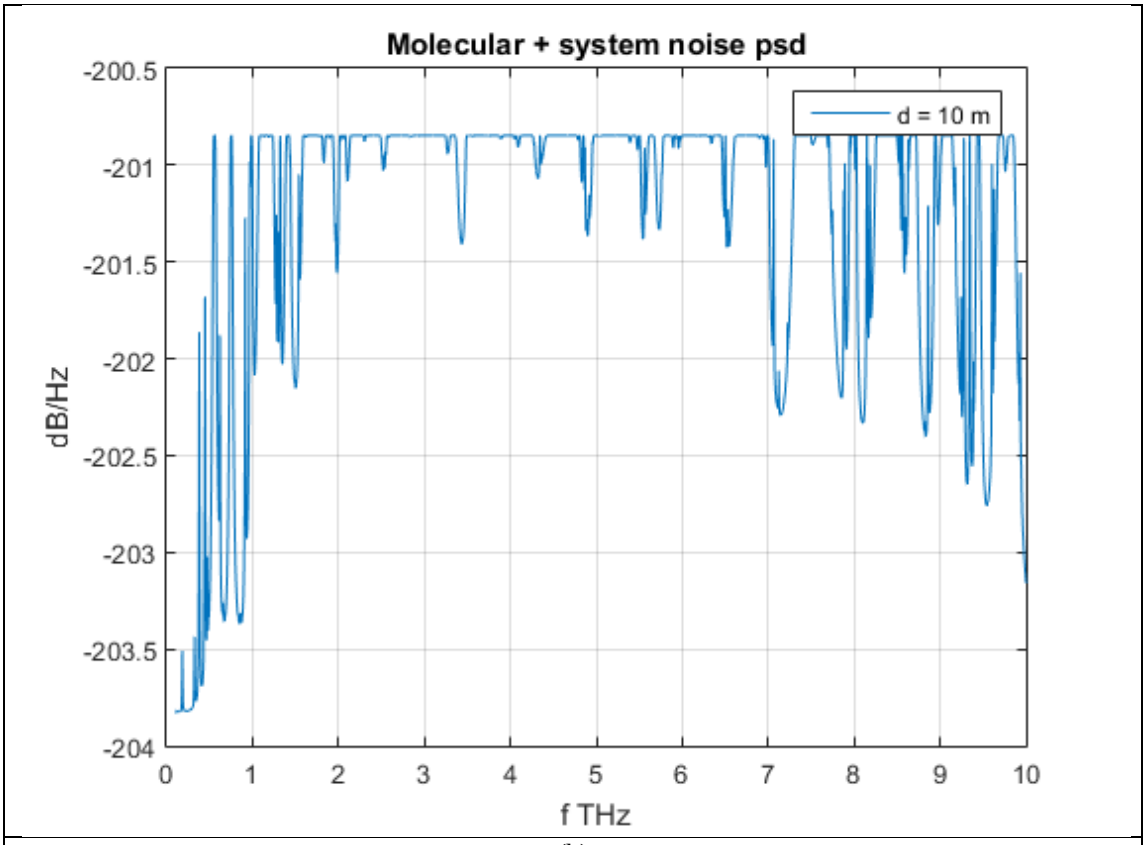
Molecular + system noise psd
d = 10 m
dB/Hz
f THz
-200.5
-201
-201.5
-202
-202.5
-203
-203.5
-204
0
1
2
3
4
5
6
7
8
9
10

(b)

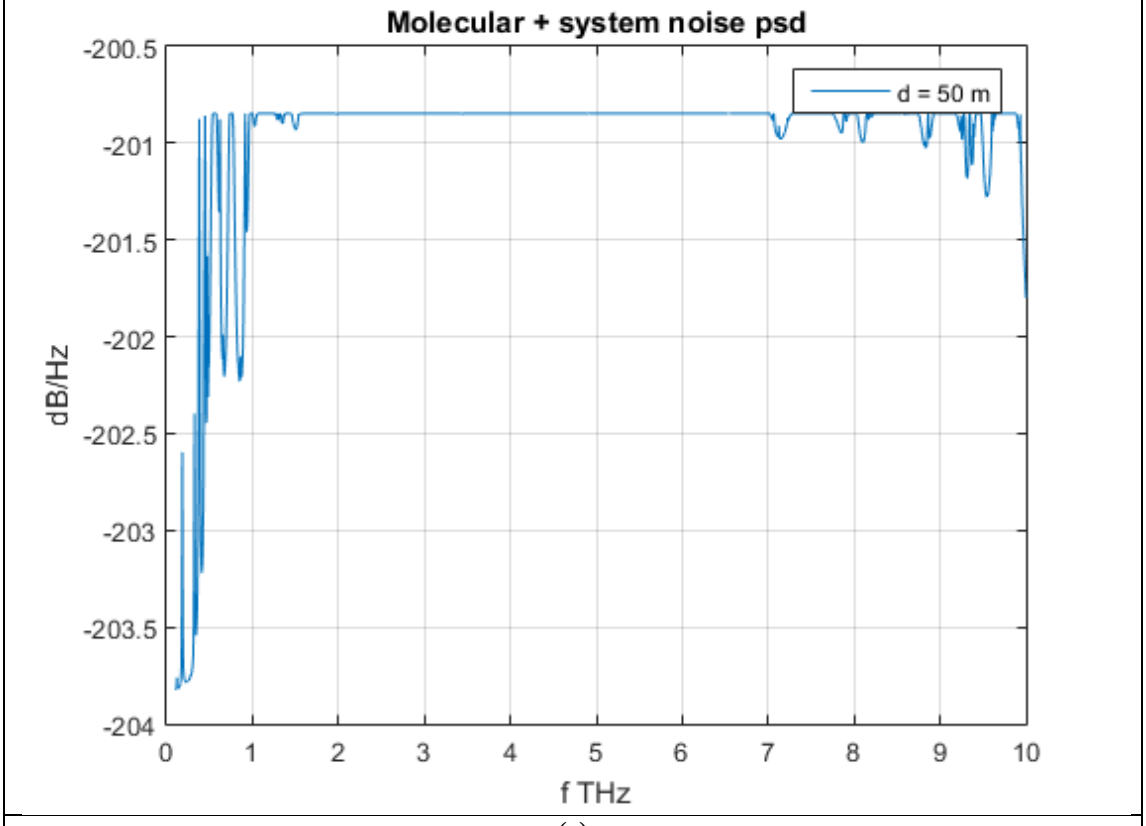
Molecular + system noise psd
d = 50 m
dB/Hz
f THz
-200.5
-201
-201.5
-202
-202.5
-203
-203.5
-204
0
1
2
3
4
5
6
7
8
9
10

(c)

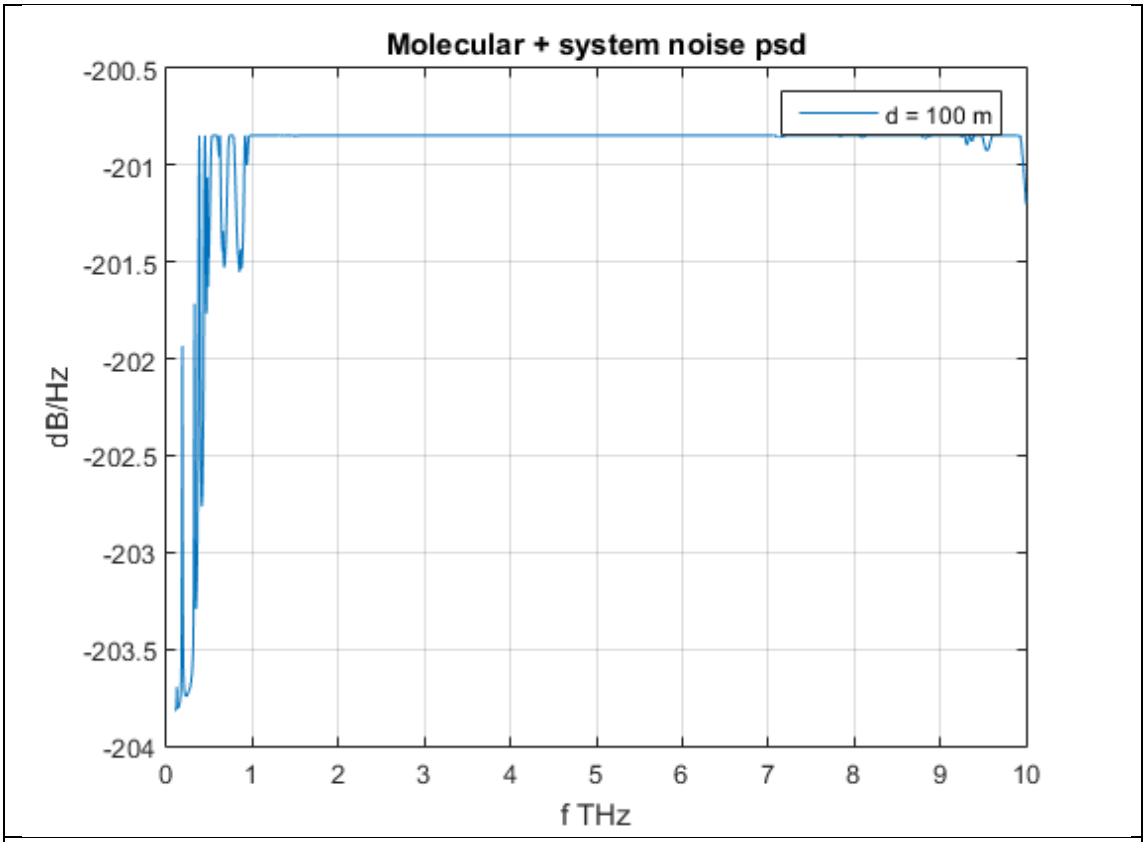

(d)

Figure 11. Noise PSD with 300K system thermal noise in 0.1 -10THz. Using HITRAN database for p = 1atm, T_0 =296K, $v.m.r$ = 0.0138, d=[1,10,50,100].

From figures 10,11 and equation (18) the linear dependency of noise PSD from temperature is evident. Maximum values of noise are obtained at the same frequency intervals as where temperature takes its maximum values. It should noted that molecular noise and generally the total noise in THz band transmissions is colored, since several peaks are present along the bandwidth.

2.3 A simplified model for THz pathloss in 275-400 GHz region

Considering the previous paragraphs describing THz channel model is obvious that calculating absorption coefficient, using HITRAN parameters, is cumbersome involving many complicated equations. In order to overcome this, efforts to create models calculating gaseous attenuations have been developed. Such a model is ITU-R P.676-8 [29] covering the region up to 1000 GHz, but as commented in [6] has some validity issues. On the other hand the novel model of molecular absorption loss in the region of 275 - 400 GHz, firstly presented in [6] yields results almost similar to those obtained using HITRAN database proving its validity. Next the channel model for this frequency range as described in [6], [23] is presented. The channel model utilized consists of the free space and molecular absorption gain, the total path gain is

$$L(f,d) = L_f L_a \tag{20}$$

where L_f , L_a respectively represent the free space and molecular absorption path gains. Note that eq. (13), (20) model total pathloss, the reason eq. (20) is called total path gain is because the gains of the transmit and receive antennas are taken into

account. The free space path gain is evaluated by radially expanding the wavefront adjusted with the transmitter and receiver antenna gains as

$$L_f(f,d) = \frac{c^2}{(4\,\pi\, f\, d)^2} G_t(\Theta_i) G_r(\Theta_r) \tag{21}$$

where $G_t(\Theta_i)$, $G_r(\Theta_r)$ are the transmitter and receiver antenna gains respectively and c is the speed of light in vacuum. It should be noted that antenna gains usually depend on the angles of incident Θ_i , Θ_r and reception. Current work assumes that the beams of transmitter and receiver are perfectly aligned, getting $G_t(\Theta_i) = G_t$, $G_r(\Theta_r) = G_r$. As stated before the current absorber of EM wave energy at THz band transmissions is the atmospheric water vapor, which dominates the loss above 200 GHz. In order to evaluate the molecular absorption loss in the 275 - 400 GHz band a simplified model for molecular absorption due to water vapor is utilized. This model was initially presented in [6]. According to this model absorption coefficient can be obtained as

$$k_a(f) = y_1(f,\mu) + y_2(f,\mu) + g(f) \tag{22}$$

and using eq. (9), (22) the molecular absorption gain is estimated as

$$L_a(f,d) = \exp(-d(y_1(f,\mu) + y_2(f,\mu) + g(f))) \tag{23}$$

where μ denotes the volume mixing ratio of water vapor. Water vapor should be conflicted with relative humidity and is given by

$$\mu = \frac{\varphi}{100} \frac{p_w^*(T,p)}{p} \tag{24}$$

where φ, p respectively stand for the relative humidity as a percentage and atmospheric pressure in hPa. Whereas the saturated water vapor partial pressure $p^*_w(T,p)$ at temperature T can be calculated according to the Buck equation [28]. The parameters of eq. (23) are

$$y_1(f,\mu) = \frac{A(\mu)}{B(\mu) + \left(\frac{f}{100c} - c_1\right)^2} \tag{25}$$

$$y_2(f,\mu) = \frac{C(\mu)}{D(\mu) + \left(\frac{f}{100c} - c_2\right)^2} \tag{26}$$

$$g(f) = p_1 f^3 + p_2 f^2 + p_3 f + p_4 \tag{27}$$

where c_1=10.835 cm^{-1} , c_2=12.664 cm^{-1} , p_1=5.54 x 10^{-37} Hz^{-3} , p_2=-3.94 x 10^{-25} Hz^{-2} , p_3=9.06 x 10^{-14} Hz^{-1} , p_4= -6.36 x 10^{-3}

and

$$A(\mu) = 0.2205\mu(0.1303\mu + 0.0294) \tag{28}$$

$$B(\mu) = (0.4093\mu + 0.0925)^2 \tag{29}$$

$$C(\mu) = 2.014\mu(0.1702\mu + 0.0303) \quad (30)$$

$$D(\mu) = (0.537\mu + 0.0956)^2 \quad (31)$$

This model was shown [6] to be very accurate to distances up to 1 km in standard atmospheric conditions (temperature 296 K and air pressure 1 atm). Also it is obvious from eq. (24) that this model can describe molecular absorption pathloss at conditions beyond of the standard. Additionally it should be noted that c_1, c_2 , p_1, p_2, p_3, p_4 , are considered relatively independent of the atmospheric conditions [6]. At this point based on eq. (20), (21), (23) the total path gain is rewritten as

$$L(f,d) = \frac{c^2}{(4\,\pi\,d\,f)^2} G_t G_r \exp(-d(y_1(f,\mu) + y_2(f,\mu) + g(f))) \quad (32)$$

From eq. (32) it is obvious that total path gain depends not only on distance and frequency but also on the transceivers gains and atmospheric conditions.

3 Fundamental performance evaluation

In the previous chapter path loss and noise mechanisms of THz EM waves where introduced. Having this knowledge metrics of spectral efficiency, capacity and theoretical SER (Symbol Error Rate) can be calculated. Using these a preliminary idea is acquired regarding the available bandwidths and possible distances that can be used for transmissions in THz band.

3.1.1 Spectral efficiency and capacity

$$C_i(d) = Df_i * log_2(1 + \frac{S(f_i)A(f_i,d)^{-1}}{N_{psd}(f_i,d)}) \text{ (bps)} \quad (33)$$

$$i \in [1, N], Df_i \leq B$$

Capacity of *i-th* sub band at distance d, around center frequency f_i , with bandwidth Df_i. The total available spectrum *B* is divided to *N* smaller bands, whose bandwidth cannot exceed that of *B*. $S(f_i)$ is the transmitted signal PSD allocated to f_i. If the sub band bandwidth is adequately small the channel can be assumed to appear as frequency non selective and noise can be considered as locally flat [1]. So the assumption of AWGN noise can be used.

$$C_{eff_i}(d) = log_2(1 + \frac{S(f_i)A(f_i,d)^{-1}}{N_{psd}(f_i,d)}) \text{ (bps/Hz)} \quad (34)$$

Spectral efficiency at distance *d* of frequency f_i belonging to *i-th* sub band of bandwidth Df_i .

3.1.2 Symbol error rate

$$P_{b(BPSK)}(f_i, d) = Q(\sqrt{2SNR_{bit}(f_i, d)}) \quad (35)$$

$$P_{s(QPSK)}(f_i, d) = 2Q\left(\sqrt{2SNR_{bit}(f_i, d)}\right) - Q^2(\sqrt{2SNR_{bit}(f_i, d)}) \quad (36)$$

$$SNR(f_i, d) = \frac{E_{s_{rx}}(f_i,d)}{N_o(f_i,d)} = \frac{E_s\, A(f_i,d)^{-1}}{k_B\, T_{noise}(f_i,d)} \quad (37)$$

$$SNR_{bit}(f_i, d) = \frac{SNR(f_i,d)}{k} \quad (38)$$

$$k = log_2(M) \quad (39)$$

$$i \in [1, N], Df_i \leq B$$

Equations (35), (36) respectively give the theoretical SER of BPSK, QPSK modulations per center frequency f_i of the *i-th* sub band having bandwidth *Dfi*. E_s is the transmitted signal power allocated to the bandwidth of the *i-th* sub band. The total available bandwidth is divided to *N* smaller sub bands, whose bandwidth cannot exceed the total. The received SNR per bit at *i-th* sub band having center frequency f_i at distance *d* is given by dividing the total SNR at this frequency with the number of

bits k belonging to the used constellation (M is the modulation order). If the sub bands bandwidth is adequately small the channel can be assumed to appear as frequency non selective and the noise can be regarded as locally flat. So the assumption of AWGN noise can be used.

3.2 Transmission windows

Molecular absorption loss is a function of both frequency and distance. At close link distances and lower frequencies, is small enough that it could be negligible. But as distance and frequency increase it can take very large values. Also molecular noise is highly frequency selective colored noise presenting several peaks in spectrum (figures 10,11).Furthermore water vapor as commented earlier is the major absorber of EM wave energy in THz, making it the greatest contributor to molecular absorption loss. This implies that THz links are prone to weather and environmental conditions. Different seasons and regions of the globe represent various atmospheric water concentrations which become more complicated if fog or rain are present, incrementing further the loss. Making it practically impossible to transmit signals using the entire frequency region. To overcome this, parts of the total available bandwidth must be selected, known as transmission windows. These windows are selected with the intention to minimize path loss and make signal transmission by THz possible. Depending on the application and its performance criteria, there is a variety of features and thresholds that can be used to locate those frequency bands. For example at a great distance (e.g. 1Km), the desired performance of a system could be to achieve an upper bound of BER (Bit Error Rate). This threshold depends on the molecular absorption loss at this distance and the SNR needed for the receiver to recognize that a transmission occurred. Another scenario could be interested in high throughputs, meaning it needs transmission windows with as low as possible molecular absorption loss, while in the meantime having great bandwidth. As there are a great number of parameters and possibilities regarding transmission window selection. Current work focuses only in locating frequency bands where molecular absorption loss takes its minimum value. This is done to begin initial research for transmission windows and also because total noise and molecular absorption loss both depend on the transmittance (see equations (10),(18)). To locate a window in the total available bandwidth at distance d , firstly the local minima of molecular absorption loss must be located. Then a threshold of x dB is defined and one should move (left and right) around a local minimum by this value to extract a transmission window.

3.3 Available bandwidth sub band division

To properly evaluate the performance using the metrics defined above they should not be calculated only for the center frequency of a used bandwidth but for all belonging in it. To simulate all frequencies, bandwidth is divided to N smaller sub bands of bandwidth Df_i , where absorption coefficient is assumed to be constant. These smaller bands have small enough bandwidth in order to assume frequency non selective noise (the noise PSD can be considered flat). This is crucial in order to employ the metrics. In addition, absorption coefficient at a frequency f is derived from HITRAN database

for a discrete set frequencies. Using these, metrics for all infinite frequencies can be calculated since they definitely belong to a sub band. To better understand this concept an example follows. Assume a vector of N absorption coefficient samples $k_i(f_i) \in [k(f_1),...,k(f_N)]$ and the matching frequency vector $f_i \in [f_1,...,f_N]$ having bandwidth $B = f_N - f_1$, then for N = 10. Sub bands are as in Table 2.

# of band *i*	Sub band limits	Absorption coefficient $k_i(f_i)$	Bandwidth Df_i (Hz)
1	$[f_1 , (f_1 + f_2)/2]$	$k(f_1)$	$(f_1 + f_2)/2 - f_1$
2	$[(f_1 + f_2)/2 , (f_2 + f_3)/2]$	$k(f_2)$	$(f_2 + f_3)/2 - (f_1 + f_2)/2$
3	$[(f_2 + f_3)/2 , (f_3 + f_4)/2]$	$k(f_3)$	$(f_3 + f_4)/2 - (f_2 + f_3)/2$
4	$[(f_3 + f_4)/2 , (f_4 + f_5)/2]$	$k(f_4)$	$(f_4 + f_5)/2 - (f_3 + f_4)/2$
5	$[(f_4 + f_5)/2 , (f_5 + f_6)/2]$	$k(f_5)$	$(f_5 + f_6)/2 - (f_4 + f_5)/2$
6	$[(f_5 + f_6)/2 , (f_6 + f_7)/2]$	$k(f_6)$	$(f_6 + f_7)/2 - (f_5 + f_6)/2$
7	$[(f_6 + f_7)/2 , (f_7 + f_8)/2]$	$k(f_7)$	$(f_7 + f_8)/2 - (f_6 + f_7)/2$
8	$[(f_7 + f_8)/2 , (f_8 + f_9)/2]$	$k(f_8)$	$(f_8 + f_9)/2 - (f_7 + f_8)/2$
9	$[(f_8 + f_9)/2 , (f_9 + f_{10})/2]$	$k(f_9)$	$(f_9 + f_{10})/2 - (f_8 + f_9)/2$
10	$[(f_9 + f_{10})/2 , f_{10}]$	$k(f_{10})$	$f_{10} - (f_9 + f_{10})/2$
			$\boldsymbol{Sum(Df_i)=B}$

Table 2. N=10 samples of $k(f)$. In each sub band $k(f)$ is constant. The summand of subband bandwidths is equal to the total used bandwidth B.

4 Performance evaluation of THz wireless systems operating in 0.1 - 1 THz band

4.1 Assumptions

In this section the results of applying the metrics described in chapter 3 are discussed. For spectral efficiency and capacity total transmit power of 10 mW is assumed. Power is then allocated to the used spectrum considering a flat transmission power allocation scheme. This is accomplished by diving the signal power with the used bandwidth yielding signal PSD at frequency f, $S_o(f)$ = 10 (mW) / B_{used} (Hz) (B_{used} is the bandwidth used for transmissions). In the case of SER calculations symbol energy of E_s=10mW is considered and a single symbol is transmitted per sub-band. Additionally SER will be calculated only for BPSK and QPSK constellations, since total losses yield low SNR making the use of higher order modulations at this point impossible. Current work deploys the metrics considering SISO system with omnidirectional transceivers in LOS path. No gain is assumed for the antennas and no transmit or receive beam forming is employed. Furthermore each transmission is independent from another meaning that they are not interfering. To apply the metrics HITRAN database [10] was queried for all wavenumbers (1/wavelength) in the interval [3.33 , 33.3] cm^{-1} ([0.1, 1] THz) for the most common atmospheric molecules, particularly H_2O, CO_2, N_2O, CO, CH_4, O_2, N_2 (hitran molecular ids: 1,2,4,5,6,7,22) and environment conditions of air temperature T=296 K, pressure p=1atm, $v.m.r$=0.0138 (50 % relative humidity). Datasets were provided by university of OULU. Using these data and the method described in chapter 3.3 a sub-band's bandwidth can be either 0.1 or 0.05 GHz.

4.2 Transmission windows

Transmission windows are located around the local minima of molecular absorption loss for a threshold of 3dB. Distances for which transmission windows are extracted are 1, 10, 100, 1000 m. The tables below give the lower and upper frequency of a window followed by its bandwidth in GHz.

window	f_{min} [THz]	f_{max} [THz]	BW [GHz]
1	0,1	0,5488	448,8
2	0,5656	0,7457	180,1
3	0,7587	0,9825	223,8

Table 3. Transmission windows 0.1 - 1THz, of molecular absorption loss at d=1m, T_0=296K, p = 1atm, $v.m.r$ = 0.0138.

window	f_{min} [THz]	f_{max} [THz]	BW [GHz]
1	0,1	0,3785	278,5
2	0,3816	0,4459	64,3
3	0,4497	0,5317	82
4	0,582	0,7333	151,3
5	0,6213	0,7314	110,1
6	0,7744	0,9126	138,2
7	0,9191	0,9642	45,1
8	0,7634	0,978	214,6

Table 4. Transmission windows 0.1 - 1THz, of molecular absorption loss at d=10m, T_0=296K, p = 1atm, $v.m.r$ = 0.0138.

window	f_{min} [THz]	f_{max} [THz]	BW [GHz]
1	0,1	0,182	82
2	0,1845	0,3229	138,4
3	0,3267	0,37	43,3
4	0,3897	0,435	45,3
5	0,4559	0,4712	15,3
6	0,4766	0,5035	26,9
7	0,6008	0,6155	14,7
8	0,6311	0,7056	74,5
9	0,805	0,8999	94,9
10	0,9257	0,9474	21,7
11	0,9734	0,9755	2,1

Table 5. Transmission windows 0.1 - 1THz, of molecular absorption loss at d=100m, T_0=296K, p = 1atm, $v.m.r$ = 0.0138.

window	f_{min} [THz]	f_{max} [THz]	BW [GHz]
1	0,1	0,1734	73,4
2	0,1932	0,3103	117,1
3	0,3333	0,3556	22,3
4	0,4004	0,4212	20,8
5	0,4612	0,467	5,8
6	0,4801	0,4852	5,1
7	0,4895	0,4959	6,4
8	0,6077	0,6123	4,6
9	0,6458	0,6553	9,5
10	0,6597	0,6919	32,2
11	0,6634	0,6821	18,7
12	0,8261	0,8873	61,2
13	0,8346	0,8584	23,8
14	0,863	0,8804	17,4
15	0,9308	0,938	7,2
16	0,9741	0,9747	0,6

Table 6. Transmission windows 0.1 - 1THz, of molecular absorption loss at d=1000m, T_0=296K, p = 1atm, $v.m.r$ = 0.0138.

4.3 Spectral efficiency

To calculate spectral efficiency at a certain distance, part of the spectrum from the available transmission windows as presented in section 4.2 will be used. In order to compare results at the same distance the following method has been chosen. The center frequency from the total bandwidth of each transmission window is located. Then as used bandwidth around that frequency, the spectrum of the smallest transmission window of this distance is chosen. Next the selected bandwidth of a window is divided into sub bands, each sub band has bandwidth *Df* . Small enough sub bands are assumed, which can simulate an infinite number of frequencies within its boundaries, where noise and absorption characteristics of the channel can be considered locally flat. Then spectral efficiency for the center frequency f_i of *i-th* sub band can be calculated and this value is constant along a sub bands spectrum.

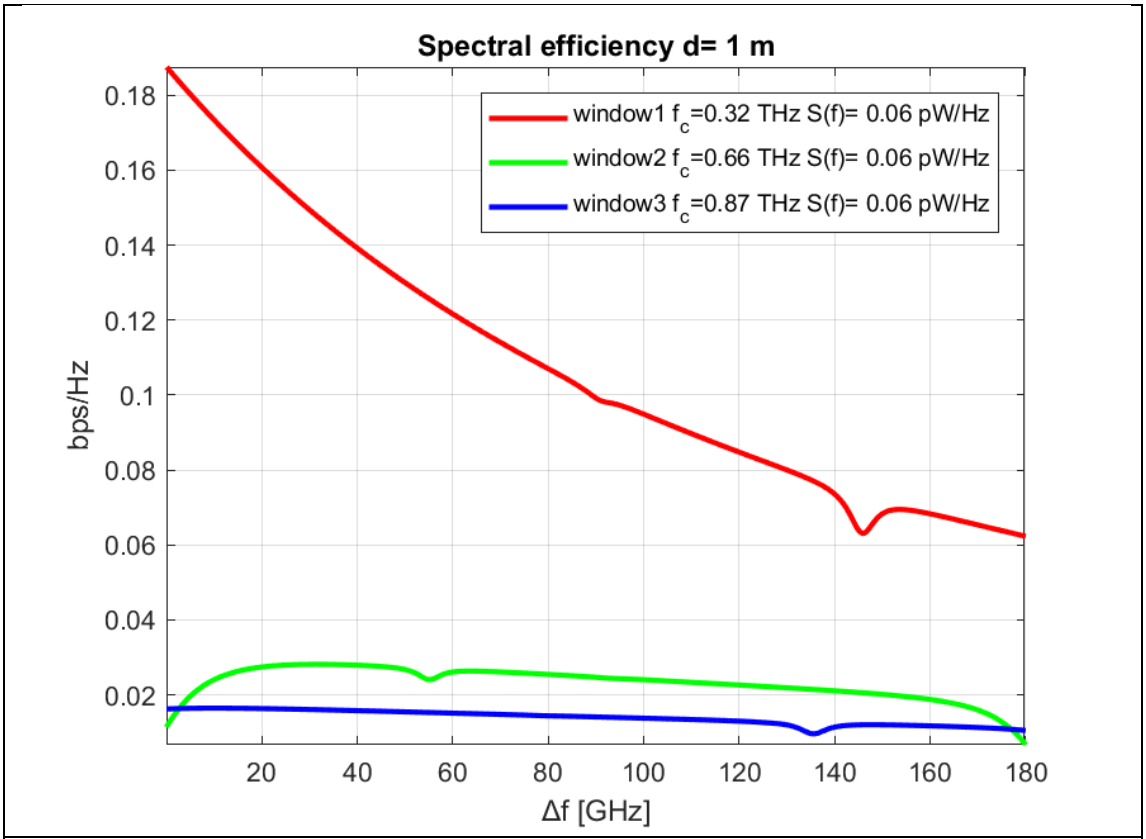

Figure 12. Spectral efficiency for each frequency window *i* (with total Bandwidth B_{used} = 180.1 GHz) at frequency $fmin_i + \Delta f$ and distance *d* = 1m, where $fmax_i - fmin_i = B_{used}$. Using absorption coefficient data derived from HITRAN database. For *p* = 1atm, T_0 =296K, *v.m.r* = 0.0138. *S(f)* is the transmitted signal PSD per frequency of the total used spectrum.

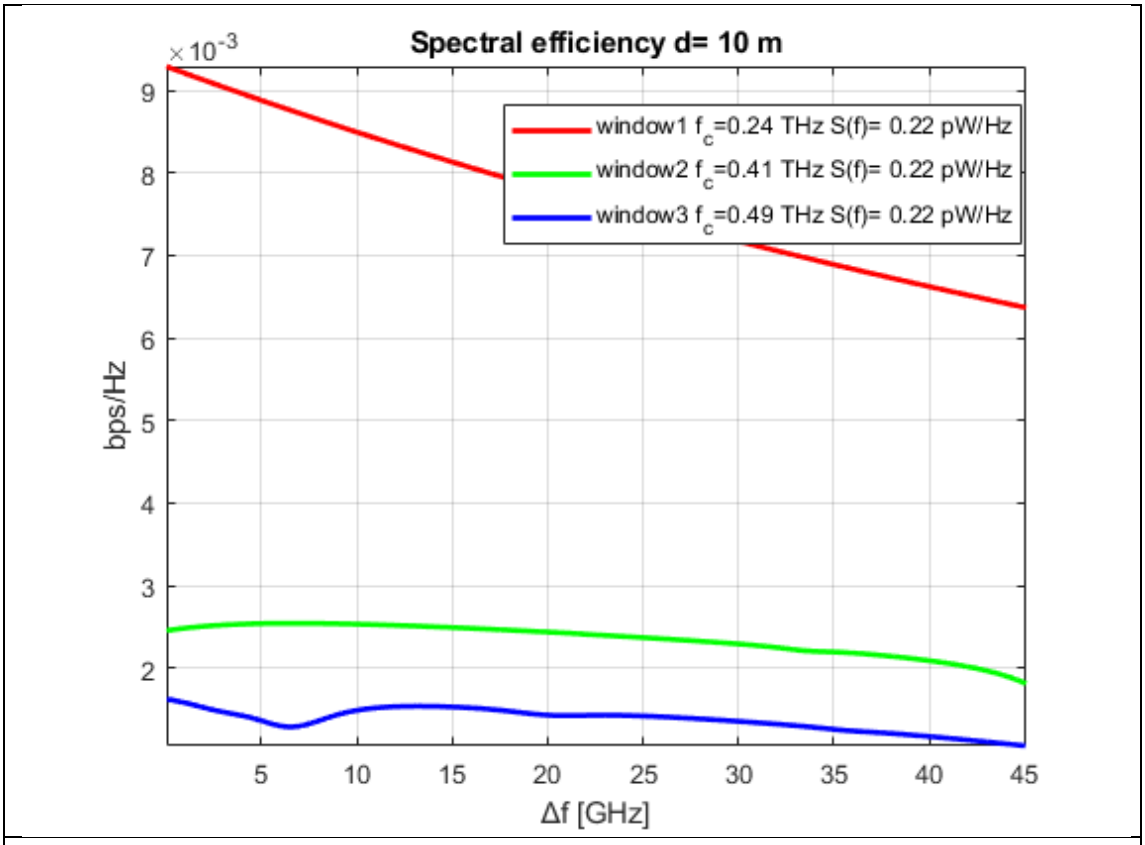

(a)

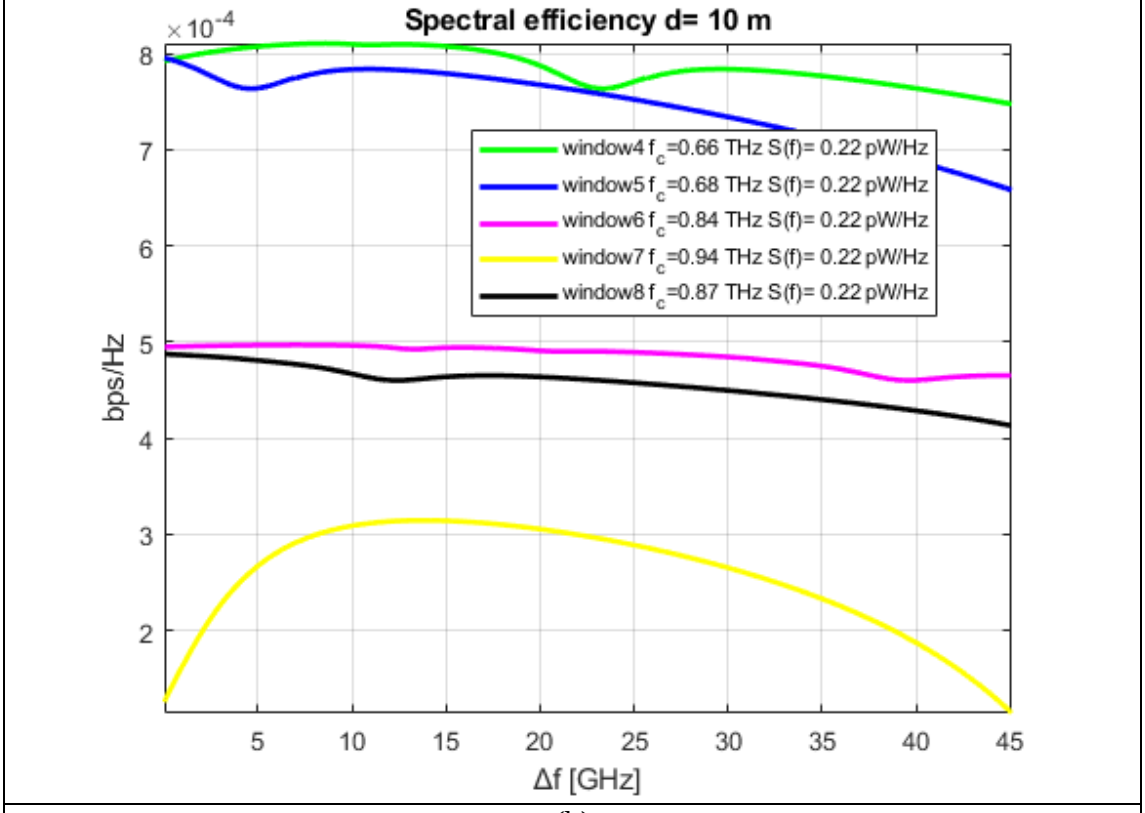

(b)

Figure 13. Spectral efficiency for each frequency window i (with total Bandwidth B_{used} = 45.1 GHz) at frequency $fmin_i + \Delta f$ and distance d = 10m, where $fmax_i$ - $fmin_i = B_{used}$. Using absorption coefficient data derived from HITRAN database. For p = 1atm, T_0 =296K, $v.m.r$ = 0.0138. $S(f)$ is the transmitted signal PSD per frequency of the total used spectrum.

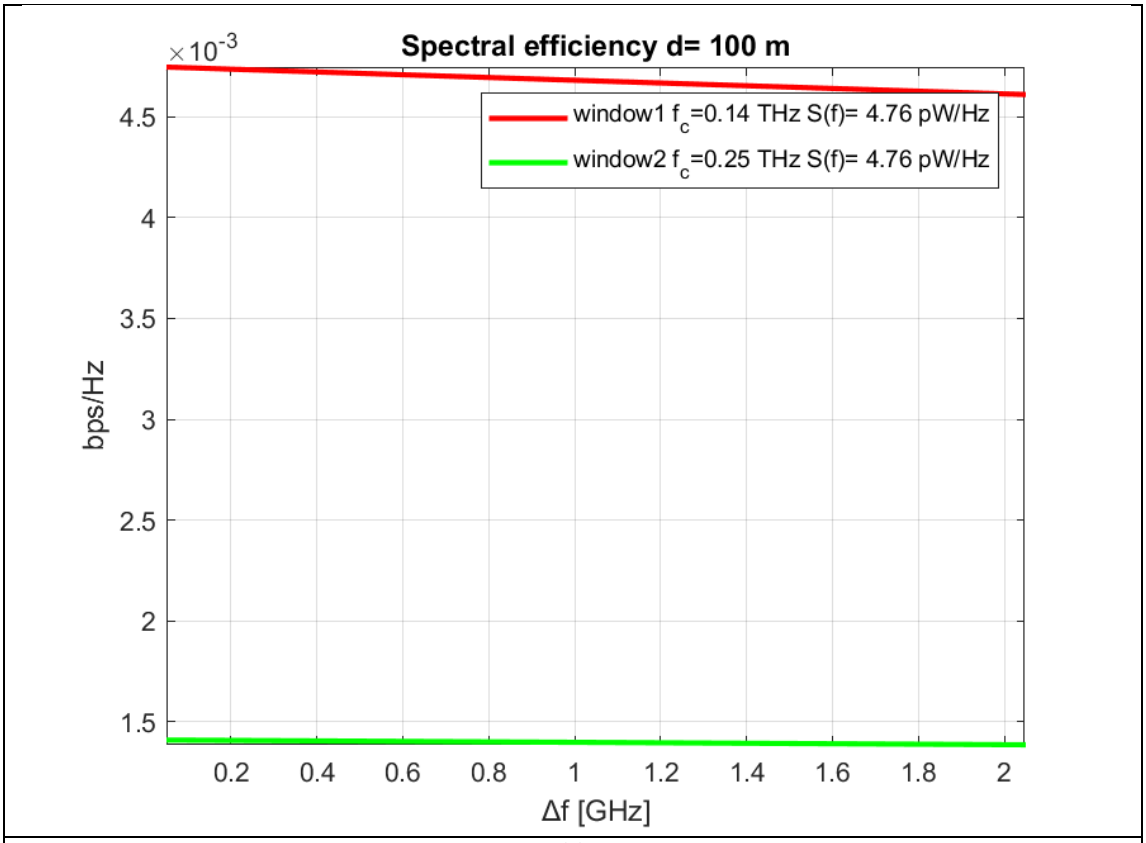
Spectral efficiency d= 100 m
×10^-3
window1 f_c=0.14 THz S(f)= 4.76 pW/Hz
window2 f_c=0.25 THz S(f)= 4.76 pW/Hz
bps/Hz
Δf [GHz]

(a)

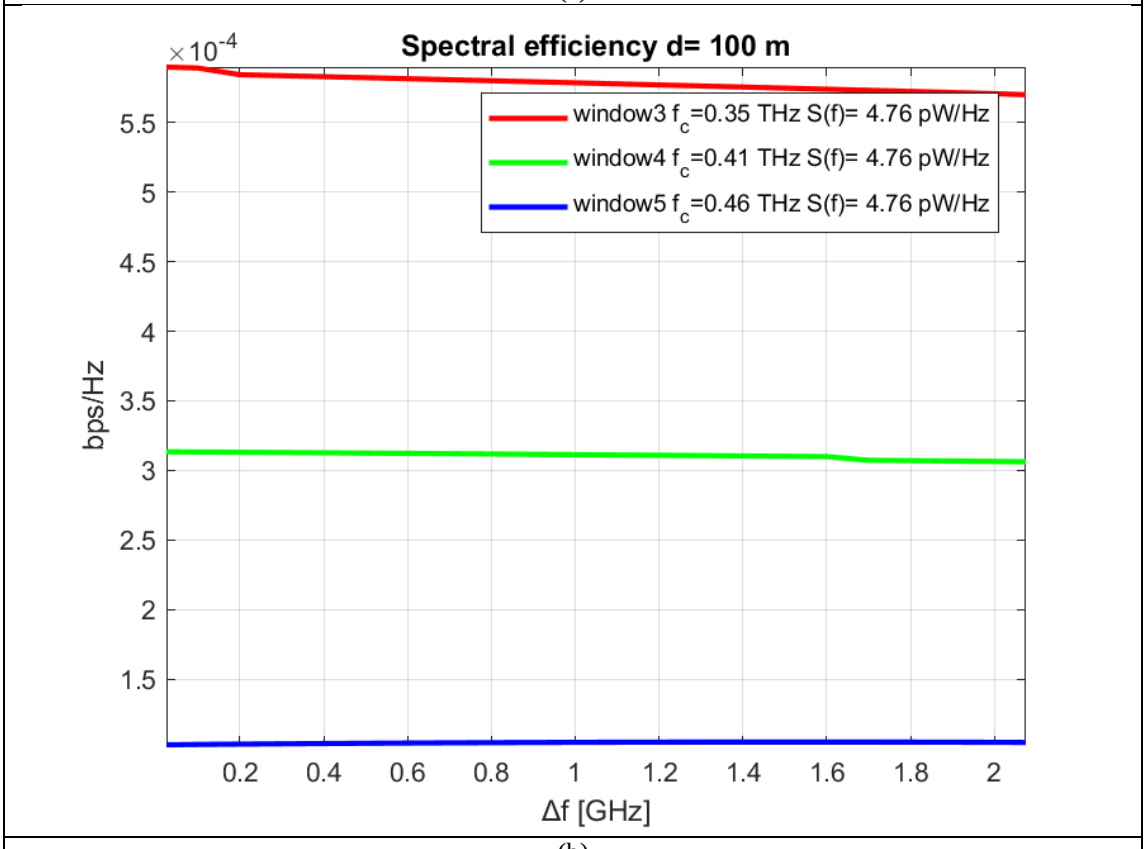
Spectral efficiency d= 100 m
×10^-4
window3 f_c=0.35 THz S(f)= 4.76 pW/Hz
window4 f_c=0.41 THz S(f)= 4.76 pW/Hz
window5 f_c=0.46 THz S(f)= 4.76 pW/Hz
bps/Hz
Δf [GHz]

(b)

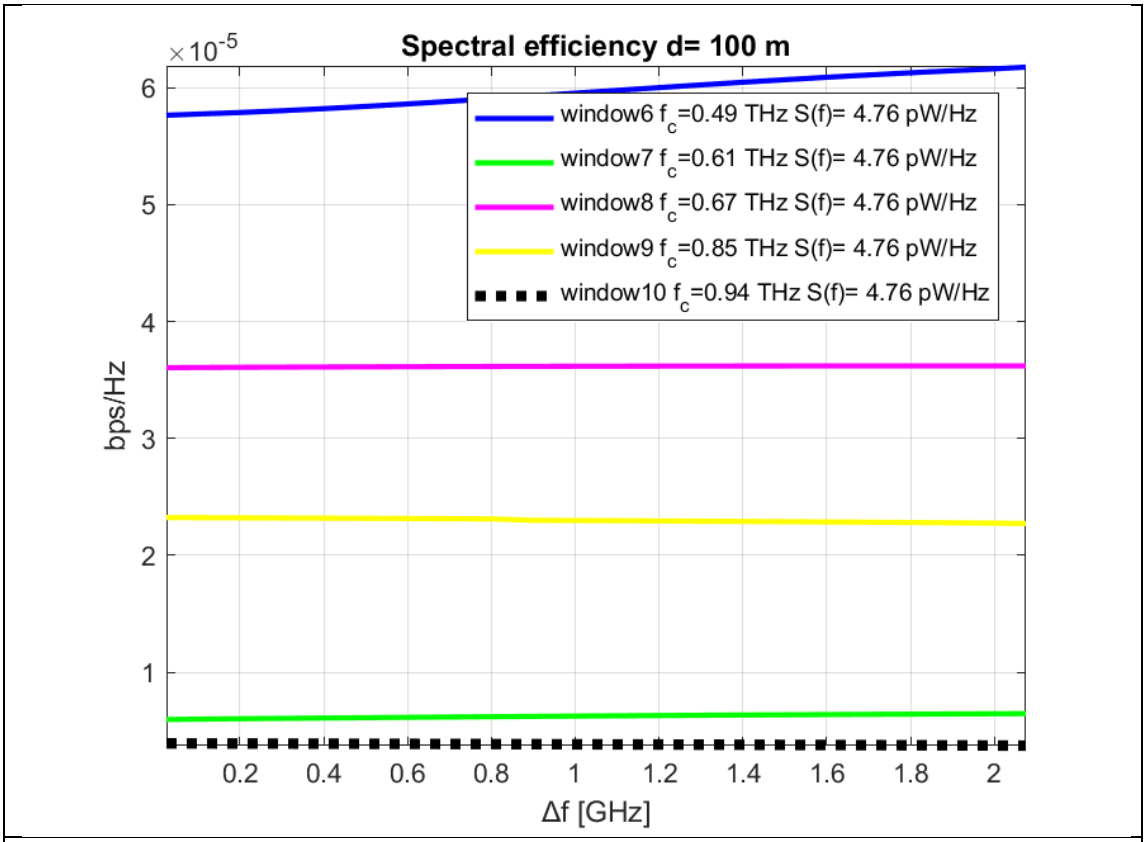

(c)

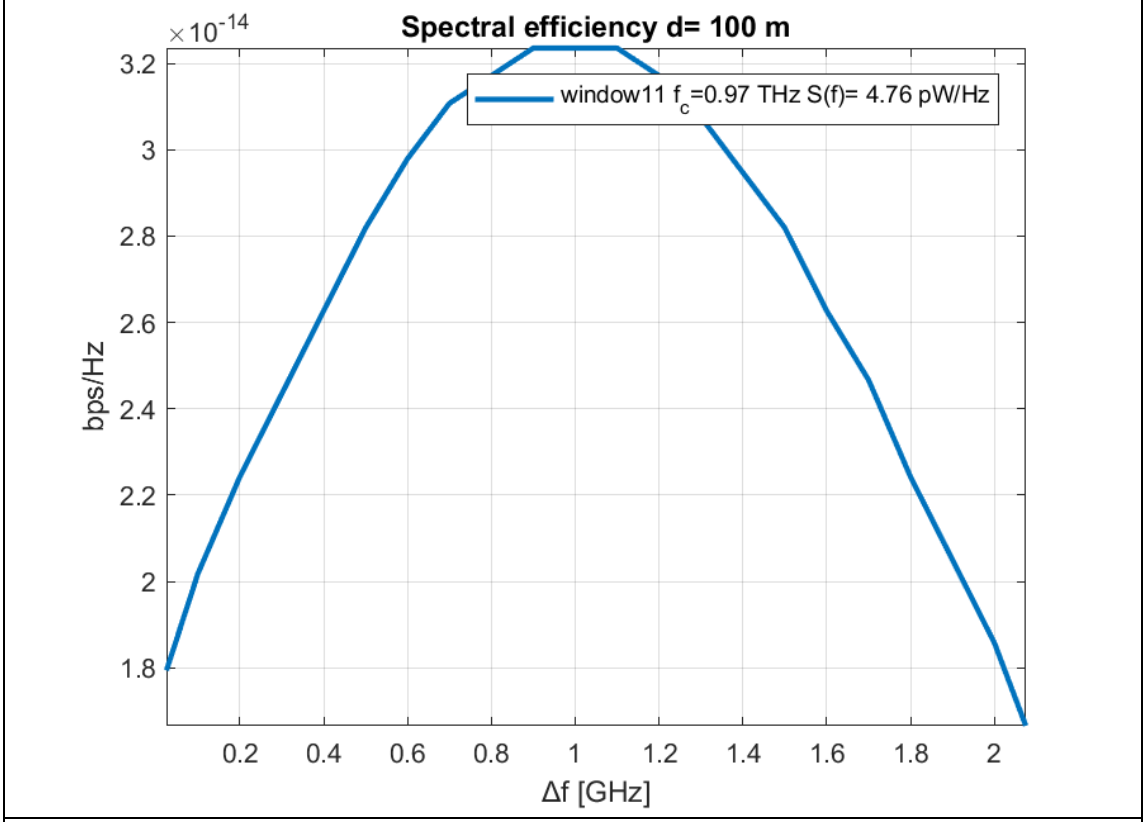

(d)

Figure 14. Spectral efficiency for each frequency window *i* (with total Bandwidth B_{used} = 2.1 GHz) at frequency $fmin_i + \Delta f$ and distance *d* = 100m, where $fmax_i$ - $fmin_i$ = B_{used} . Using absorption coefficient data derived from HITRAN database. For *p* = 1atm, T_0 =296K, *v.m.r* = 0.0138. *S(f)* is the transmitted signal PSD per frequency of the total used spectrum.

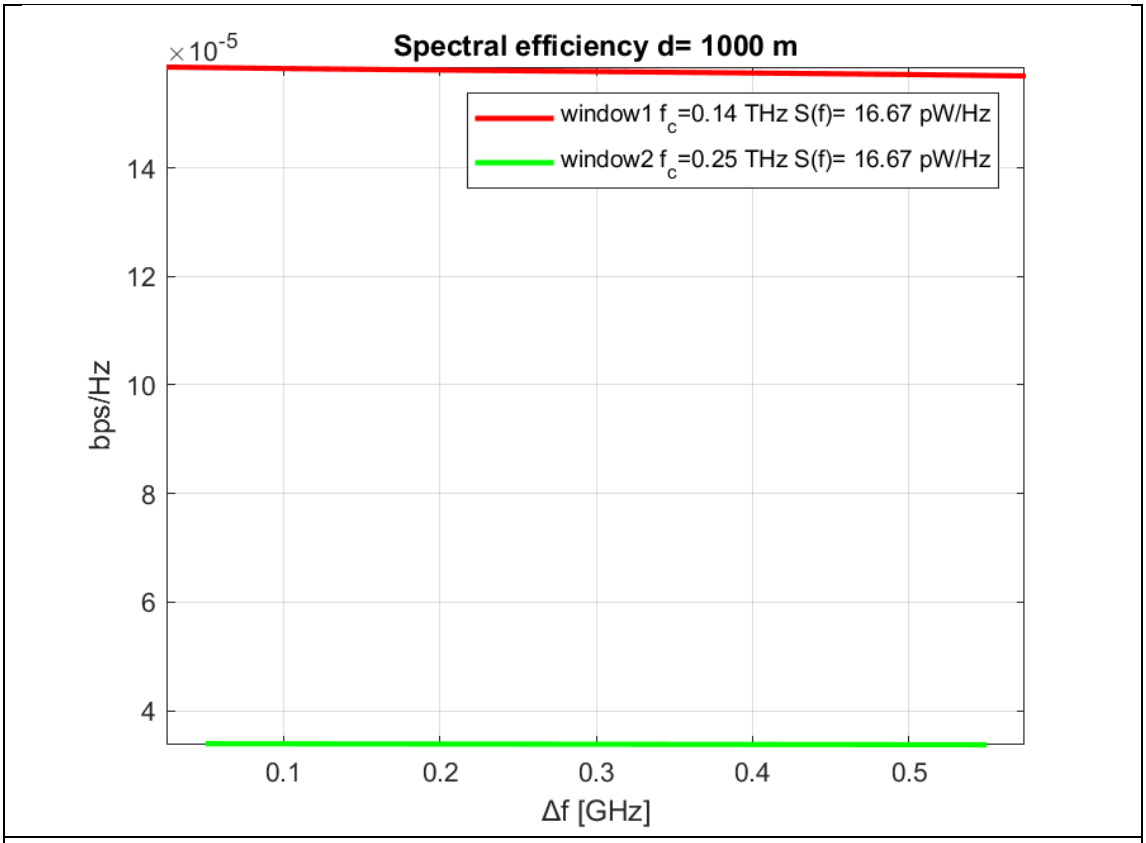
Spectral efficiency d= 1000 m
×10^-5
window1 f_c=0.14 THz S(f)= 16.67 pW/Hz
window2 f_c=0.25 THz S(f)= 16.67 pW/Hz
bps/Hz
Δf [GHz]

(a)

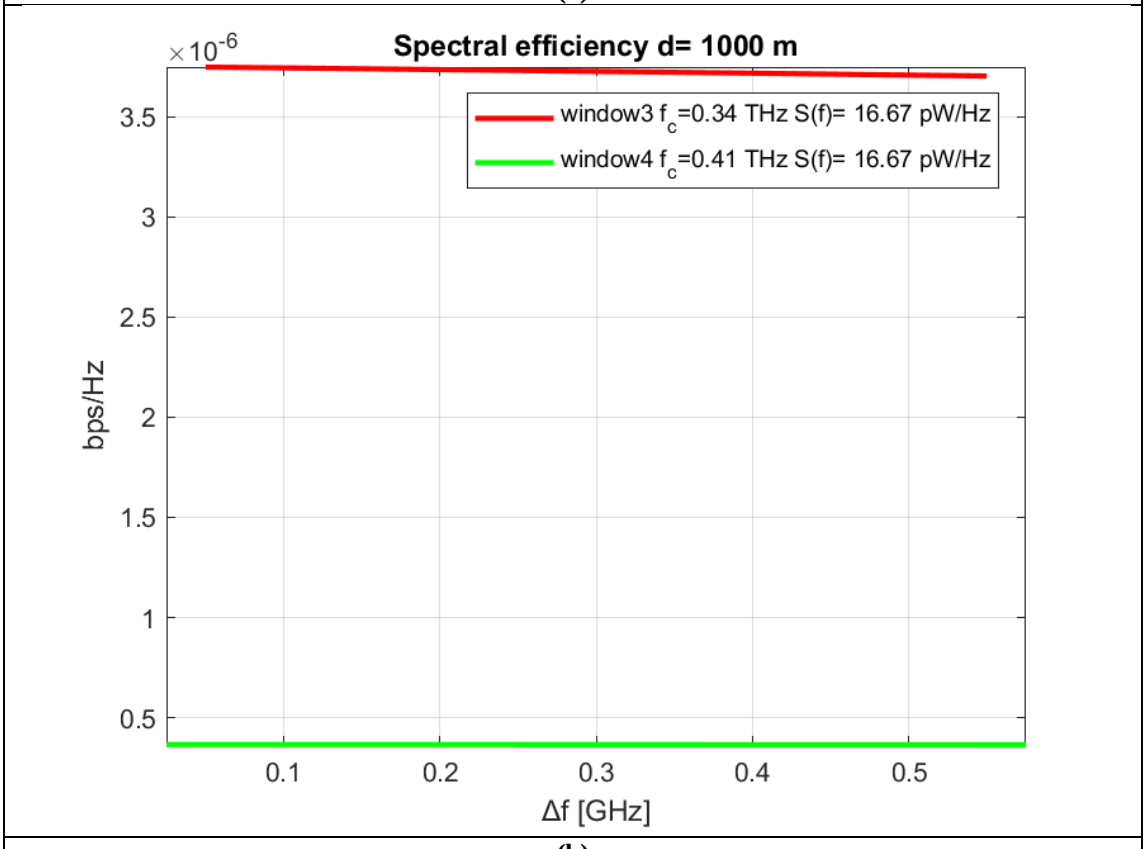
Spectral efficiency d= 1000 m
×10^-6
window3 f_c=0.34 THz S(f)= 16.67 pW/Hz
window4 f_c=0.41 THz S(f)= 16.67 pW/Hz
bps/Hz
Δf [GHz]

(b)

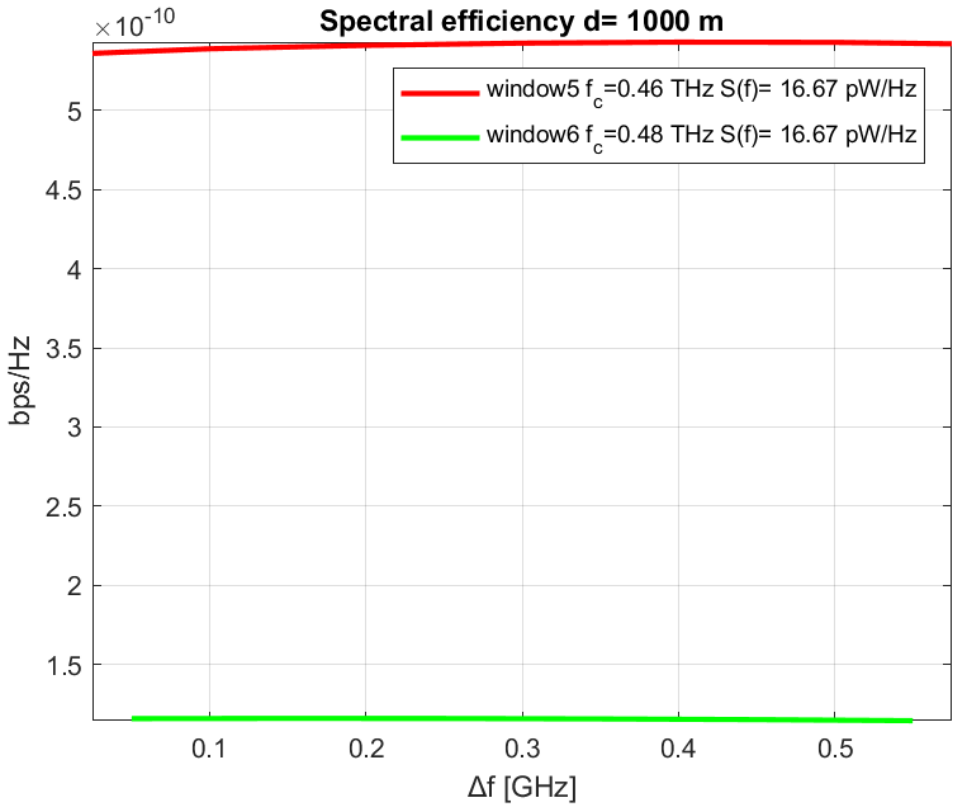

(c)

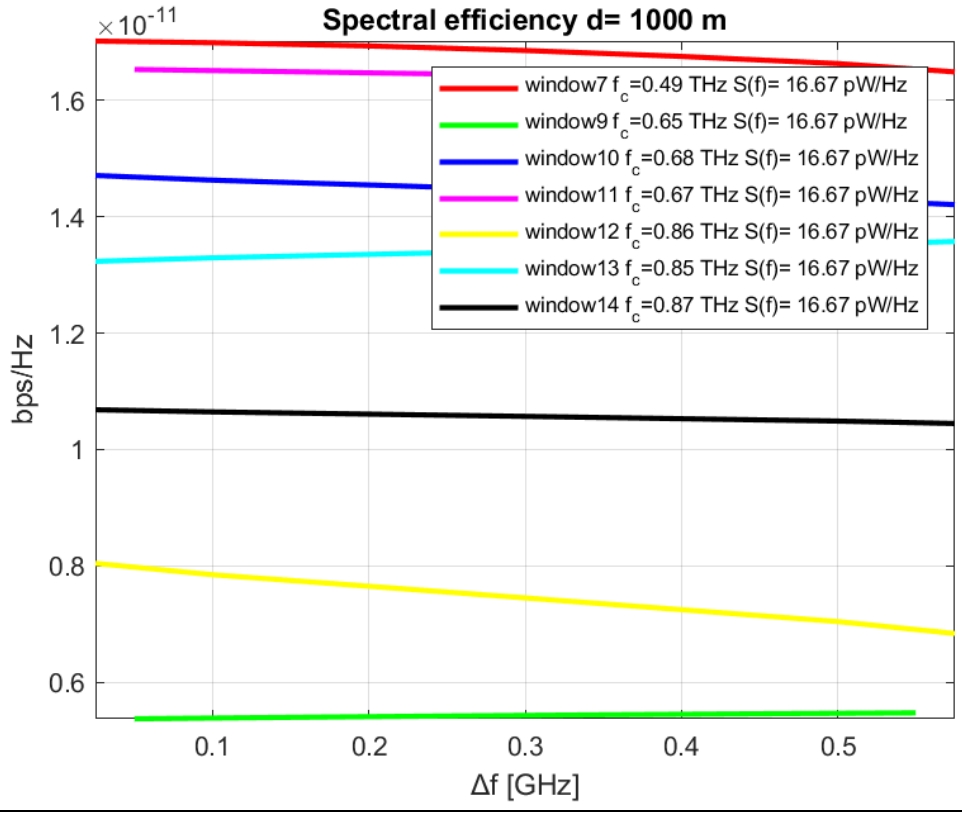

(d)

Figure 15. Spectral efficiency for each frequency window *i* (with total Bandwidth B_{used} = 0.6 GHz) at frequency $fmin_i + \Delta f$ and distance *d* = 1000m, where $fmax_i - fmin_i = B_{used}$. Using absorption coefficient data derived from HITRAN database. For *p* = 1atm, T_0 =296K, *v.m.r* = 0.0138. *S(f)* is the transmitted signal PSD per frequency of the total used spectrum.

Figures 12,13,14,15 illustrate spectral efficiency for each frequency window i , with total bandwidth B_{used} , at link distances 1, 10, 100, 1000 m respectively. At frequency $fmin_i+\Delta f_j$, where $fmin_i$ is the first frequency of *i-th* window and Δf_j is *j-th* sub-band's bandwidth. It is obvious that transmission windows at smaller link distances yield better spectral efficiency per sub-band. Also for the same distance, transmission windows containing frequencies lower in the THz spectrum yield better results with exceptions observed at fig. 14 (c) (window 7 with f_c=0.61 THz), fig. 15 (d) (windows 9, 12, 14 with f_c=0.65 , 0.86, 0.87 THz respectively), caused by the frequency selectivity of molecular absorption loss. The reason of spectral efficiency degradation is the decrease of achievable SNR per sub-band caused by the severe total path loss. Due to the use of transmission windows, FSPL way exceeds molecular absorption losses making it the major cause of received signal PSD decrease. Furthermore noise PSD at the receiver is far lower compared to total pathloss. It is observed that noise PSD at all transmission windows and distances is close to -203 dB/Hz much lower when compared to the total losses. In order to comprehend the severity of the losses some indicative values for the range of total pathloss for the used link distances are presented. For d=1 m at the first transmission window losses are in the interval of [80-84] dB, at the second in [88-93] dB. For d=10m at the first transmission window losses are in the interval of [99-100] dB, the second [104-106] dB, at the third in [106-108] dB. The results of observing spectral efficiency figures suggest that in order to increase it more measures need to be taken. Such as transmit and receive beamforming combined with high antenna gains.

4.4 Capacity

To calculate capacity at a certain distance, part of the spectrum from the available transmission windows as presented in section 4.2 will be used. In order to compare results at the same distance the following method has been used. The center frequency from the total bandwidth of each transmission window is located. Then as used bandwidth around that frequency, the spectrum of the smallest transmission window of this distance is chosen. Next the selected bandwidth of a window is divided into sub bands, each sub band has bandwidth Df . Small enough sub bands are assumed, which can simulate an infinite number of frequencies within its boundaries, where noise and absorption characteristics of the channel can be considered locally flat. Then capacity for the center frequency f_i of *i-th* sub band can be calculated and this value is constant along a sub bands spectrum.

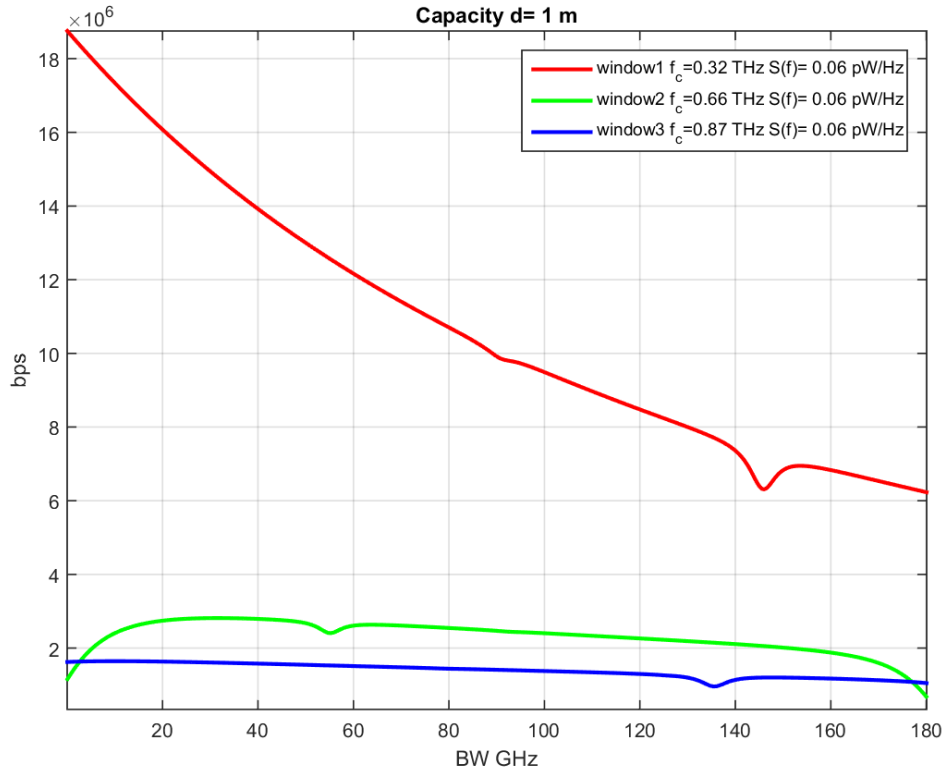

Figure 16. Capacity for each frequency window *i* (with total Bandwidth B_{used}=180.1 GHz) at frequency $fmin_i + \Delta f$ and distance *d*=1m, where $fmax_i - fmin_i = B_{used}$. Using absorption coefficient data derived from HITRAN database. For *p* = 1atm, T_0 =296K, *v.m.r* = 0.0138. *S(f)* is the transmitted signal PSD per frequency of the total used spectrum.

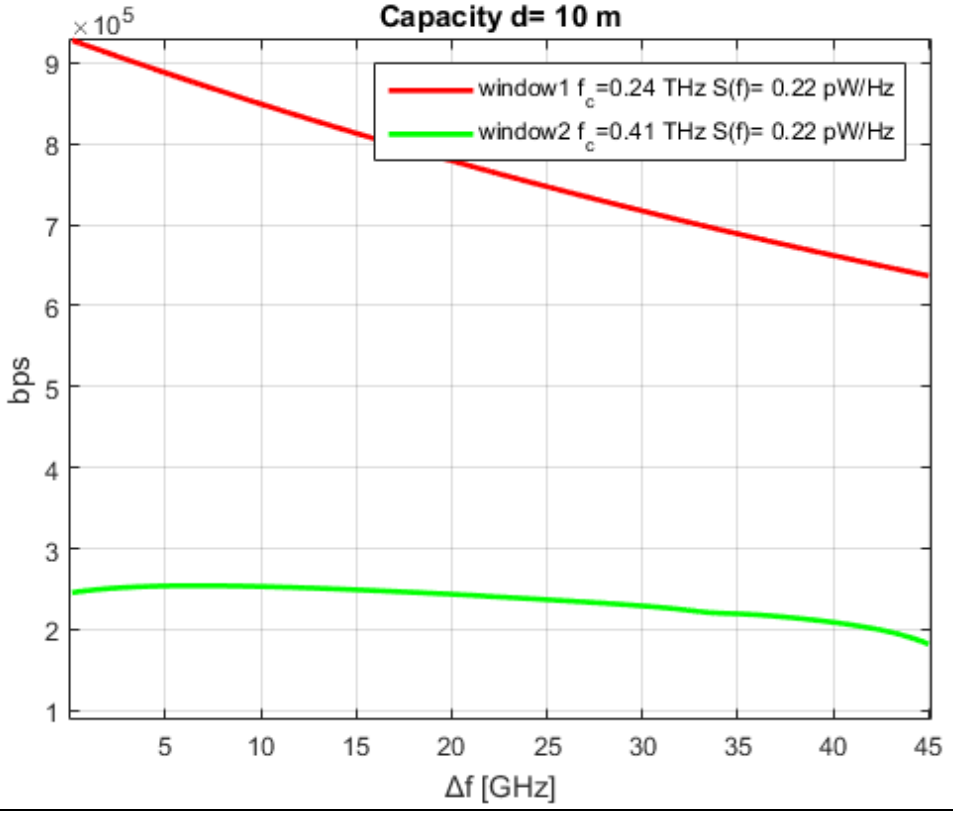

(a)

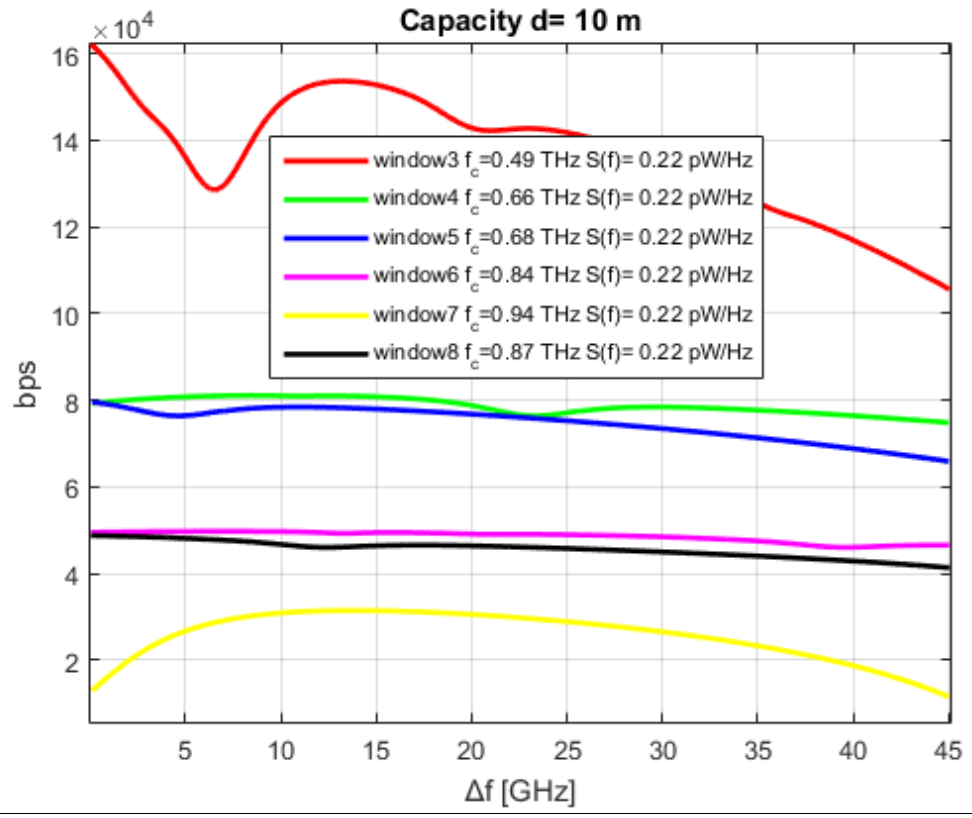

(b)

Figure 17. Capacity for each frequency window i (with total Bandwidth B_{used}=45.1 GHz) at frequency $fmin_i + \Delta f$ and distance d=10m, where $fmax_i$ - $fmin_i$ = B_{used} . Using absorption coefficient data derived from HITRAN database. For p = 1atm, T_0 =296K, $v.m.r$ = 0.0138. $S(f)$ is the transmitted signal PSD per frequency of the total used spectrum.

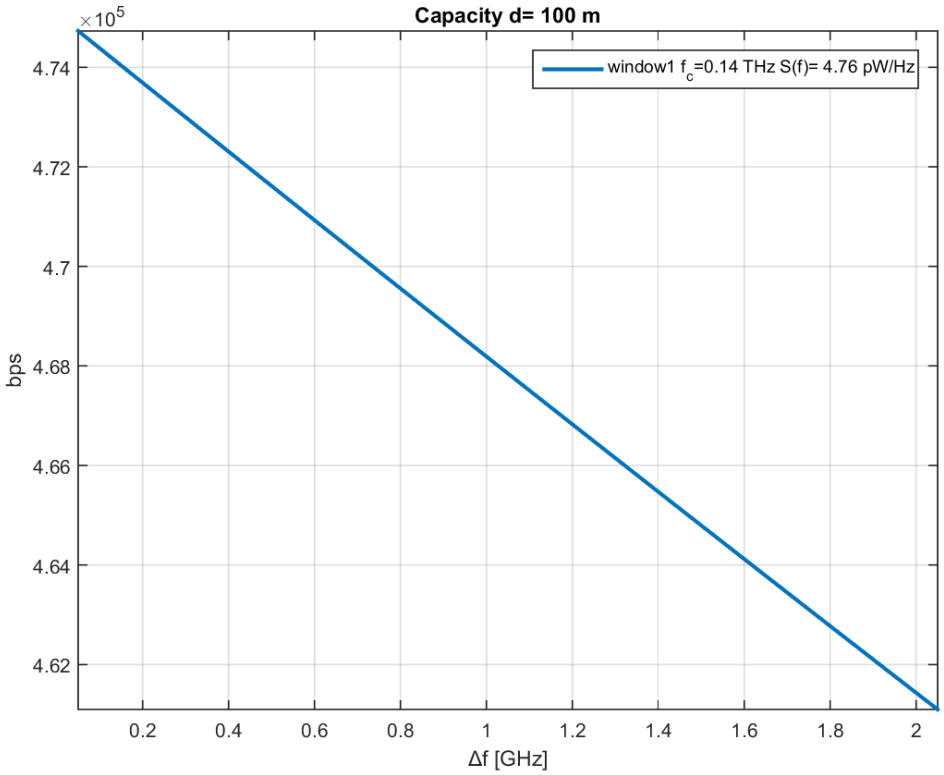
Capacity d= 100 m
×10^5
4.74
4.72
4.7
4.68
4.66
4.64
4.62
bps
0.2
0.4
0.6
0.8
1
1.2
1.4
1.6
1.8
2
Δf [GHz]
window1 f_c=0.14 THz S(f)= 4.76 pW/Hz

(a)

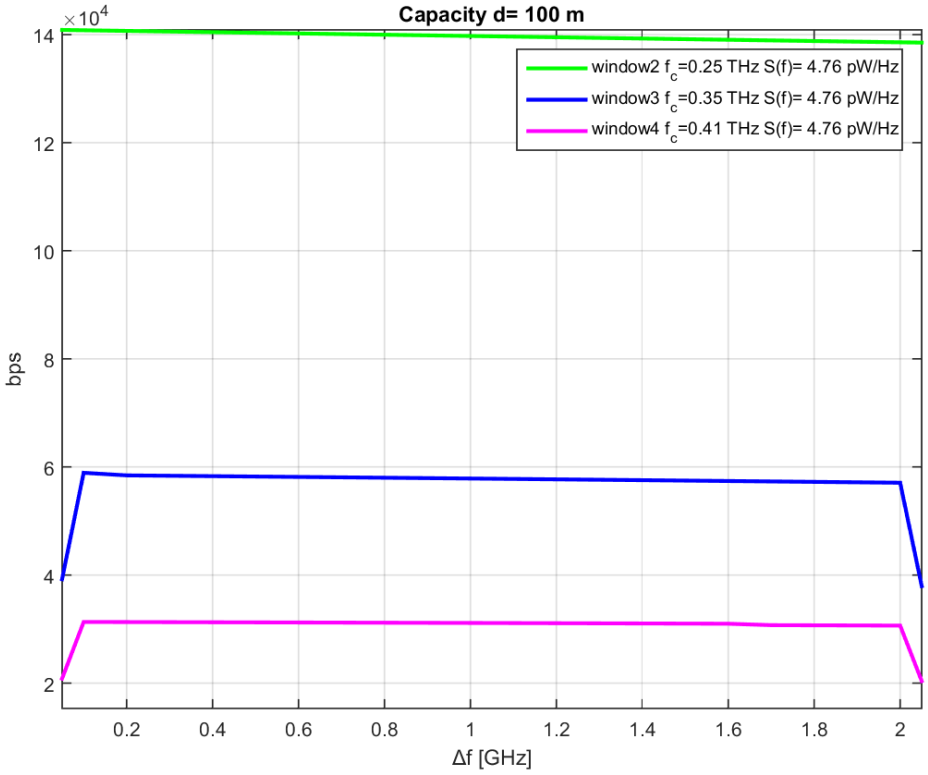
Capacity d= 100 m
×10^4
14
12
10
8
6
4
2
bps
0.2
0.4
0.6
0.8
1
1.2
1.4
1.6
1.8
2
Δf [GHz]
window2 f_c=0.25 THz S(f)= 4.76 pW/Hz
window3 f_c=0.35 THz S(f)= 4.76 pW/Hz
window4 f_c=0.41 THz S(f)= 4.76 pW/Hz

(b)

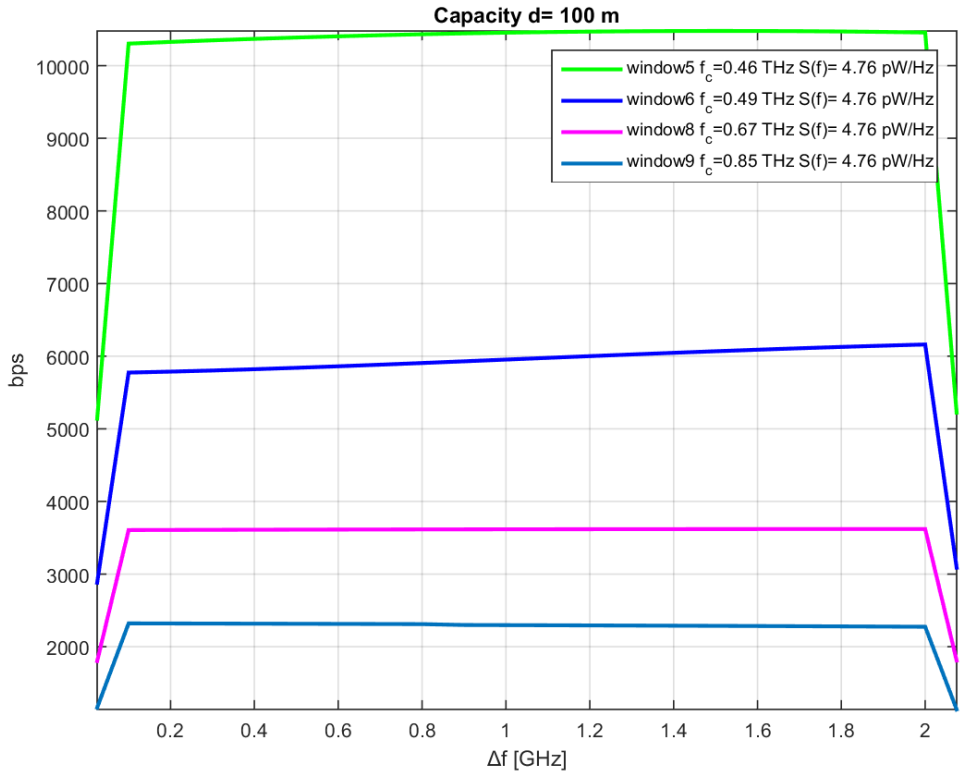
Capacity d= 100 m
window5 f_c=0.46 THz S(f)= 4.76 pW/Hz
window6 f_c=0.49 THz S(f)= 4.76 pW/Hz
window8 f_c=0.67 THz S(f)= 4.76 pW/Hz
window9 f_c=0.85 THz S(f)= 4.76 pW/Hz
bps
Δf [GHz]

(c)

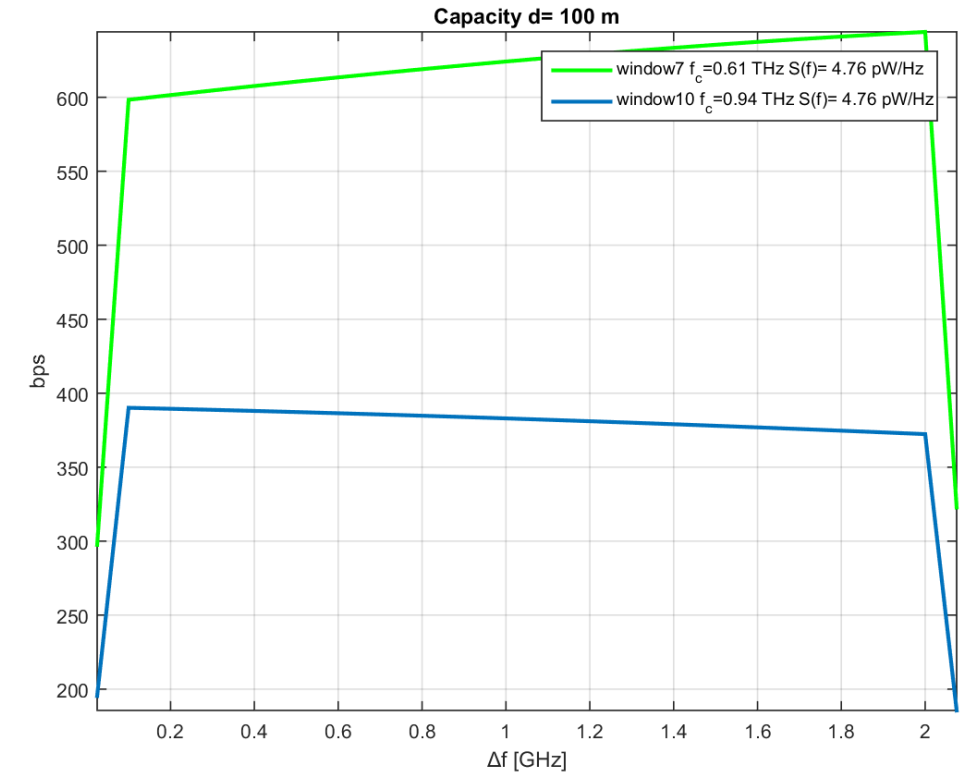
Capacity d= 100 m
window7 f_c=0.61 THz S(f)= 4.76 pW/Hz
window10 f_c=0.94 THz S(f)= 4.76 pW/Hz
bps
Δf [GHz]

(d)

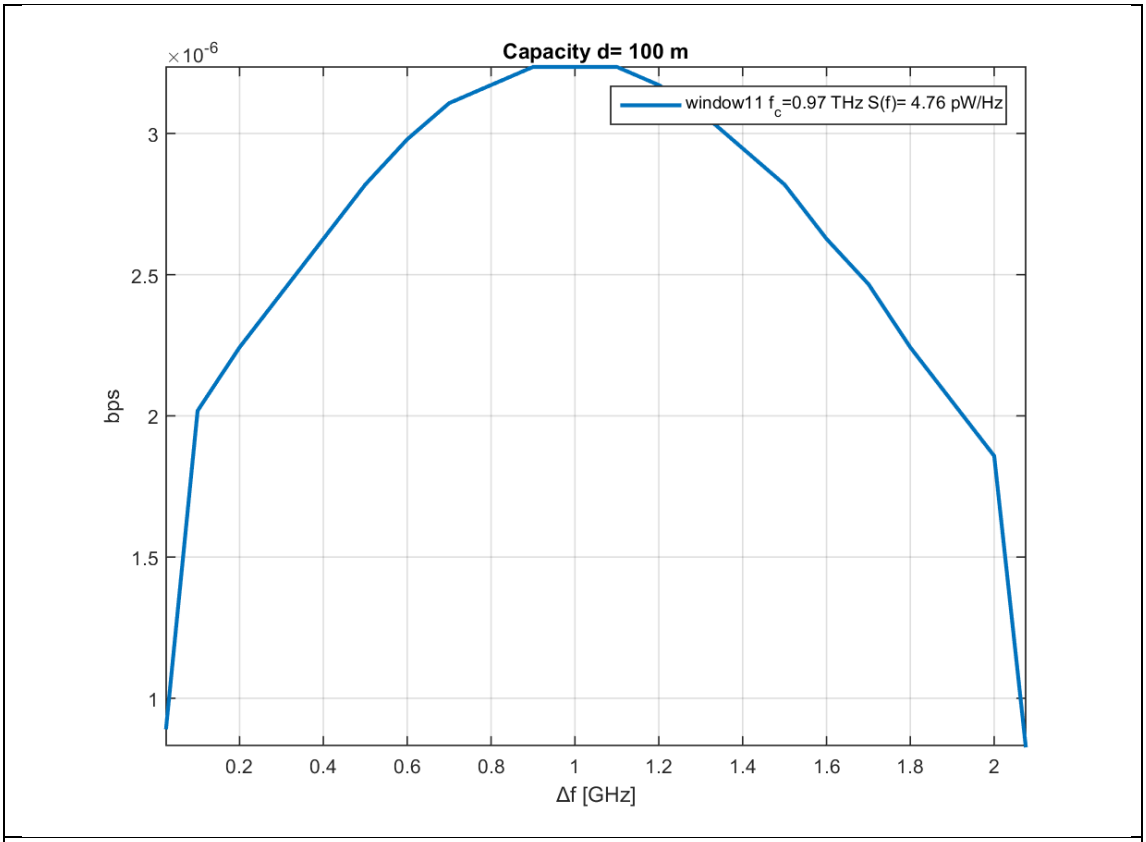

(e)

Figure 18. Capacity for each frequency window *i* (with total Bandwidth B_{used}=2.1 GHz) at frequency $fmin_i + \Delta f$ and distance *d*=100m, where $fmax_i - fmin_i = B_{used}$. Using absorption coefficient data derived from HITRAN database. For *p* = 1atm, T_0 =296K, *v.m.r* = 0.0138. *S(f)* is the transmitted signal PSD per frequency of the total used spectrum.

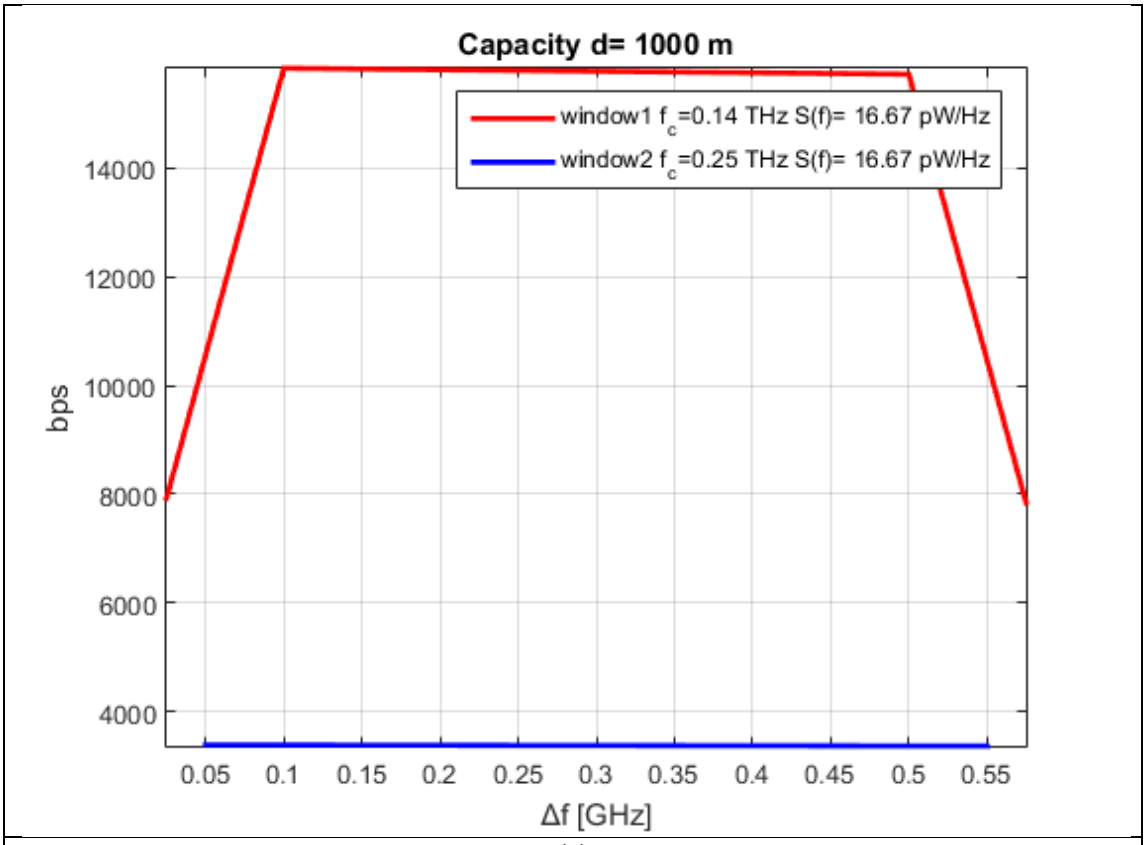
Capacity d= 1000 m
window1 f_c=0.14 THz S(f)= 16.67 pW/Hz
window2 f_c=0.25 THz S(f)= 16.67 pW/Hz
bps
14000
12000
10000
8000
6000
4000
0.05 0.1 0.15 0.2 0.25 0.3 0.35 0.4 0.45 0.5 0.55
Δf [GHz]

(a)

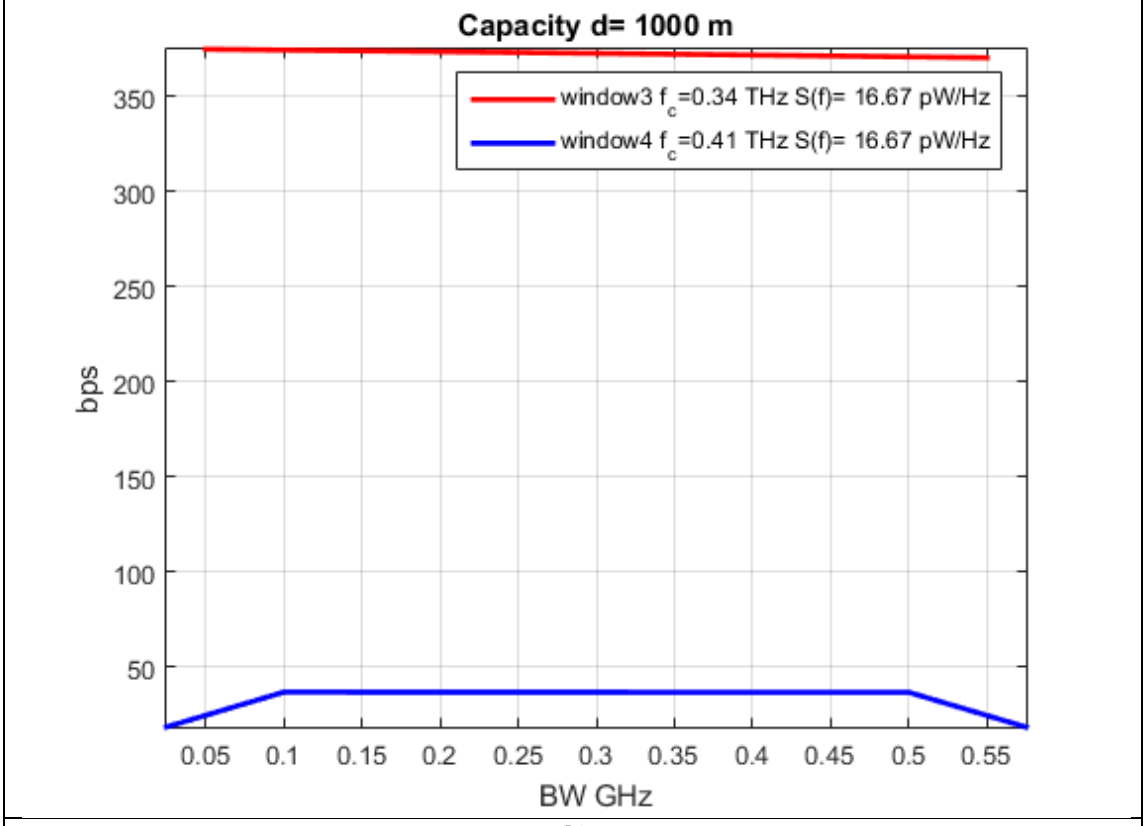
Capacity d= 1000 m
window3 f_c=0.34 THz S(f)= 16.67 pW/Hz
window4 f_c=0.41 THz S(f)= 16.67 pW/Hz
bps
350
300
250
200
150
100
50
0.05 0.1 0.15 0.2 0.25 0.3 0.35 0.4 0.45 0.5 0.55
BW GHz

(b)

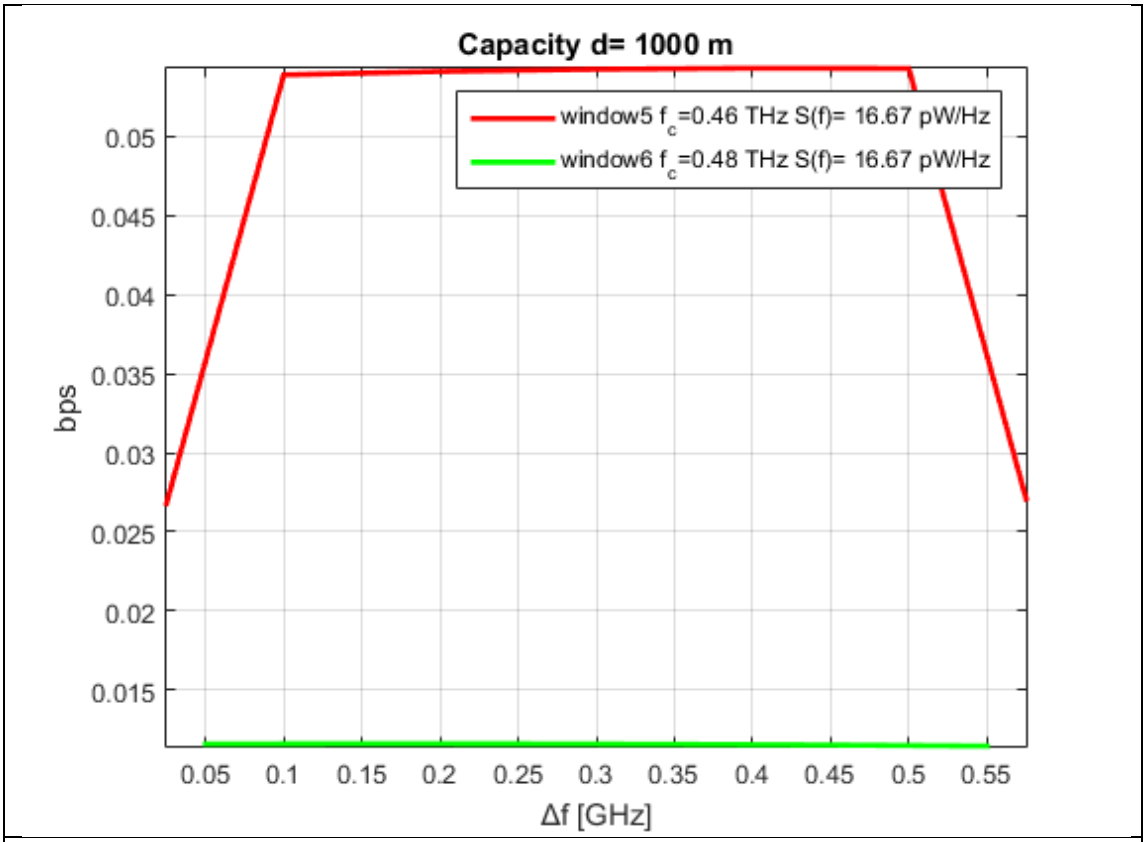

(c)

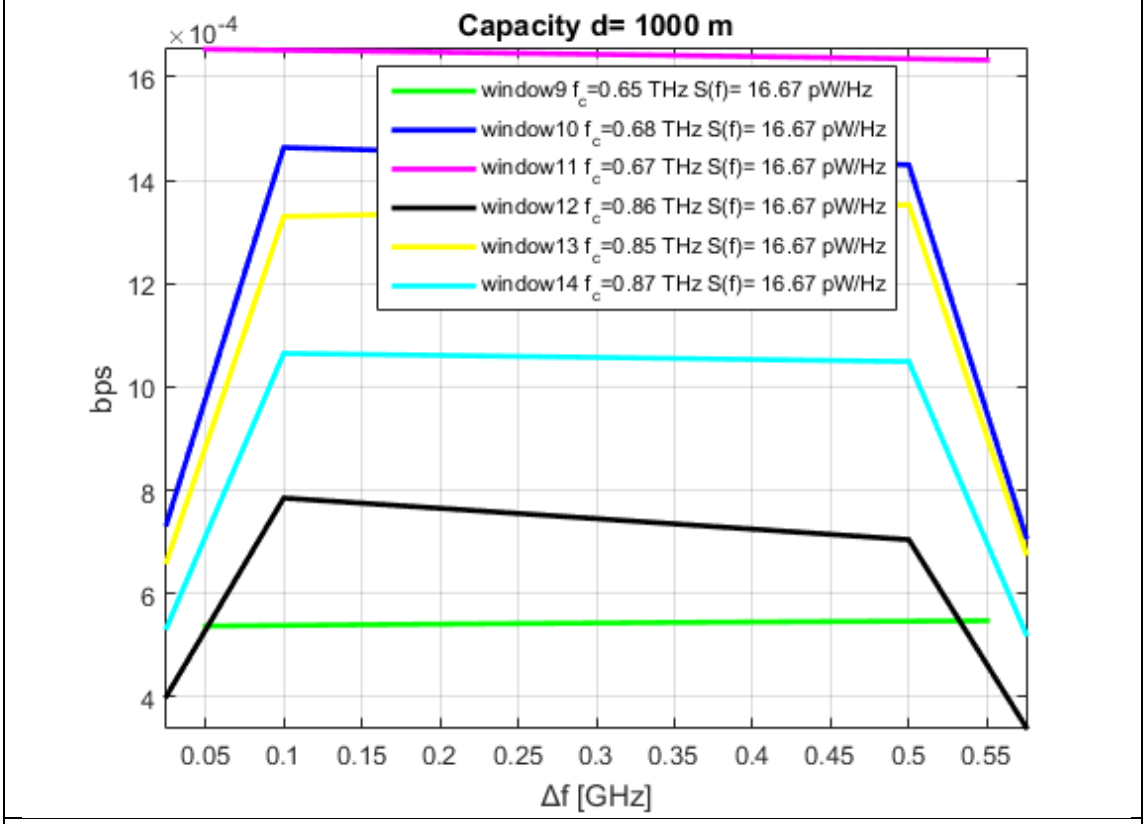

(d)

Figure 19. Capacity for each frequency window *i* (with total Bandwidth B_{used}=0.6 GHz) at frequency $fmin_i + \Delta f$ and distance *d*=1000m, where $fmax_i - fmin_i = B_{used}$. Using absorption coefficient data derived from HITRAN database. For *p* = 1atm, T_0 =296K, *v.m.r* = 0.0138. *S(f)* is the transmitted signal PSD per frequency of the total used spectrum.

Figures 16,17,18 illustrate capacity for each frequency window i , with total bandwidth B_{used} at link distances 1,10,100,1000 m. At frequency $fmin_i+\Delta f_i$, where $fmin_i$ is the first frequency of *i-th* window and Δf_j is *j-th* sub-bands bandwidth. The same observations done for spectral efficiency also apply to capacity. The severity of pathloss narrows achievable capacity in the order of a few kbps and only when transmission windows containing lower frequencies of THz spectrum are used.

4.5 Symbol error rate

To calculate symbol error rate at a certain distance, part of the spectrum from the available transmission windows as presented in section 4.2 will be used. In order to compare results at the same distance the following method has been used. The center frequency from the total bandwidth of each transmission window is located. Then as used bandwidth around that frequency, the spectrum of the smallest transmission window of this distance is chosen. Next the selected bandwidth of a window is divided to sub bands each sub band has bandwidth *Df*. Small enough sub bands are assumed, which can simulate an infinite number of frequencies within its boundaries, where noise and absorption characteristics of the channel can be considered locally flat. Then SER for the center frequency f_i of *i-th* sub band can be calculated and this value is constant along a sub bands spectrum.

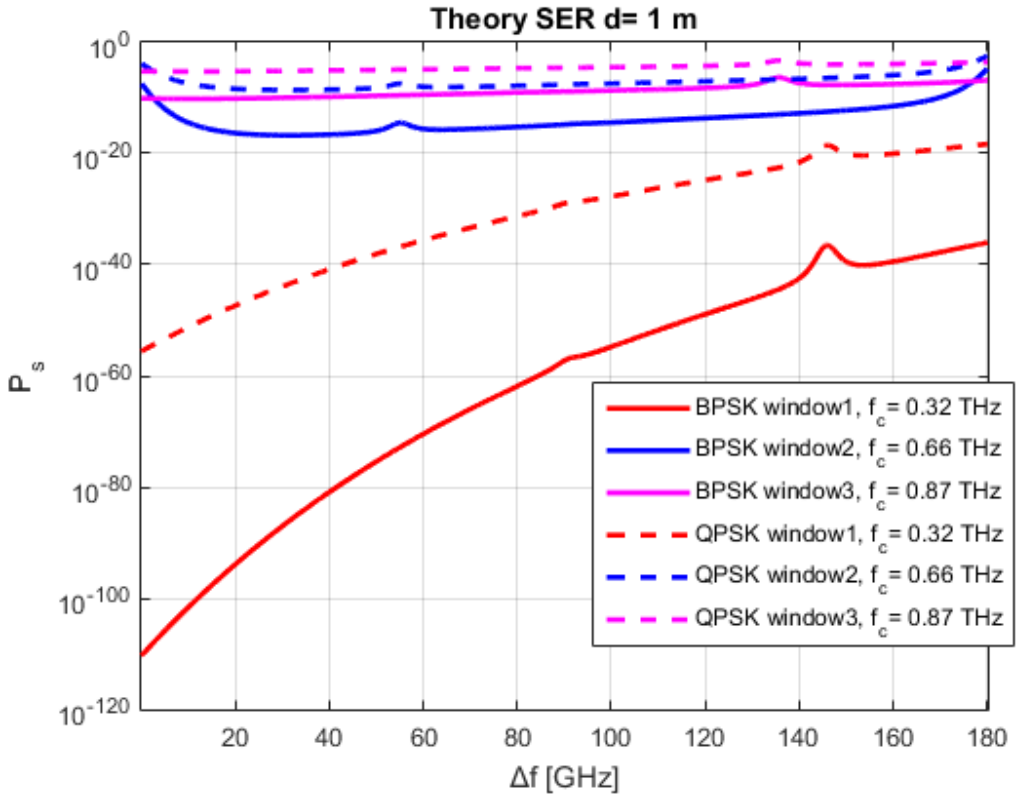

Figure 20. Theoretical SER for each frequency window i (with total Bandwidth B_{used}=180.1 GHz) at frequency $fmin_i + \Delta f = B_{used}$ and distance d=1m, where $fmax_i - fmin_i = B_{used}$. Using absorption coefficient data derived from HITRAN database. For p = 1atm, T_0 =296K, $v.m.r$ = 0.0138. E_s=10 mW, is the transmitted signal power per sub band center frequency. In the same figure QPSK and BPSK, SER for the same window and bandwidth are presented.

Figure 20 illustrates theoretical SER probability for each frequency window i , with total bandwidth B_{used} at link distance 1m. At frequency $fmin_i+\Delta f_j$, where $fmin_i$ is the first frequency of *i-th* window and Δf_j is *j-th* subbands bandwidth. For every window as expected BPSK error is lower than QPSK. Specifically window 1 yields lower error for both modulations, this due to lower path loss compared to the other two bands. Windows 2,3 have close error probabilities for the respective constellations.

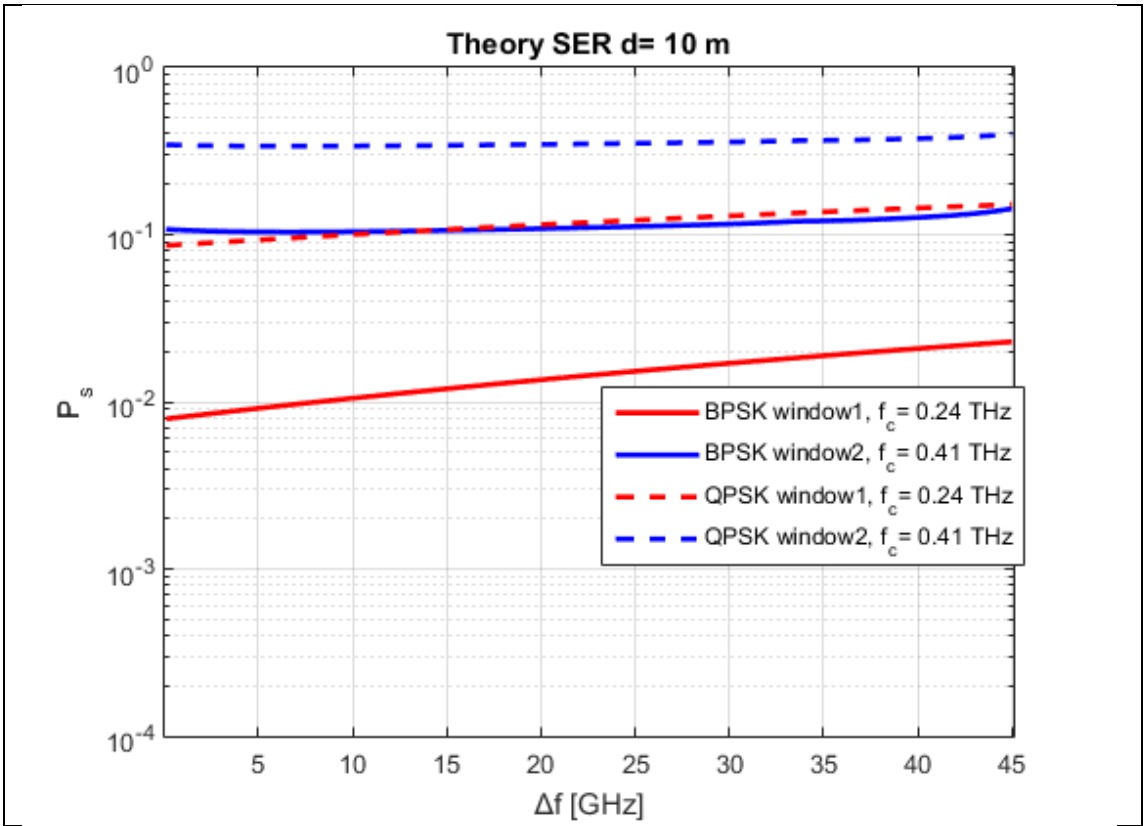

(a)

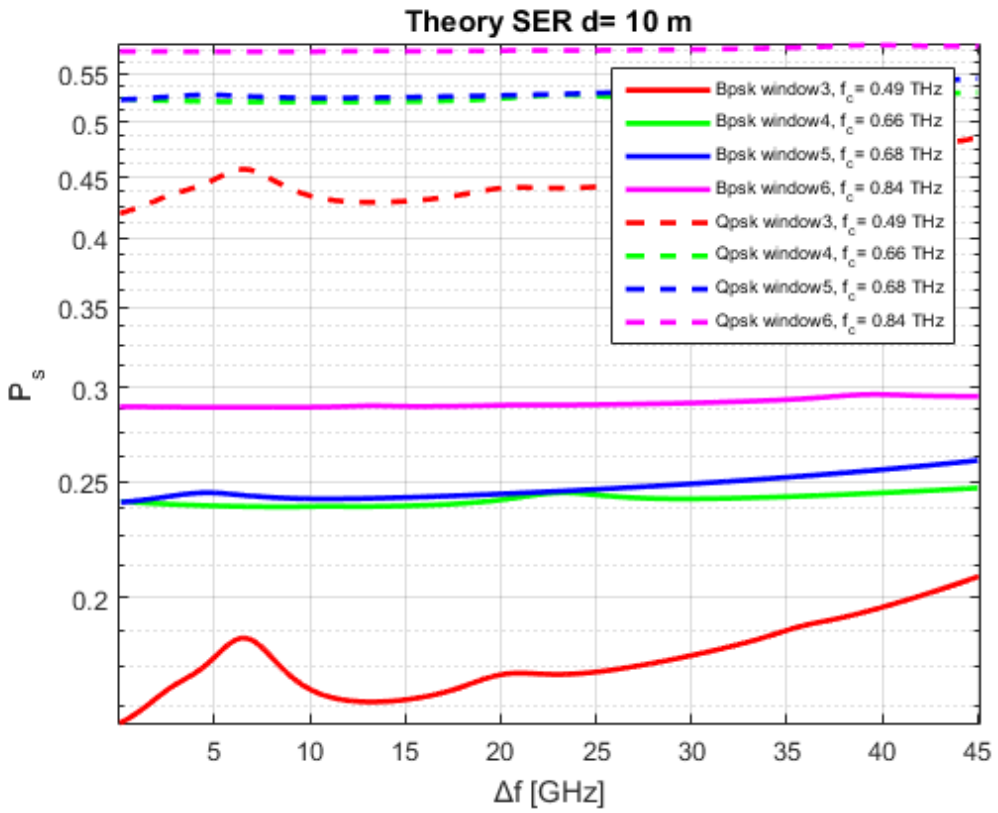

(b)

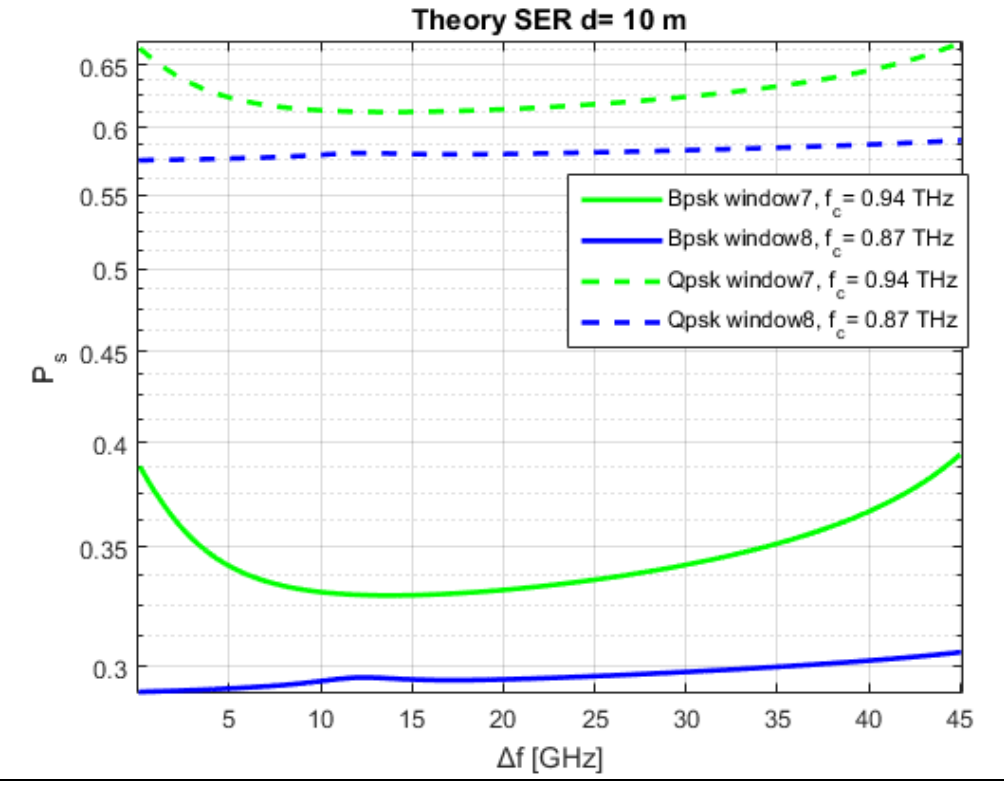

(c)

Figure 21. Theoretical SER for each frequency window *i* (with total Bandwidth B_{used}=45.1 GHz) at frequency $fmin_i + \Delta f = B_{used}$ and distance d=1m, where $fmax_i - fmin_i = B_{used}$. Using absorption coefficient data derived from HITRAN database. For p = 1atm, T_0 =296K, $v.m.r$ = 0.0138. E_s=10 mW, is the transmitted signal power per sub band center frequency. In the same figure QPSK and BPSK, SER for the same window and bandwidth are presented.

Figure 21 illustrates theoretical SER probability for each frequency window i , with total bandwidth B_{used} at link distance 10m. At frequency $fmin_i+\Delta f_j$, where $fmin_i$ is the first frequency of *i-th* window and Δf_j is *j-th* subbands bandwidth. For every window as expected BPSK error is lower than QPSK. Windows 1, 2 from fig. 21 (a), give the lowest SER compared to the rest in fig. 21 (b), (c). Error at those bands is significant and reaches the theoretical upper bounds of the used modulations. Due to this deterioration no SER results for transmission windows at further link distances are presented.

5 Performance evaluation of THz wireless systems operating in 275 - 400 GHz band

In this chapter performance evaluation for 275 - 400 GHz band using the simplified pathloss model presented in chapter 2.3 will be done. It is assumed that flat transmission PSD allocation is performed and every frequency belonging in the transmission spectrum is assigned with constant S_o (W/Hz) as

$$S_f(f) = \begin{cases} S_o, \ for\ f\ \in B \\ 0, \ elsewhere \end{cases} \quad (40)$$

Also it is assumed that both transmitter and receiver employ analog beamforming with their beams being perfectly aligned meaning that the angles of incident and reception (Θ_i , Θ_r) can be neglected in calculations giving $G_t(\Theta_i) = G_t$, $G_r(\Theta_r) = G_r$. Furthermore rewriting eq. (33) taking into account the transmit and receive antenna gains introduced in eq. (32) capacity equivalently is

$$C_i(d) = Df_i \ log_2(1 + \frac{S_o L(f_i,d)}{N_{psd}(f_i,d)}) \quad (41)$$

also the fraction in eq. (41) can be written as

$$\tilde{\gamma}(f_i, d) = \frac{S_o G_t G_r}{N_{psd}(f_i,d)} \left(\frac{c}{4\,\pi\, d}\right)^2 \left(\frac{1}{f_i}\right)^2 \exp(-d(y_1(f_i,\mu) + y_2(f_i,\mu) + g(f_i))) \quad (42)$$

and a constant value of g dB, for the fraction of $g = \frac{S_o G_t G_r}{N_{psd}(f_i,d)}$ can be assumed.

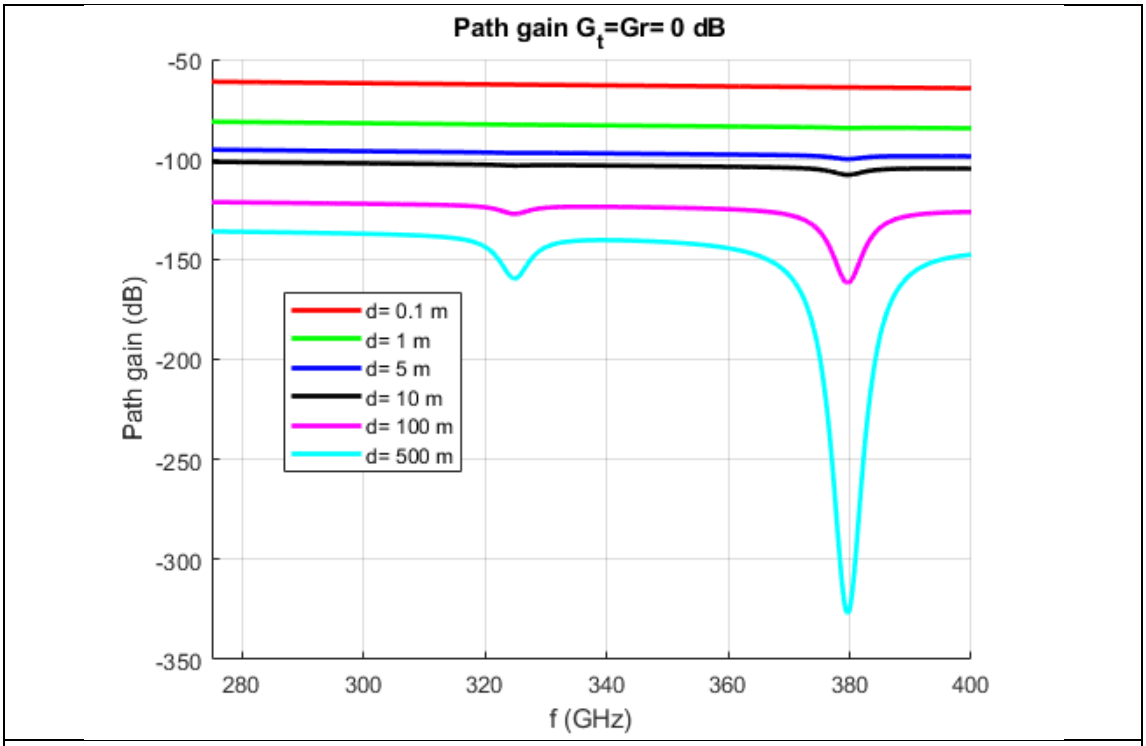

Figure 22. Path gain as a function of frequency for different transmission distances, assuming G_t=G_r=1 and p=1 atm, T=296 K

Figure 22 presents the path gain as a function of frequency for different link distances, assuming standard atmospheric conditions (p=1 atm, T=296 K), equal transmitter and receiver gains equal to G_t=G_r=1. As it is expected when THz frequency path gain (path loss) is investigated, when transmission distance increases path gain decreases. For example for f=380 GHz as distance increases from 0.1 to 100m path gain decreases about 100% (from almost -50 dB drops to -150 dB). This yet again indicates the importance of employing beamforming schemes in order to increase transmitter and receiver gains to countermeasure the effect of pathloss. Furthermore the results of the used loss model as those derived using HITRAN indicate that frequency selectivity becomes more severe as distance increases.

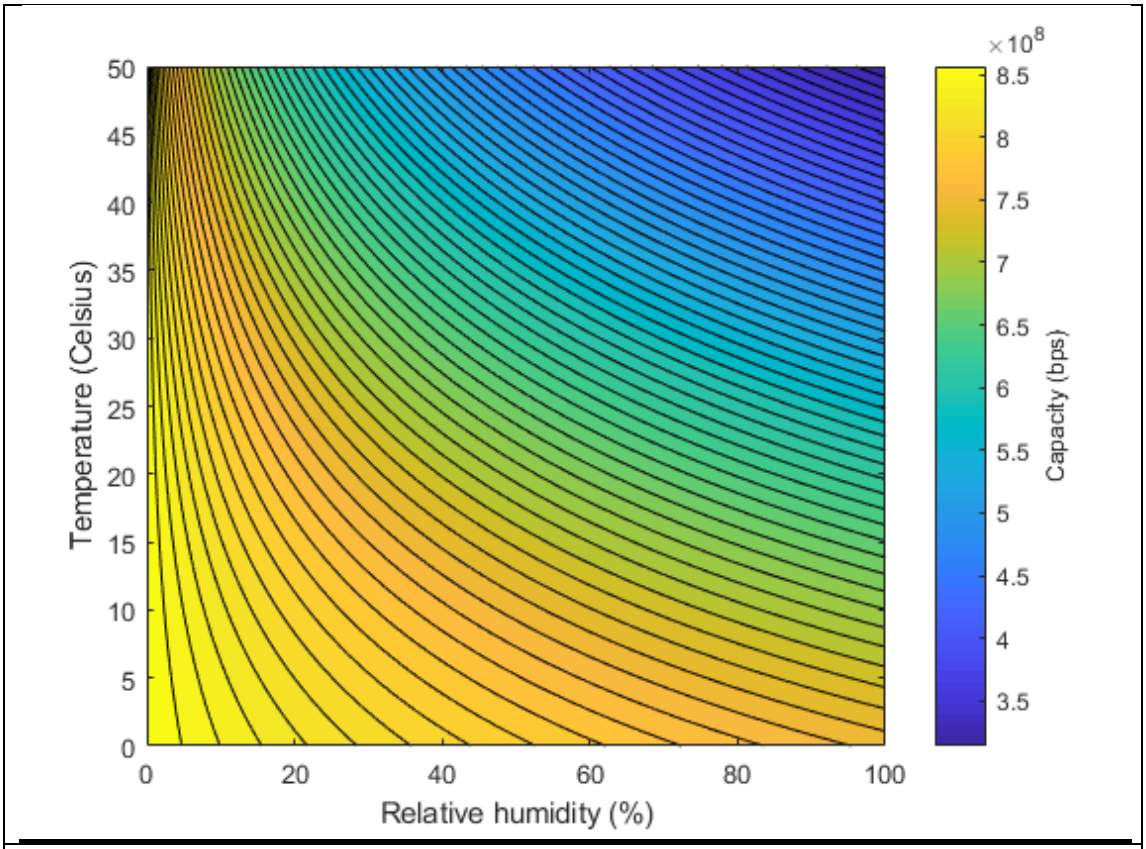

Figure 23. Capacity as a function of the temperature and relative humidity, for d=100m, assuming flat transmission signal PSD, g=100 dB, bandwidth B=125 GHz, *p*=1atm and *T*=296 K

Figure 23 depicts the capacity as a function of temperature and relative humidity for link distance *d*=100m, g=100 dB using bandwidth of B=125 GHz and assuming flat transmission signal PSD and standard atmospheric conditions. For a given temperature e.g. $T=25^{o}$ C almost 10 % capacity deterioration occurs as the relative humidity increases from 60 to 90 %. Also for a given relative humidity value as the temperature increases the capacity decreases. For example for relative humidity equal to 50 % the capacity deteriorates by almost 54 % as the temperature increases from 20 to 50^{o}C. These observations make evident that the impact of temperature variation is more severe compared to humidity variations in THz wireless links. Furthermore it should be noted that even for flat transmission signal PSD allocation the assumptions of gains at the transmit and receive antennas result to capacity far more improved compared to the case where no gains were used (figures 16,17,18).

6 Conclusion & further work

Current work presented the distance, frequency dependence of THz EM waves propagation. In particular the spectrums of 0.1 - 1 THz and 0.1-10THz were firstly investigated in terms of noise temperature and path loss. In the 0.1 - 1 THz total noise temperature at link distance 1m presents peaks close to the upper bound of 600 K in the frequency sub intervals of 0.5 - 0.6, 0.7 - 0.8, 0.9 - 1 THz, while in the rest of the spectrum is relatively low close to the constant thermal noise floor of 300K. As distance increases the upper bound of temperature is shown to spread wider in the

aforementioned frequency intervals, while in the meantime new peaks arise at other spectrum parts. This distance frequency dependence of temperature is even more eminent at 0.1 - 10THz. In compliance with noise temperature, noise power spectral density shows the same results. Reaching its maximum at the same frequency intervals. Observing the figures of FSPL and molecular absorption loss in 0.1 - 1THz band at distance 1m, molecular loss is almost flat, when compared to FSPL. Some local maxima peaks of molecular loss appear within sub intervals of 0.5 - 0.6, 0.7 - 0.8 and 0.9 - 1 THz. As link distance increases molecular absorption peaks become wider occupying the entire aforementioned frequency regions and exceed FSPL, while also peaks of absorption loss appear at other frequencies. The increase of molecular loss is even more intense in 0.1 - 10THz. This distance, frequency dependence of THz propagation leads to the need of evaluation of possible transmissions in 0.1 - 1THz region, using parts of the spectrum where molecular loss presents local minima. Spectral efficiency and capacity were calculated for each frequency window i , with total bandwidth B_{used} at frequency $fmin_i+\Delta f$ and sub band bandwidth Δf. At every case it was shown, that windows containing lower frequencies suffer less from noise and losses, yielding better results. Similar observations were made for SER. Information theory metrics suggest that THz channel particularities make it impossible to transmit signals without any measures to improve SNR at the receiver. This was verified by the capacity calculations results using the channel model for the 275-400 GHz band, where gains for the transmit and receive antennas were assumed. There it was shown that even for the link distance of 100m, 125 GHz bandwidth and different environmental conditions way better results were achieved. It is apparent that the main task of future work is to improve received SNR. So in order to achieve acceptable performance in long range links, high gain antennas and transmission PSD designs which take into account the extreme path losses are necessary. Furthermore MIMO transmission schemes must be employed in combination with highly directive pencil beam forming. At last another step that could possibly boost further research is the development of molecular absorption loss models covering wider areas of the THz spectrum.

References

[1] J. M. Jornet and I. F. Akyildiz, "Channel Modeling and Capacity Analysis for Electromagnetic Wireless Nanonetworks in the Terahertz Band", IEEE Trans. Wireless Commun., vol. 10, no. 10, pp. 3211-3221, Oct. 2011

[2] A. A. Boulogeorgos, A. Alexiou, T. Merkle, C. Schubert, R. Elschner, A. Katsiotis, P. Stavrianos, D. Kritharidis, P. K. Chartsias, J. Kokkoniemi, M. Juntti, J. Lehtomaki, A. Teixeira, F. Rodrigues, "Terahertz Technologies to Deliver Optical Network Quality of Experience in Wireless Systems Beyond 5G", IEEE Communications Magazine.

[3] J. D. Park ,"Fully Integrated Silicon Terahertz Transceivers for Sensing and Communications Applications", Electrical Engineering and Computer Sciences University of California at Berkeley, Technical Report No. UCB/EECS-2013-36

[4] J. Kokkoniemi, J. Lehtomäki, M. Junnti, "A discussion on molecular absorption noise in the terahertz band", Nano Communication Networks, vol. 8, pp. 35-45, June 2016

[5] P. Boronin, V. Petrov, D. Moltochanov, Y. Koucheryavy, J. M. Jornet, "Capacity and throughput analysis of nanoscale machine communication through transparency windows in the terahertz band", Nano Communications Networks, vol. 5, issue 3, pp. 72-82, Sept. 2014

[6] J. Kokkoniemi, J. Lehtomäki, M. Junnti, "Simplified Molecular Absorption Loss Model for 275-400 Gigahertz Frequency Band"

[7] S. Chandrasekhar, "Radiative Transfer", Dover Publications Inc., 1960

[8] R. M. Goody, Y. L. Yung, "Atmospheric Radiation: Theoretical Basis", second edition. Oxford University Press, 1989

[9] L. S. Rothman et al., "The HITRAN 2012 molecular spectroscopic database", J. Quant. Spectrosc. Radiat. Transfer., vol. 130, no. 1, pp. 4-50, Nov. 2013

[10] "HITRAN", Molecular spectroscopic database, "http://hitran.org/"

[11] S. Paine, "The am atmospheric model", Tech. Rep. 152, Smithsonian Astrophysical Observatory (2012)

[12] J. H. Van Vleck, V. F. Weisskopf, "On the shape of collision broadened lines", Rev. Mod. Phys., vol. 17, no. 2-3, pp. 227-236, 1945.

[13] J. H Van Vleck, D. L. Huber, "Absorption, emission and line breadths: A semihistorical perspective", Rev. Mod. Phys., vol 49, no. 4, pp. 939-959, 1977

[14] F. Box, "Utilization of atmospheric transmission losses for interference resistant communications", IEEE Trans. Commun., vol. 34, no. 10, pp. 1009-1015, Oct. 1986.

[15] P. Boronin, D. Moltchanov, Y. Koucheryavy, "A molecular noise model for THz channels", Proc. IEEE Int. Conf. Commun., 2015, pp. 1286 - 1291.

[16] E. K. Smith, "Centimeter and millimeter wave attenuation and brightness temperature due to atmospheric oxygen and water vapor", Radio Sci. 17 (6) (1982) 1455-1464.

[17] P. M. Robitaille, "Kirchhoffs law of thermal emission: 150 years, Progress", Physics vol. 4, Oct. 2009.

[18] L. S. Rothman et al., "The HITRAN molecular spectroscopic database and HAWKS (HITRAN atmospheric workstation): 1996 edition", J. Quant. Spectrosc. Radiat. Transfer, vol. 60, no. 5, pp. 665-710, Nov. 1998

[19] J. M. Jornet, and I. F. Akyildiz, "Channel Capacity of Electromagnetic Nanonetworks in the Terahertz Band", in Proc. of IEEE, ICC, May 2010, pp. 1-6.

[20] H. J. Song , T. Nagatsuma, “Present and future of Terahertz communications,” in

IEEE Trans. Terahertz Sci. Technol., vol. 1, no. 1, pp. 256–263, Sep. 2011

[21] "The European table of frequency allocations and applications in the frequency range 8.3 kHz to 3000 GHz (ECA TABLE)", Electronic Communications Committee) within the European Conference of Postal and Telecommunications Administrations (CEPT)

[22] T. Merkle, “Testbed for phased array communications from 275 to 325 GHz,” in IEEE Compound Semiconductor IC Symposium (CSICS), Oct. 2017.

[23] A.–A. A. Boulogeorgos, E. N. Papasotiriou, J. Kokkoniemi, J. Lehtomäki, A. Alexiou, M. Juntti, “Performance evaluation of THz wireless systems operating on 275-400 GHz band,” submitted for possible publication in the IEEE 87th Vehicular Technology Conference 2018, International Workshop on THz Communication Technologies for Systems Beyond 5G.

[24] C. Lin and G. Y. Li, "Indoor Terahertz communications: How many antenna arrays are needed?", in IEEE Trans. Wireless Commun., vol. 14, no. 6, pp. 3097-3107, Jun. 2015

[25] S. Rajagopal, S. Abu-Surra, M. Malmirchegini, "Channel feasibility for outdoor non-line-of-sight mmwave mobile communication", in IEEE Vehicular Technology Conference, Sep. 2012, pp. 1-6

[26] R. Zhang, K. Yang, Q. H. Abbasi, K. A. Qarage, A. Alomainy, "Analytical characterization of the terahertz in vivo nano-network in the presence of interference

based on TS-OOK communication scheme", in IEEE Access, vol. 5, pp. 10 172-10 181, 2017.

[27] N. Akkari, J. M. Jornet, P. Wang, E. Fadel, L. Elrefaei, M. G. A. Malik, S. Almasri, I. F. Akyildiz, "Joint physical and link layer error control analysis for nanonetworks in the terahertz band", in Wireless Networks, vol. 22, no. 4, pp. 1221-1233, May 2016.

[28] O. A. Alduchov and R. E. Eskridge, "Improved magnus form approximation of saturation vapor pressure", J. Appl. Meteor., vol. 35, no. 4, pp. 601-609, Apr. 1996

[29] ITU-R (2009) Recommendation P.676-8, Attenuation by atmospheric gases, International Telecommunication Union Radiocommunication Sector Std.